Max-Planck-Institut
für Meteorologie

MAX-PLANCK-GESELLSCHAFT

International Max Planck Research School
on Earth System Modelling

Impact of the multidecadal variations in the North Atlantic Sea Surface Temperature on European summer climate

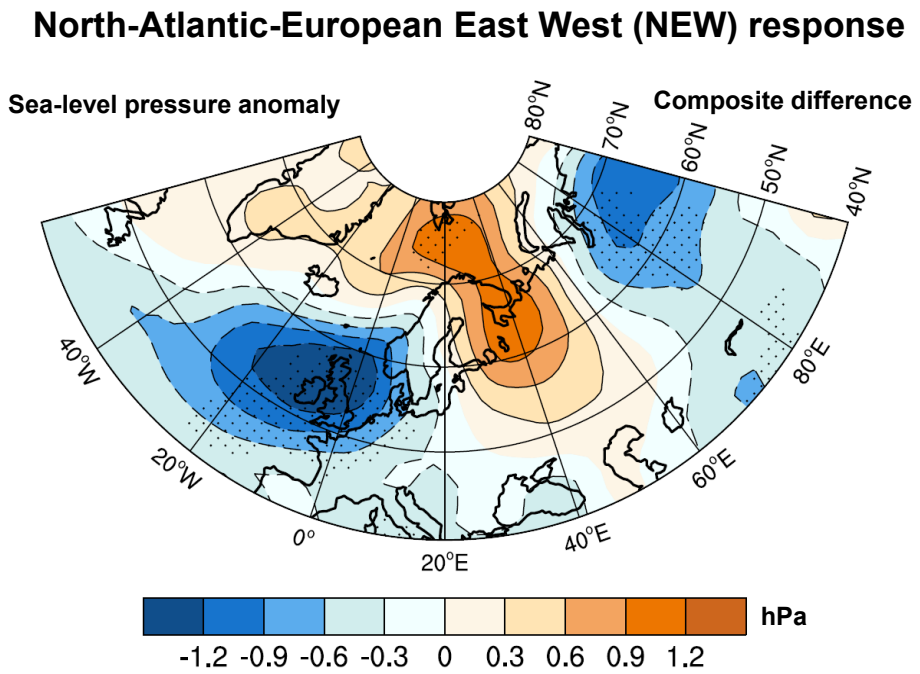

Rohit Ghosh

Hamburg 2017

Berichte zur Erdsystemforschung
Reports on Earth System Science

189
2017

Hinweis

Die Berichte zur Erdsystemforschung werden vom Max-Planck-Institut für Meteorologie in Hamburg in unregelmäßiger Abfolge herausgegeben.

Sie enthalten wissenschaftliche und technische Beiträge, inklusive Dissertationen.

Die Beiträge geben nicht notwendigerweise die Auffassung des Instituts wieder.

Die "Berichte zur Erdsystemforschung" führen die vorherigen Reihen "Reports" und "Examensarbeiten" weiter.

Notice

The Reports on Earth System Science are published by the Max Planck Institute for Meteorology in Hamburg. They appear in irregular intervals.

They contain scientific and technical contributions, including Ph. D. theses.

The Reports do not necessarily reflect the opinion of the Institute.

The "Reports on Earth System Science" continue the former "Reports" and "Examensarbeiten" of the Max Planck Institute.

Anschrift / Address

Max-Planck-Institut für Meteorologie
Bundesstrasse 53
20146 Hamburg
Deutschland

Tel./Phone: +49 (0)40 4 11 73 - 0
Fax: +49 (0)40 4 11 73 - 298

name.surname@mpimet.mpg.de
www.mpimet.mpg.de

Layout

Bettina Diallo and Norbert P. Noreiks
Communication

Copyright

Photos below: ©MPI-M
Photos on the back from left to right:
Christian Klepp, Jochem Marotzke,
Christian Klepp, Clotilde Dubois,
Christian Klepp, Katsumasa Tanaka

Impact of the multidecadal variations in the North Atlantic Sea Surface Temperature on European summer climate

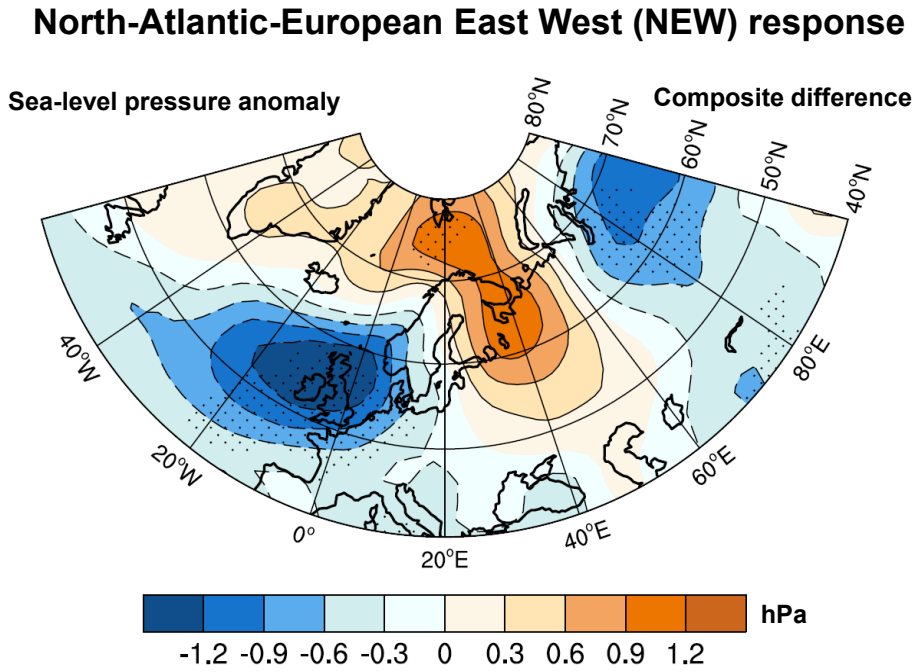

Dissertation with the aim of achieving a doctoral degree
at the Faculty of Mathematics, Informatics and Natural Sciences
Department of Earth Sciences of Universität Hamburg

submitted by

Rohit Ghosh

Hamburg 2017

Rohit Ghosh

Max-Planck-Institut für Meteorologie
Bundesstrasse 53
20146 Hamburg

Tag der Disputation: 24.01.2017

Folgende Gutachter empfehlen die Annahme der Dissertation:

Dr. Wolfgang A. Müller
Prof. Dr. Johanna Baehr

Berichte zur Erdsystemforschung / Max-Planck-Institut für Meteorologie 189
Reports on Earth System Science / Max Planck Institute for Meteorology 2017

ISSN 1614-1199

Abstract

The observed multidecadal variations in the central to eastern (C-E) European summer temperature are closely related to the Atlantic Multidecadal Variability (AMV). Using the Twentieth Century Reanalysis project version 2 data for the period of 1930 to 2012, we present a mechanism by which the multidecadal variations in the C-E European summer temperature are governed by a linear baroclinic atmospheric response to the AMV-related surface heat flux (Ghosh et al., 2016). Our results suggest that over the north-western Atlantic, the positive heat flux anomaly triggers a surface baroclinic pressure response with a negative surface pressure anomaly to the east of the heat source. Further downstream, this response induces an east-west wave-like pressure anomaly. The east-west wave like sea level pressure structure, to which we refer as North-Atlantic-European East West (NEW) mode, is independent of the summer North Atlantic Oscillation and is the principal mode of variations during summer over the Euro-Atlantic region at decadal means. The NEW mode causes warming of the C-E European region by favouring an atmospheric blocking-like situation. This NEW mode is also responsible for the multidecadal variations in precipitation over the British Isles and north-western Europe due to warm and moist air advection from the subtropics.

Further, by using coupled climate model MPI-ESM, we investigate the model response to AMV type of SST and its similarities and differences from the response in the reanalysis. In the control simulations, both low resolution (LR) and high (HR) resolution versions of MPI-ESM can simulate a similar AMV type of SST pattern like in 20th century reanalysis. The LR is found to be more sensitive to the tropical branch of the SST and thus the North-Atlantic-European (NAE) climate is mainly influenced by the stationary Rossby wave response from the tropics. In HR, the impact of the tropical SST variations on the extra-tropics is weaker due to lesser eddy-mean flow interactions. However the NEW mode is not found in any of these control simulations.

The coupled models have a strong SST bias in the North Atlantic which may restrict the model and associated heat fluxes to produce the observed NEW mode. Therefore a set of AMIP-like sensitivity experiments with prescribed observed AMV type SST pattern is conducted, using the atmospheric component of the MPI-ESM-LR, ECHAM version 6.3. The results from the experiments reveal that in the positive phase of the AMV, the North-Atlantic-European (NAE) climate is mainly influenced by the tropical branch of the AMV. Here a stationary Rossby wave response from the tropics is associated with negative surface air temperature (SAT) anomalies over the C-E Europe, which is opposite to what is

found in the case of decadal means in the re-analysis. However, in the case of the negative phase of AMV, NAE climate variations are mainly governed by the extra-tropical branch of SST through a baroclinic-like response. Over C-E Europe, negative SAT anomalies are found with respect to the negative phase of AMV, which is similar to what is found in Ghosh et al. (2016). Hence, the model can simulate the observed baroclinic response with the AMV type of SST forcing, but only in the negative phase of the AMV SST. For the positive phase, in agreement with the previous findings, the model is very sensitive to the tropical branch of the AMV SST.

Zusammenfassung

Die beobachteten multidekadischen Variationen der zentralen-osteuropäischen Temperaturen sind eng verknüpft mit der Atlantischen Multidekadischen Variabilität (AMV). Unter Berücksichtigung der Daten der NOAA 20. Jahrhundert Re-Analysen für eine Periode von 1930 bis 2012, weisen wir den Mechanismus nach, durch welchen die multidekadischen Variationen der Sommertemperaturen über Europa über einen baroklinen Austausch zwischen Bodendruck und diabatischer Erwärmung respektive Wärmeflüsse erklärt werden kann. Im weiteren Verlauf induziert dieser Prozess ein wellenartiges Druckmuster in Ost-West Ausrichtung. Diese Ost-West-artige Ausprägung der Druckstruktur an der Oberfläche, welche wir im Folgenden den NEW ("North-Atlantic-European East West“) Mode bezeichnen, ist unabhängig von der bekannten sommerlichen Nordatlantischen Oszillation und gemeinhin das dominante Muster der dekadischen Variabilität über Europa. Der NEW Mode geht einher mit blockierenden Wetterlagen über Zentraleuropa und induziert somit die Variationen der sommerlichen Temperaturen. Der NEW Mode geht auch einher mit der Advektion von warmer und feuchter Luft aus dem subtropischen Atlantik und beschreibt die multidekadischen Variationen von Niederschläge über den Britischen Inseln und Nord-West Europa.

Mit Hilfe des MPI-ESM untersuchen wir ferner inwieweit ein Klimamodell diese Prozesse simulieren kann und inwiefern sie sich von den Ergebnissen aus den Re-Analysen unterscheiden. Kontrollsimulationen in niedriger (LR) und hoher (HR) Auflösung des MPI-ESM weisen zunächst eine ähnliche AMV Struktur auf wie in den NOAA 20. Jahrhundert Re-Analysen. Die LR Konfiguration weist jedoch eine erhebliche Sensitivität des europäischen Klimas hinsichtlich der tropischen Meeresoberflächentemperatur (SST) auf. In der Atmosphäre ist dies über einen starken Anteil der tropisch angeregten stationären Rossby-Wellen erkennbar. In der HR Konfiguration ist dieser Einfluss geringer, vorwiegend durch eine geringere Wechselwirkung zwischen synoptischen Störungen und mittlerer Grundströmung. Grundsätzlich aber ist der NEW Mode in den Kontrollexperimenten nicht identifiziert.

Die gekoppelten Modelle weisen im Nordatlantik grundsätzlich einen starken SST Fehler auf, der die modellierten Wärmeflüsse und somit auch den NEW Mode beeinträchtigen. Zu diesem Zweck werden AMIP-artige Sensitivitätsexperimente mit vorgegebener SST durchgeführt, hier mit der atmosphärischen Komponente des MPI-ESM ECHAM 6.3. Die Ergebnisse dieser Experimente zeigen, dass in der positiven Phase der AMV, das nordatlantisch-europäische Sommerklima hauptsächlich über den tropischen Anteil der AMV gesteuert ist. Die tropisch angeregte Rossby-Welle geht einher mit negativen Oberflächentemperaturanomalien (SAT) über Europa, und ist gegensätzlich zu den Ergebnissen der dekadischen

Mittel in den Re-Analysen. Im Falle der negativen Phasen der AMV hingegen, sind die Klimavariationen über Zentraleuropa tatsächlich auf den baroklinen Prozess des extra-tropischen Atlantiks zurückzuführen. Über Zentraleuropa geht hier die negative Phase der AMV einher mit negativen SAT Anomalien, so wie beschrieben in Ghosh et al. (2016). Somit kann das Modell den beobachteten baroklinen Prozess simulieren, allerdings nur in der negativen Phase der AMV. In der positiven Phase der AMV wird das Modell vom tropischen Anteil der AMV dominiert.

Table of contents

Chapter 1

Introduction

1.1 Multidecadal variations of the summer North Atlantic sea surface temperature

The observed North Atlantic ocean sea surface temperature (SST) exhibits variability on multi-decadal time scales over the last century in all the seasons (Bjerknes, 1964; Delworth and Mann, 2000; Kushnir, 1994; Schlesinger and Ramankutty, 1994). A typical proxy for the variability is the Atlantic Multidecadal Variability (AMV) index, which shows distinct alternating warm and cool phases with a periodicity of 65-70 years (Fig 1.1). The strong shifts in the AMV such as during the 1920s and 1990s have been associated with the changes in the Arctic-Atlantic climate system (e.g Bengtsson et al., 2004; Polyakov et al., 2005).

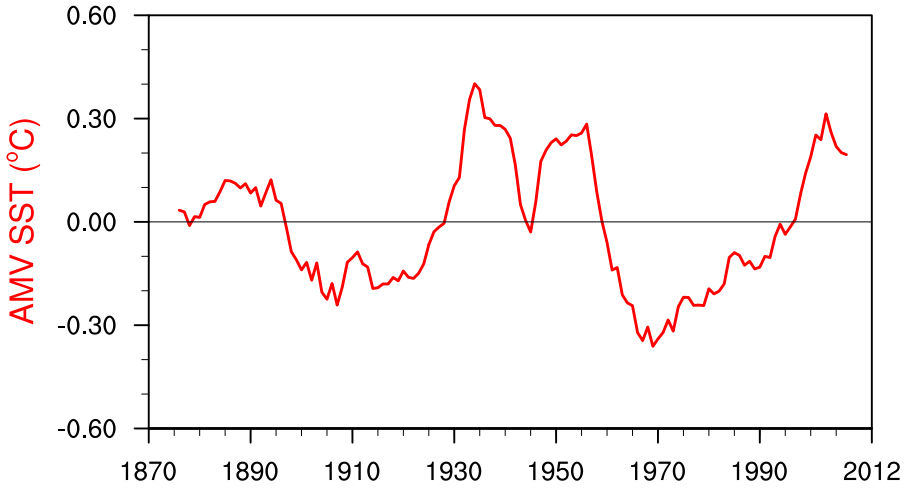

Fig. 1.1 The 11 year running mean times series of the detrended average SST anomaly during summer (JJA) over the region 35°- 50°N and 75°W - 7.5°W for the period 1871-2012 taken from Hadley Center Sea Ice and SST (HadISST) 1.1 (Rayner et. al., 2003). This is known as Atlantic Multidecadal Variability (AMV) index. Units are in °C.

The spatial pattern of the North Atlantic SST anomalies associated with the warm minus cold phase of the summer AMV index is shown in figure 1.2. It presumably shows warm SST anomalies all over the North Atlantic Ocean in the warm phase of the AMV. Over the tropical Atlantic Ocean, higher anomalies are seen over the eastern tropical Atlantic. However, most intense SST anomalies are seen just east of the Newfoundland ($\sim 0.9\ ^{\circ}C$) which is consistent with the previous studies (Sutton and Hodson, 2007, 2005).

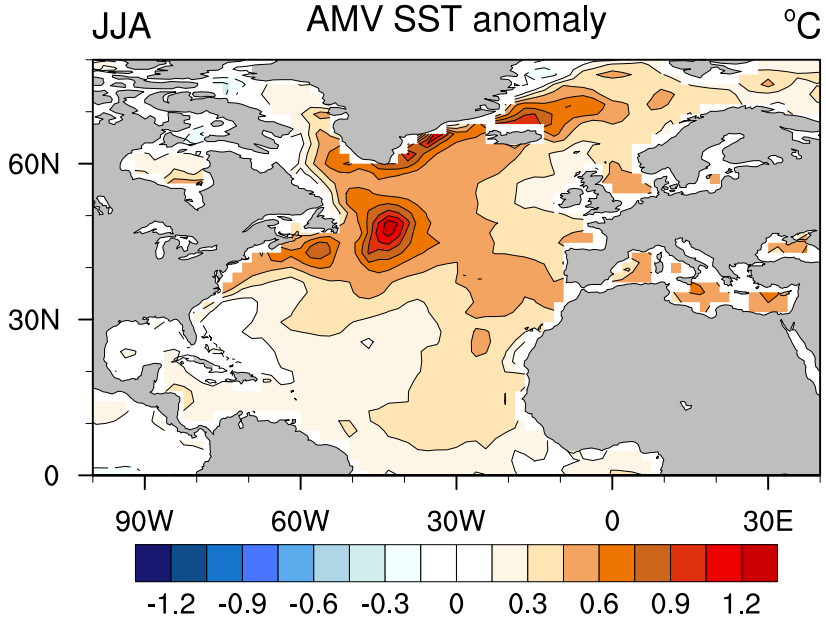

Fig. 1.2 The composite SST anomalies in summer (JJA) over the North Atlantic Ocean which is defined as the difference in the average SST anomalies between the warm and cold phases in the AMV index from figure 1.1. The warm or cold phases are all those years when the AMV index is above or below 1 or -1 standard deviation. Units are in $^{\circ}C$.

SST is clearly associated with the turbulent heat fluxes, which is a key proccess for atmosphere-ocean interaction. A recent study with observed data over the mid-latitude North Atlantic Ocean shows that on multi-decadal time scales the turbulent heat flux, is indeed driven by the ocean and may force the atmosphere (Gulev et al., 2013). The amplitude of the AMV is found to be large in comparison to the interannual North Atlantic SST variability (Sutton and Hodson, 2007). In this context, the AMV and associated heat fluxes provide the physical framework to significantly impact surrounding continents on multi-decadal time scales.

In fact, there are studies which show links between observed AMV and atmospheric features over the North Atlantic European region for distinct seasons (Enfield et al., 2001; McCabe et al., 2004; Sutton and Hodson, 2005). The robustness of these links are established through year long control simulations of a climate model (e.g Knight et al., 2006). Regarding the reasons behind the link of AMV and North American summer climate, some studies further explored the mechanism and proposed plausible atmospheric pathway (Hodson et al.,

2010; Sutton and Hodson, 2007). However, a detailed description of the link of the AMV and European climate in summer remains unclear.

1.2 AMV related Multidecadal variations in European summer climate

Previous studies suggest that the AMV affects European summer climate (Müller et al., 2014; Robson et al., 2012; Sutton and Dong, 2012; Sutton and Hodson, 2005). As an example, the observed differences between the warm phase (1931-1960) and the cold phase (1961-1990) of the AMV shows warmer summer SATs over C-E Europe to be associated with a warm phase of the AMV and vice versa (Sutton and Hodson, 2005). Similar results are found for the transition from a cold phase to a warm phase in the 1920s (Müller et al., 2014) and the transition from a warm phase to a cold phase in the 1960s during the North Atlantic cooling (Robson et al., 2012; Sutton and Dong, 2012).

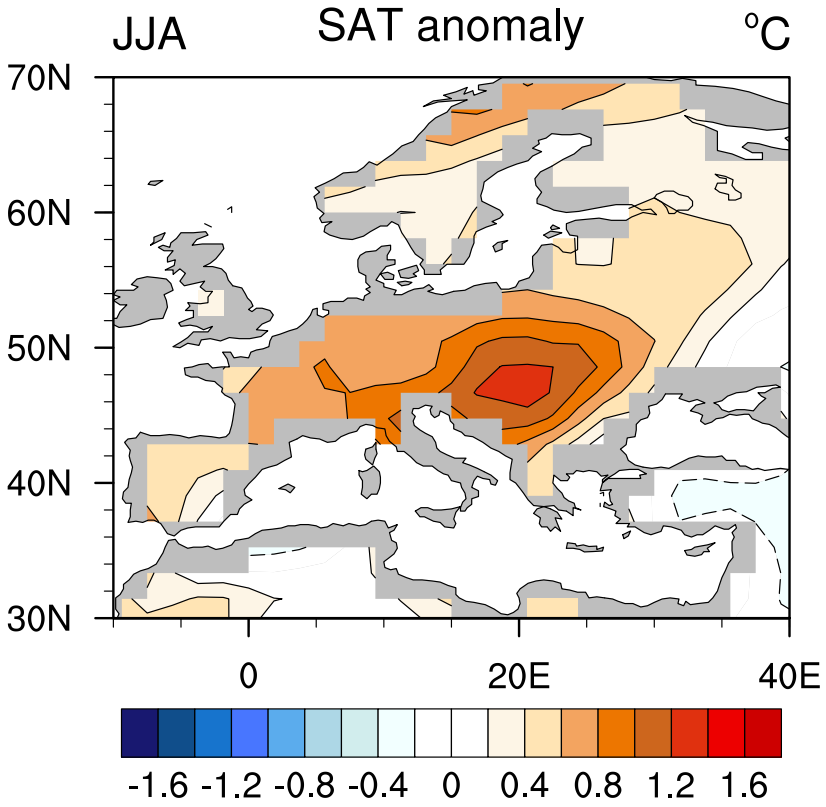

Fig. 1.3 Same as figure 1.2 but for the composite of 2m surface air temperature (SAT) anomalies in summer (JJA) over the European region. The SAT data is taken from 20th Century reanalysis (Compo et al., 2011). Units are in °C.

As an illustration, the composite of the surface air temperature (SAT) anomalies over Europe from Twentieth Century Reanalysis Project version 2 (20CRv2) with respect to the warm minus cold phase of the AMV index is shown in figure 1.3. There are positive anomalies all over Europe with a prominent warming over the central to eastern (C-E) Europe in a range of ~ 1.5 °C. Hence, it is evident that AMV is strongly associated with the multidecadal variations of European summer climate. However, a mechanism describing the atmospheric pathway from the AMV to European summer climate has not yet been established.

1.3 AMV related plausible atmospheric response to European summer climate

Previous studies revealed two possibilities of how atmosphere responses to AMV and thus potentially link to European summer climate. One is a tropical response based on a Gill-type response to sub-tropical heating and another is an extra-tropical response forced by the diabatic heating anomalies in the extra-tropical North Atlantic. Both are briefly described here.

1.3.1 Response from the tropical AMV SST anomalies

General circulation models have been used to show that decadal scale variability in the tropical Atlantic SST can impact the climate over the North Atlantic-European (NAE) region (Davini et al., 2015; Terray and Cassou, 2002). It is shown that a Gill-type of reponse from the off-equatorial diabatic heating of the tropical Atlantic ocean consists of a strong upper level wind divergence. This tropical wind divergence acts as a source of stationary Rossby wave response which then propagates pole-ward and influences the midlatitude climate (Hoskins and Karoly, 1981; Terray and Cassou, 2002). The vertical structure of the response is baroclinic in the tropics and barotropic in the mid and high latitudes and the temperature response shows heating in the tropics, cooling in the extra-tropics, and warming at the high latitudes throughout the troposphere, indicating poleward heat transport (Terray and Cassou, 2002). However, these studies were addressing the winter season and the response could be different during summer due to a different mean climate state (Peng and Whitaker, 1999).

By considering seasonal mean quantities, Gastineau and Frankignoul (2015) examined the atmospheric responses during summer from the 20CRv2 data. With a lead of 3 months (March-April-May, MAM) in SST, they performed maximum covariance analysis (MCA) with the 500hPa geopotential pattern in summer (JJA). Using the time series of the first mode of MCA and then performing a regression analysis on the 200hPa velocity potential, they showed a decrease in velocity potential over the tropics is associated with the large scale ascending motion over the tropical Atlantic positive SST anomalies. This is an indication of stationary Rossby wave propagation (Terray and Cassou, 2002). However, their analysis is

based on seasonal means. It could have a different characteristics while considering decadal means in summer, which only represents the impact from the low frequency variability in the climate system.

The atmospheric response over the surrounding regions from the AMV in summer is exclusively investigated through idealized model experiments where an AMV SST anomaly pattern is added to the climatological global SST, which is then used as a forcing of the atmospheric model (Hodson et al., 2010; Sutton and Hodson, 2007, 2005). These experiments also showed robust linear response from the tropical branch of the AMV SST anomaly which affects the North American climate. The response was attributed to an off-equatorial Gill response to diabatic heating which is also the reason of stationary Rossby wave generation (Terray and Cassou, 2002). However, these studies did not show any impact of the AMV through stationary Rossby waves on NAE climate and specifically on European summer climate where we have seen a prominent response from AMV in the observations (Fig 1.3). Moreover, these studies have addressed the impact of the tropical branch of the AMV in a model set up. The impact of the tropical branch of the AMV in observations is still to be explored.

1.3.2 Response from the extra-tropical AMV SST anomalies

An alternative mechanism is reffered to the baroclinic atmospheric response related to the extra-tropical SST anomalies (Hoskins and Karoly, 1981; Kushnir, 1994; Kushnir and Held, 1996). According to the linear quasigeostrophic theory, in the extra-tropics, a diabatic heating induces a surface low east of the centre of heating. The surface low deviates the colder polar wind towards the heating region and drives sub-tropical warmer air to the east of the centre of the low pressure (Hoskins and Karoly, 1981). This warmer air can increase humidity and SAT over Europe by temperature advection. This mechanism is shown by a schematic diagram in Figure 1.4.

Kushnir (1994) found a similar pressure response for interdecadal variations of the SST in the extra-tropical Atlantic ocean over all seasons. Kushnir (1994) inferred that the atmospheric response to SSTs over the North Atlantic sector differs between interannual and interdecadal time scales. Similar results were found with atmospheric general circulation model experiments by prescribing the SST anomalies over the extra-tropical Atlantic Ocean (Kushnir and Held, 1996). Moreover, Gulev et al. (2013) showed that the surface heat flux over the north western Atlantic region shows similar multidecadal variations as the AMV and thus may produce the diabatic heating background required for such a baroclinic response. These results strongly motivate us to further investigate the response related to the diabatic heating of the extra-tropical branch of AMV SST and its impact on European summer climate in observations as well as in the model.

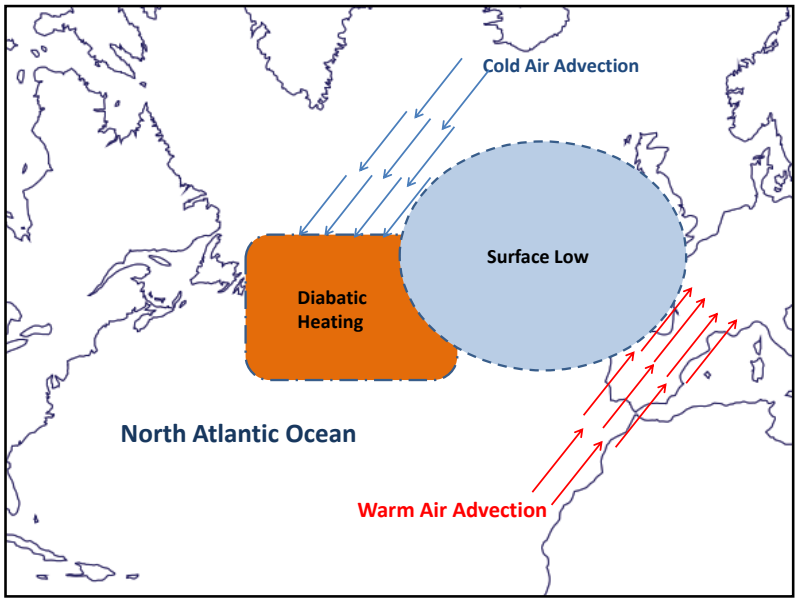

Fig. 1.4 The schematic diagram showing the linear baroclinic response from the diabatic heating of the North Atlantic Ocean following the linear quasi-geostrophic theory (Hoskins and Karoly, 1981). It shows the diabatic heating over the North-West Atlantic Ocean (red box) induces a surface low (blue oval) east of the heating which drives colder polar winds (blue arrows) towards the heating region and advects warmer subtropical winds (red arrows) towards the European region.

1.4 Motivations and Thesis outline

Based on the previous studies mentioned above, the main question which remained unanswered is about the reason behind the observed link between AMV and European summer climate. The main motivation of this thesis is to first describe the observed atmospheric pathway between AMV and European summer climate and then to establish a plausible mechanism explaining the dynamical reason of the atmospheric pathway. Subsequently we investigate whether the observed atmospheric pathway between AMV and European summer climate can be found in a climate model. For this, we examine the control simulations of the coupled model MPI-ESM and the idealized experiments with AMV like SST forcing.

For addressing the above-mentioned motivations, the thesis is divided into three main chapters, each addressing a particular aspect. They are the following

Chapter 2: What is the observed atmospheric pathway between AMV and European summer climate? What is a plausible dynamical mechanism which can lead to the observed atmospheric pathway?

– The answers are provided through the analysis of the 20th Century Reanalysis data (Compo et al., 2011) which is used as a proxy of the observations. This chapter has already been published in the journal of Climate Dynamics (Ghosh et al., 2016).

Chapter 3: What is the relation of the AMV and European summer climate in a coupled climate model? Can it represent the observed link and the atmospheric pathway?

– The answers are given through the analysis of the Max Planck Institute Earth System Model (MPI-ESM) pre-industrial control simulations for both low and high resolutions.

Chapter 4: What is the relation of the AMV and European summer climate in idealized sensitivity experiments with observed AMV like SST pattern? Can we find the observed response over Europe and associated atmospheric pathway?

– The answers are given by performing a set of sensitivity experiments with both positive and negative phase of the AMV SST anomaly forcing, using the atmospheric component of the MPI-ESM, ECHAM 6.3.

Chapter 2

Impact of observed Atlantic Multidecadal Variability to European summer climate: a linear baroclinic response to surface heating

Abstract: The observed prominent multidecadal variations in the central to eastern (C-E) European summer temperature are closely related to the Atlantic Multidecadal Variability (AMV). Using the Twentieth Century Reanalysis project version 2 data for the period of 1930 to 2012, we present a mechanism by which the multidecadal variations in the C-E European summer temperature are associated to a linear baroclinic atmospheric response to the AMV-related surface heat flux. Our results suggest that over the north-western Atlantic, the positive heat flux anomaly triggers a surface baroclinic pressure response to diabatic heating with a negative surface pressure anomaly to the east of the heat source. Further downstream, this response induces an east-west wave-like pressure anomaly. The east-west wave like response in the sea level pressure structure, to which we refer as North-Atlantic-European East West (NEW) mode, is independent of the summer North Atlantic Oscillation and is the principal mode of variations during summer over the Euro-Atlantic region at multidecadal time scales. The NEW mode causes warming of the C-E European region by creating an atmospheric blocking-like situation. Our findings also suggest that this NEW mode is responsible for the multidecadal variations in precipitation over the British Isles and north-western Europe.

2.1 Introduction

The AMV has a profound impact on European summer climate (Knight et al., 2006; Sutton and Hodson, 2005). Substantial increase of temperature in central Europe is observed during a strong phase of the AMV (Sutton and Hodson, 2005). The AMV-related atmospheric pathway to the European summer climate, however, is still not understood. Previous studies

considered the summer North Atlantic Oscillation (SNAO, Folland et al. (2009)) and associated meridional shifts in the storm tracks explaining variations of the European summer climate (Bladé et al., 2012; Dong et al., 2012). Even though a direct link of the AMV to the SNAO is still controversial. In addition to the summer North Atlantic Oscillation (SNAO), an alternative atmospheric response could be the baroclinic atmospheric response to shallow diabatic heating anomalies in the extra-tropics (Hoskins and Karoly, 1981; Kushnir, 1994; Smagorinsky, 1953). Such diabatic heating can result from AMV-related surface heat fluxes as recently shown in the analysis of observations (Gulev et al., 2013). Here, we investigate the atmospheric response to such diabatic heating in the North Atlantic and we identify a remote pathway which explains the observed multidecadal variations of European summer climate.

The central to eastern (C-E) European summer climate exhibits prominent multidecadal variations as shown by surface air temperature (SAT) in figure 1a. For example, there is a likelihood of appearance of high SATs between 1930 and 1960, and from 1990 onwards, and low SATs between 1960 and 1990. Similar multidecadal variations, however, have also been observed for other parameters, for example for the precipitation over the British Isles and north-western European (BE) region (Fig 1b), suggesting that BE precipitation and C-E European SATs stem from the same dynamical response at multidecadal time scales.

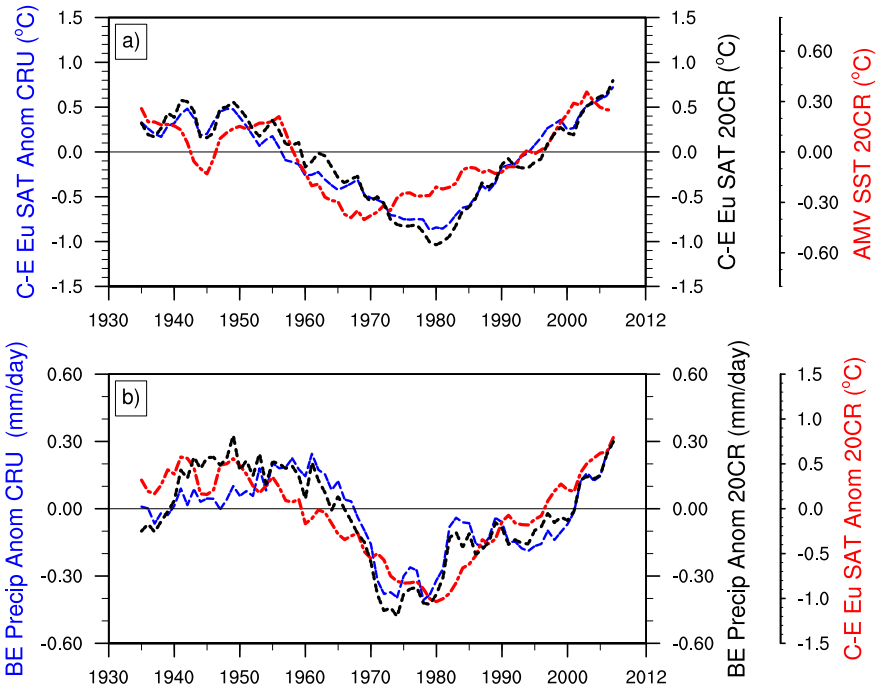

Fig. 2.1 a) Time series of averaged central to eastern (C-E) European (40°N - 55°N, 10 °E - 30°E) summer SAT (Surface Air Temperature) with 11 year running mean from 20CRv2 (black), from CRU TS3.2 (blue) and SST over the region 35°N - 50°N and 7.5°W - 75°W (red) for the summer (JJA) months from 20CRv2 (Compo et al., 2011) (units in °C). b) Time series of averaged British Isles and north-western European (BE) (50°N - 60°N, 0 °E - 15°E) region summer precipitation with 11 year running mean from 20CRv2 (black), from CRU TS3.2 (blue) (units in mm/day) and C-E European SAT with 11 year running mean (red) for the summer (JJA) months from 20CRv2 (Compo et al., 2011) (units in °C).

Multidecadal variations of C-E European SATs and multidecadal variations of North Atlantic sea surface temperatures (SSTs), the AMV, have similar temporal variations with a correlation of 0.84 (Fig 1a). Previous studies suggested that the AMV affects European summer climate (e.g. Müller et al., 2014; Robson et al., 2012; Sutton and Dong, 2012; Sutton and Hodson, 2005). The observed differences between the warm phase (1931-1960) and the cold phase (1961-1990) of the AMV have shown warmer summer SATs over C-E Europe to be associated with a warm phase of the AMV and vice versa (Sutton and Dong, 2012; Sutton and Hodson, 2005). Similar results are found for the transition from a cold phase to a warm phase in the 1920s (Müller et al., 2014) and the transition from a warm phase to a cold phase in the 1960s during the North Atlantic cooling (Robson et al., 2012; Sutton and Dong, 2012). These studies also showed, during the warm phase of AMV, a positive summer precipitation anomaly over northern Europe including the BE region, thus suggesting a close association between the multidecadal variations of C-E European SATs and BE precipitation in summer. In summary, the AMV is accepted as a governing factor for multidecadal variations of European summer climate. However, a mechanism describing the atmospheric pathway from the AMV to European summer climate has yet to be established.

The principal mode of interannual variability in summer sea-level pressure (SLP) over the NAE region is usually referred to as SNAO which has a typical North-South dipole-like structure in SLP with the southern lobe over the north-western Europe. Vertically, the SNAO is near equivalent barotropic in structure and on interannual time scales, it has significant impact on the climate over the north-western Europe by varying the position of the North Atlantic storm track (Bladé et al., 2012; Dong et al., 2012; Folland et al., 2009). Additionally, Bladé et al. (2012) found the influence of SNAO on Mediterranean climate in interannual as well as multidecadal time scales. However, SNAO and AMV are not found to be significantly related on multidecadal time scales. Moreover, on multidecadal time scales to our knowledge no previous research identified any robust relation of the SNAO with C-E European SATs and BE precipitation. Therefore, the AMV-related multidecadal variations of C-E European SAT are unlikely to be due to an SNAO type of atmospheric response.

An alternative mechanism to the SNAO is the baroclinic atmospheric response related to the extra-tropical SST anomalies (Hoskins and Karoly, 1981; Kushnir, 1994; Kushnir and Held, 1996). According to the linear quasigeostrophic theory, in the extra-tropical ocean, a shallow diabatic heating induces a surface low east of the centre of heating. The surface low deviates the colder polar wind towards the heating region and drives sub-tropical warmer air to the east of the centre of the low pressure (Hoskins and Karoly, 1981). Kushnir (1994) found a similar pressure response for interdecadal variations of the SST in the extra-tropical Atlantic ocean over all seasons. From that he inferred that the atmospheric response to SSTs over the North Atlantic sector differs between interannual and interdecadal time scales. Similar results were found in an atmospheric general circulation model experiment by prescribing the SST anomalies over the extra-tropical Atlantic Ocean (Kushnir and Held, 1996). Moreover, Gulev et al. (2013) showed that the surface heat flux over the north western Atlantic region shows similar multidecadal variations as the AMV and thus may produce the diabatic heating background required for such a baroclinic response. In addition, Gastineau and Frankignoul

(2015) recently showed that such heating during summer is shallow in nature. These results strongly suggest an investigation of a linear baroclinic response to diabatic heating and its impact on the multidecadal variations of C-E European SAT.

Previous studies emphasize on limitations of such baroclinic response to diabatic heating under the influence of transient eddies (Kushnir et al., 2002). The transient eddies can change the baroclinic nature of the response to equivalent barotropic, which indeed is the case in winter (Czaja and Frankignoul, 2002). However, the strength of the transient eddy forcing depends on the climatological mean state of the season (Peng and Whitaker, 1999). Therefore, it could be possible that the eddy forcing in summer is not as strong as winter which we must ensure to confirm the linear baroclinic response to extra-tropical heating.

We use the National Center for Environmental Prediction (NCEP) 20CRv2 data (Compo et al., 2011) to asses the nature of multidecadal variations in the C-E European summer SAT and to establish an atmospheric pathway from the AMV to the C-E European SAT. Similarly, we show a plausible cause of multidecadal variations for the BE precipitation as a manifestation of the same dynamical mechanism.

2.2 Data and Methods

Here, we use the 20CRv2 data as a proxy for observations (Compo et al., 2011). The data are based on the experimental version of the NCEP Global Forecast System model, whose setup we briefly describe here. The observed variables were derived using synoptic surface pressure data records from the International Surface Pressure Databank (ISPD). The monthly observed SST and sea ice concentration data from HadISST 1.1 were used as boundary condition during the simulations (Rayner et al., 2003). The reanalysis fields were generated for 6 hourly temporal and 2°horizontal resolution on 24 vertical levels. A 'deterministic' type Ensemble Kalman Filter algorithm was used for the assimilation (Compo et al., 2006; Whitaker et al., 2004). An ensemble of 6-hourly global fields was performed for the entire period of the simulation. Here, we use for our analysis the monthly mean fields derived from the 6-hourly fields covering the period 1930 to 2012. For further verification, we use the SAT and precipitation data, stem from the CRU TS3.2 and covering the period 1930-2012 with 0.5°resolution (Harris et al., 2014). For reasons explained in section 3.2, we restrict our analysis to the time period between 1930 and 2012 in 20CRv2.

To analyse the governing factors behind the multidecadal variations of the European summer climate, we apply for all variables a 11 year running mean to the detrended time series of seasonal (June-July-August (JJA)) means. We remove the trend by a linear fit. Composites of the respective variables are constructed on the basis of a pre-defined index such as the AMV or the SAT index over a certain region. The composites of the corresponding parameters are defined as the difference of the epochs above and below zero line of the reference index. The significance of the composites is tested using a bootstrap algorithm where the composite at each grid point is calculated on the basis of permutation of the reference index for 1000 times where a block of 11 years is permuted to consider the effect

of smoothing (11 year running mean) in the data. If the 975 out of the 1000 composite values at any grid point is greater or less than the actual composite value, then according to a two-tailed test that grid point is considered significant at 95% level (Matthews and Kiladis, 1999; Schreck et al., 2013).

For defining the relevant period considered in this study (1930-2012), we perform running correlation between two reference indexes (AMV and Heat Flux) using a 70 year time window. The significance of the running correlation is calculated through permutation of the indexes for 1000 times and forming a null distribution on the basis of the highest correlation found in each attempt. We permute a block of 11 years to account for the auto-correlation in the time series due to smoothing.

In case of Pearson's correlation coefficient values mentioned in the paper, for the period 1930-2012, any correlation value above 0.75 (0.66) is significant at 95% (90%) level according to a two-sided student t-test with an equivalent sample size of 7 which accounts for the auto-correlation in the data due to smoothing. Similarly, for the entire period of 20CRv2 (1871-2012) the 95% significance level of correlation is 0.58 with equivalent sample size of 12.

To find the principle mode of variations in a parameter, the empirical orthogonal functions (EOF) of the spatial variations are calculated from the parameters by using their anomaly covariance matrix (North et al., 1982). This procedure is also known as principal component analysis (PCA). The robustness of the orthogonal modes is checked by rotating the EOFs using Kaiser row normalization and the varimax criterion (Mestas-Nunez, 2000). The coupled mode of variations between two parameters are further calculated using the singular value decomposition (SVD) technique on their covariance matrix (Bretherton et al., 1992).

For understanding the role of the synoptic eddies, the transient component of the velocity and temperature fields are calculated using a 2-6 day band pass Lanczos filter on the field of daily data over a particular season (Duchon, 1979).

For deriving the blocking frequency, the blocking index is used in its extension to two dimensions (Scherrer et al., 2006). The daily 500 hPa geopotential height (Z500) data from 20CRv2 are used to construct the blocking index. For the two dimensional extension of the index, all grid latitudes between 35°N to 75°N are accounted as central latitudes. A latitude gradient of 15°north and south is taken around every central latitude to calculate the Z500 gradient. A grid point is considered as blocked if the northern Z500 gradient is less than -10 *m* and southern Z500 gradient is more than 0 *m* for a minimum 5 of consecutive days.

2.3 Multidecadal Variations of European summer SAT

2.3.1 Central to Eastern European SAT Index

We first define the C-E European SAT index, using the first mode of the principal component analysis of summer (JJA) 2 meter air temperature (11 year running mean) over the region 35°N - 75°N and 20°W - 50°E (Fig 4.2a). The spatial distribution of the first mode covers much of the central to eastern (C-E) European area and its time series shows strong multidecadal variations. This mode explains 63% of the total variability. The temporal variations of this mode are similar to the AMV (Fig 4.2b) (temporal correlation = 0.82) and thus indicate the close correspondence of the C-E European temperature in summer with the North Atlantic SST variations.

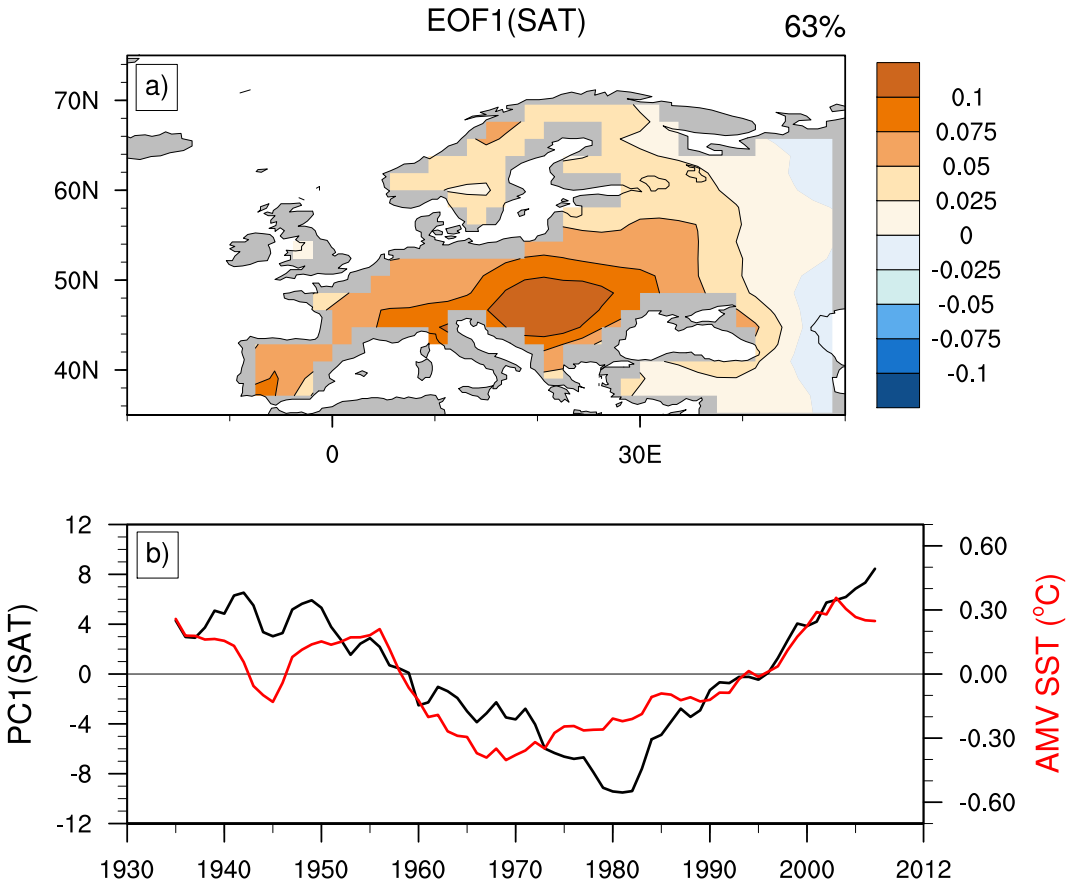

Fig. 2.2 a) The EOF1 of the summer (JJA) 2m air temperature in °C (11 year running mean) for the time period 1930-2012. The explained variance is 63%. b) First principal component (PC1) of EOF SAT (black) with AMV index (red) which is constructed on the basis of the averaged SST (in °C) over the region 35°N - 50°N and 7.5°W - 75°W.

2.3.2 Relation between European summer SAT and North Atlantic heat flux

Before considering the atmospheric pathways, we investigate the nature of the relation between the North Atlantic surface (sensible + latent) heat fluxes and the AMV in 20CRv2 for the entire period (1871 -2012). A composite of the heat flux based on the AMV index identifies the region of the most intensified heat fluxes at the central subpolar gyre region and eastern subtropical Atlantic and shows mostly positive heat fluxes over the North Atlantic except over the western Atlantic and Labrador Sea (Fig 2.3a).

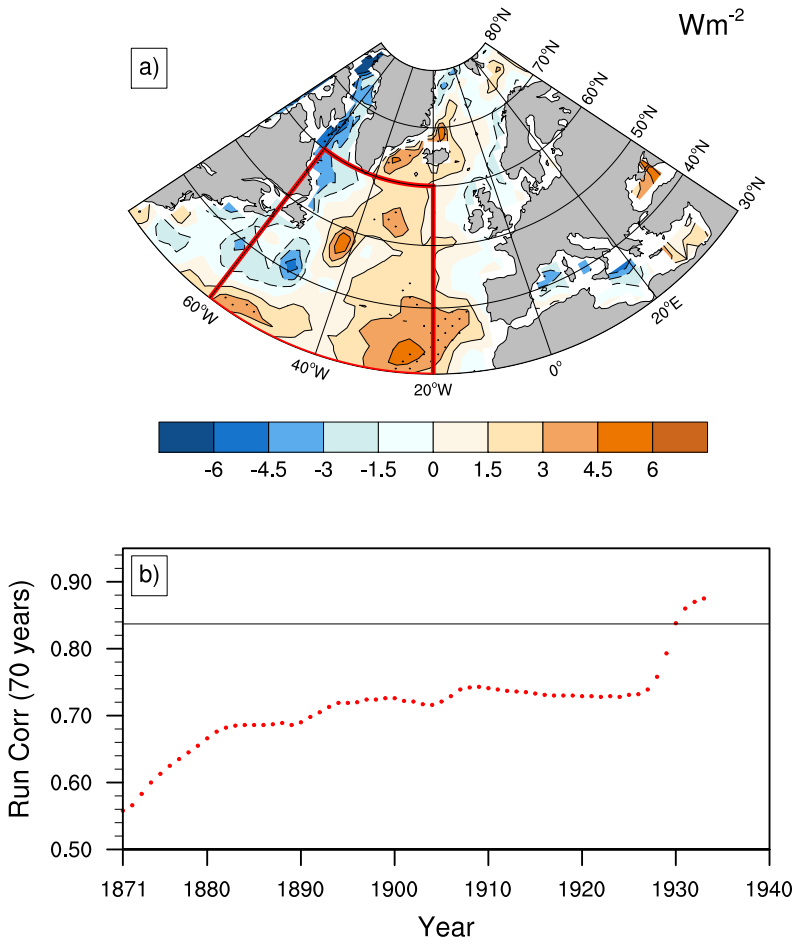

Fig. 2.3 a) Composite of total (sensible + latent) surface heat flux anomaly (11 year running mean) in Wm^{-2} over the ocean with respect to the positive-negative phase of the AMV index (1871-2012). Positive values denote that the ocean is releasing heat to the atmosphere. The dotted regions denote areas with significance at 95% level based on block-bootstrap test. The red box is the area considered for constructing averaged heat flux anomaly over the north-west Atlantic. Only the significant grid points inside the red box are taken for making the average. b) Running correlation of AMV index and the averaged heat flux (both 11 year running mean) for 70 year windows. The value of the correlation is plotted as red dots at the starting point of the correlation window. The horizontal black line is showing the 95% significance level of the running correlation based on block-bootstrap test.

This spatial pattern is similar to the findings of Gulev et al. (2013), who use observations. Next, we use an average of all heat flux anomalies that are significant at 95% level over the north-western Atlantic ocean to relate the heat flux anomalies to the AMV. The evolution of a 70 year time window running correlation is shown in figure 2.3b. The overall correlation between the AMV and heat flux is 0.69, which is mainly due to stronger relation in the later part of the record. The values of the running correlation are low and not significant at the beginning of the record. Only from 1930 onward, the correlations are above the significance level of 95% (0.837). One reason for the temporally changing relation between the AMV and heat flux could be the limited number of observations assimilated at beginning of the 20CRv2 compared to later periods (Gastineau and Frankignoul, 2015; Krueger et al., 2013). Since the diabatic heating of the north-western Atlantic ocean is the foundation of our proposed atmospheric response generated from AMV, the significant relation between these two parameters is essential. Hence, we restrict our entire analysis to the period from 1930 onwards from 20CRv2.

Given the close relation of C-E European SAT and the AMV, composites of the surface heat flux with respect to the C-E European SAT index shows a similar response as for the AMV (Fig 4.10).

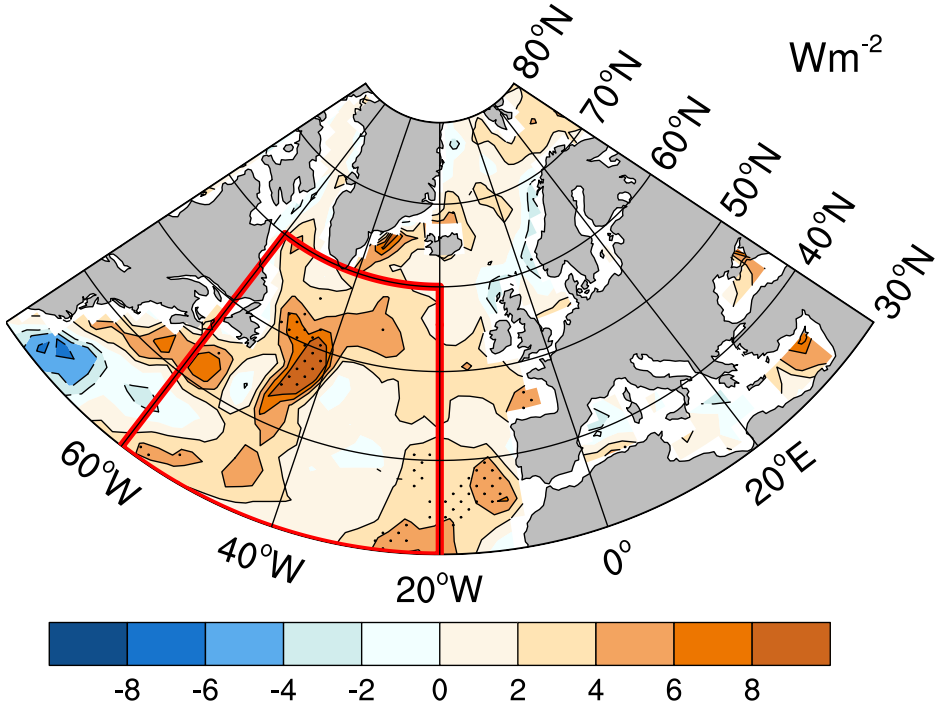

Fig. 2.4 Composite of total (sensible + latent) summer surface heat flux anomaly (11 year running mean) in Wm^{-2} over the ocean (color) with respect to the positive-negative phase of the C-E European SAT Index (1930-2012). Positive values denote that the ocean is releasing heat to the atmosphere. The dotted regions denote areas significant at 95% level based on block-bootstrap test. The red box is the area considered for constructing averaged heat flux anomaly over north-west Atlantic. Only the significant grid points inside the red box are taken for making the average.

The heat flux composite shows an area in the north-western Atlantic which is significantly and positively related to the C-E European SAT. The averaged surface heat flux over this region is of the order $\sim 6\ W/m^2$. Vertically, the warming is maximum within $\sim 700\ hPa$ (not shown) which is in accordance to previous studies (Gastineau and Frankignoul, 2015; Kushnir et al., 2002). Hence, considering the depth of the heating as up to 700 hPa (~ 2 km) the heating rate would be of magnitude $\sim 0.1 - 0.2\ K/day$. Apart from that, the eastern subtropical gyre also provides some heat to the atmosphere.

The temporal variations of the heat flux anomaly over the north-western Atlantic region (30°N - 60°N, 20°W - 60°W), the variations of the SAT index and the AMV index, all show similar multidecadal variations over the last century (Fig 2.5). Here, only the grid points showing significance at 95% level with respect to SAT index are considered when calculating the average of the heat flux anomaly over the above mentioned area. The averaged heat flux anomaly has a temporal correlation with the SAT index of 0.89. The close association of the C-E European SAT with the north-western Atlantic heat flux provides the basis to examine the dynamical atmospheric response in 20CRv2, which can eventually affect the European summer climate at multidecadal time scales.

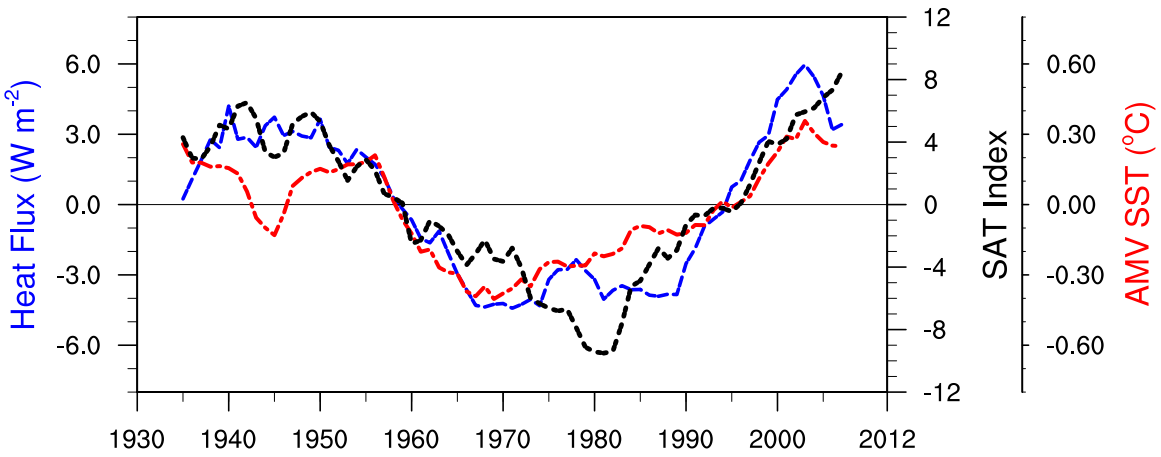

Fig. 2.5 Time series of heat flux anomaly in Wm^{-2} (average of significant grid points within the red box in figure 3) (blue), SAT (Surface Air Temperature) index (PC1 SAT from figure 1b) with 11 year running mean (black), and AMV SST (red) in °Celsius for the summer (JJA) months.

2.4 NEW mode: A linear baroclinic response

In a conceptual framework, Hoskins and Karoly (1981) examined the atmospheric response to extra-tropical diabatic heating within a baroclinic model. In particular they showed that a shallow diabatic heating forces a negative surface pressure anomaly east of the centre of the heating. The composite of the 20CRv2 SLP anomalies (11 year running mean) during summer (JJA) shows a low pressure anomaly situated over the north-eastern Atlantic region and an east-west wave like response further downstream (Fig 4.3). The low pressure anomaly

over the North Atlantic exceeds 1 hPa at the centre of the system and is located eastward of the positive heat flux (Fig 4.10). This SLP anomaly is associated to SST anomaly of $\sim 1\ K$ which is consistent with the study of Kushnir (1994). The subsequent high pressure anomaly is built over the central to north-eastern European region. The high pressure anomaly is followed by low and high pressure anomalies with downstream decreasing intensity. This wave like response could be the result of a baroclinic response to the diabatic heating in the mid-latitudinal Atlantic ocean (Kushnir, 1994).

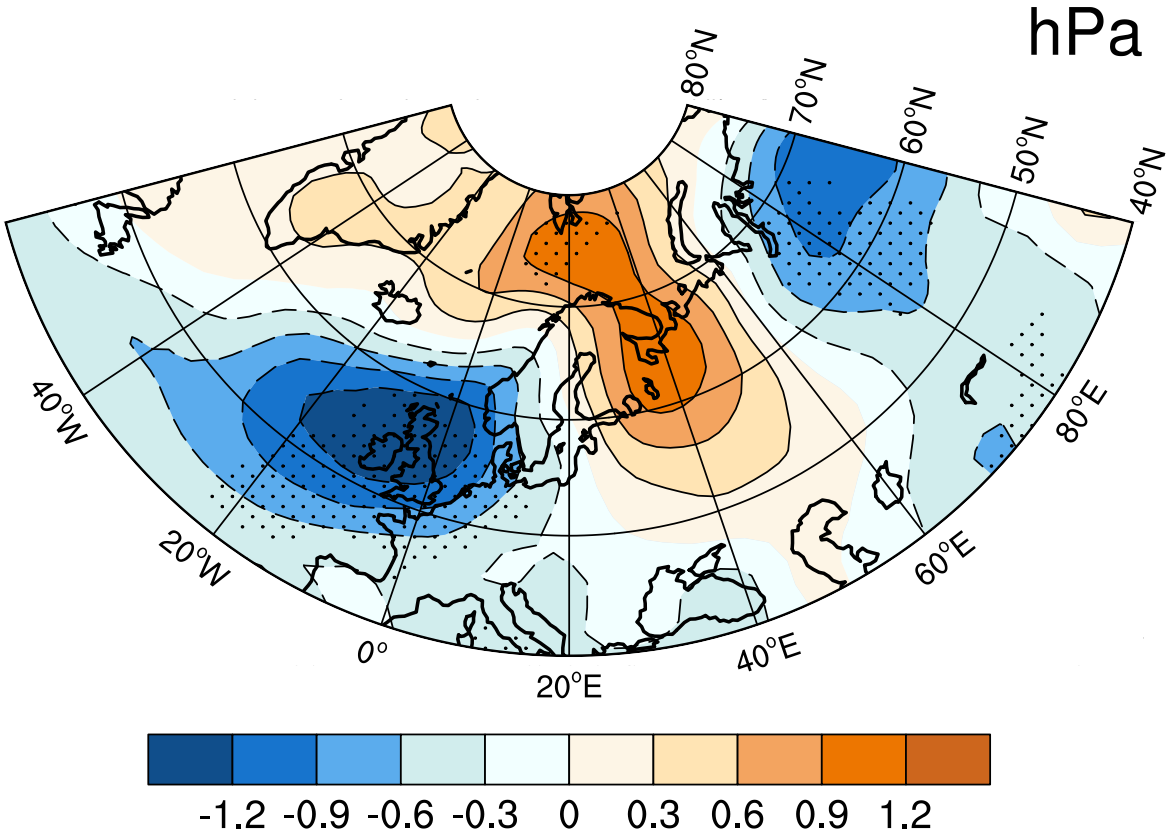

Fig. 2.6 Composite of 11 year running mean SLP in summer (JJA) in hPa with respect to the positive-negative phase of the C-E European SAT index. The dotted regions denote areas with significance at 95% level based on block-bootstrap test.

The formation of the low pressure anomaly at the east of the mid-latitudinal heating is also in accordance with the framework of the linear quasi-geostrophic (QG) theory. According to that theory, the surface low balances the excess heating by driving colder sub-polar winds towards the extra-tropical heat source through horizontal temperature advection (Hoskins and Karoly, 1981). As a result of the formation of this low pressure anomaly, the warmer sub-tropical air would also be driven towards the extra-tropics at the east of the center of the low pressure anomaly. This advection of warmer air is suggested to lead (at least partially) to the warming of the European region at multidecadal time scales; situated just east of the

center of the low pressure (Fig 4.3). The findings from the analysis of the composite of the heat flux (Fig 4.10) and of the SLP (Fig 4.3) suggest that the diabatic heating at the surface of north-western Atlantic ocean leads to the development of the low pressure anomaly and the subsequent wave like response downstream as a linear baroclinic response.

Before continuing with the QG framework, we show the east-west wave-like SLP response is the primary mode of variations on multidecadal time scales. Previous studies showed that the SNAO plays a major role over the extra-tropical Atlantic region from interannual time scales to inter decadal time scales (e.g. Bladé et al., 2012; Folland et al., 2009). However, in contrast to the north-south SNAO SLP structures, the composites of SLP with respect to the C-E European SAT index (Fig 4.3) reveals an east-west wave like structure over the NAE region. To examine the differences of the east-west wave like SLP response from the SNAO, an EOF analysis is performed for SLP over the domain 40°N - 80°N and 60°W - 100°E (Fig 2.7).

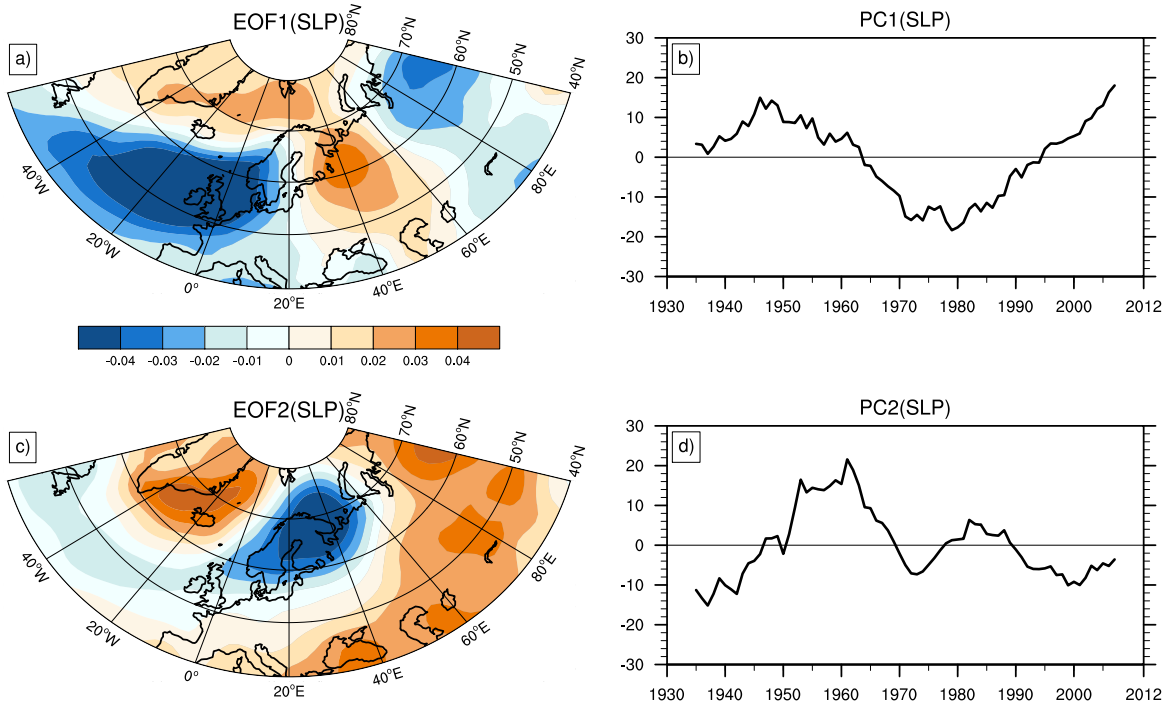

Fig. 2.7 a) EOF1 and c) EOF2 of SLP in summer (11 year running mean) in hPa over the region shown in the figure for the period 1930-2012. EOF1 and EOF2 explain 37% and 29% of the total variance respectively. b) and d) are the corresponding PC1 and PC2 of the EOFs.

The principal mode shows the east-west wave like response in SLP similar to the SLP composites in figure 4.3 (Fig 2.7a). The time series of the principal mode explains 36% of the total variance and exhibits multidecadal variations with negative values from 1960-1990 and positive values before 1960 and after 1990 (Fig 2.7b). Based on the spatial location, we name the principle mode as North-Atlantic-European East West (NEW) mode. The correlation of

the C-E European SAT index with the time series of the principal component of the North-Atlantic-European East West (NEW) mode is significant (r = 0.85). This analysis confirms that the first mode of SLP is associated to the multidecadal variations in the C-E European SAT. The second mode (Fig 2.7c) shows the characteristic north-south SLP structure of the SNAO in its negative phase, and explains 29% of the total variability. The temporal variations of the second mode (Fig 2.7d) is similar to Folland et al. (2009) and has no substantial relation with the multidecadal variations of C-E European SAT (r = -0.07). The same results are found after rotating the EOFs (not shown). Therefore, these two modes are robust over the NAE region.

We perform a SVD of geopotential height in vertical with respect to SLP to understand the vertical structure of the two multidecadal modes (NEW and SNAO) (Fig 2.8). Figure 2.8b,e show the heterogeneous pressure-longitude cross-section correlation maps of geopotential height over the NAE region averaged from 50°N to 60°N. The corresponding homogeneous SLP modes are shown in Fig 2.8a,d.

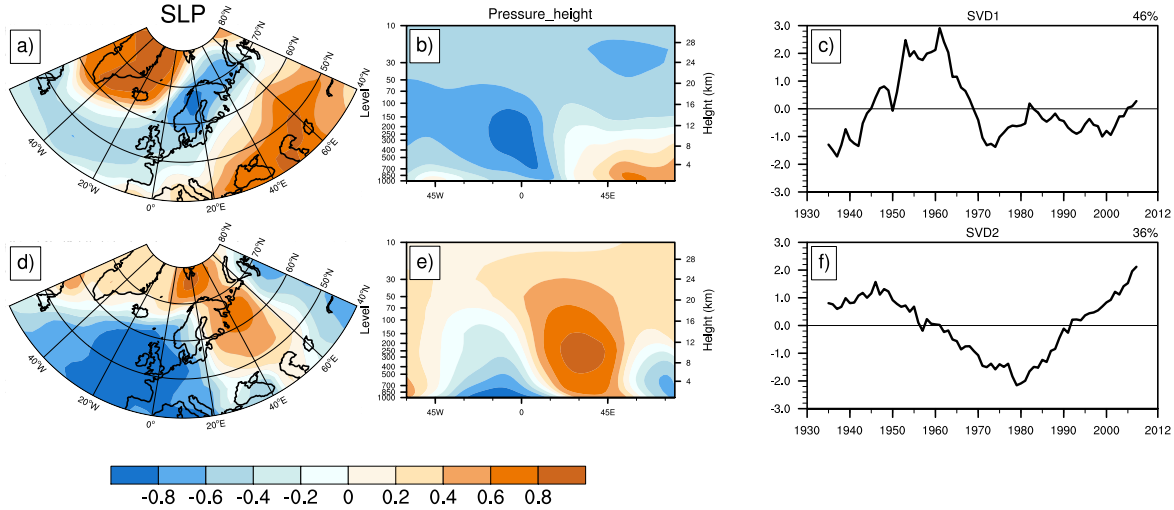

Fig. 2.8 SVD1 of a) SLP with b) pressure-longitude cross-section of geopotential height (11 year running mean) and SVD2 of d) SLP with e) pressure-longitude cross-section of geopotential height in summer (11 year running mean) over the respective regions for the period 1930-2012. The pressure-longitude cross-section of geopotential height is the average of the latitude extent 50°N - 60°N. SVD1 and SVD2 explain 46% and 36% of the total covariance respectively and the spatial patterns represent the correlation maps. c) and f) are the corresponding PC1 and PC2 of the SVDs representing the time series of the normalized expansion coefficients.

While considering the vertical structure, the first mode of SLP co-variability becomes the SNAO mode which explains 46% of the co-variance over this region. The second mode reveals the NEW mode which explains 36% of the co-variance. The equivalent barotropic structure of the SNAO mode kept the footprint of this mode on upper levels of the atmosphere and hence, the SNAO mode becomes the principle mode of co-variance. For the NEW mode, the low pressure anomaly at the surface over the north-eastern Atlantic is still present at 500 hPa but it diminishes considerably in magnitude from its strength at the surface which

is an indication of a linear baroclinic-like response to midlatitude surface heating (Kushnir and Held, 1996). Moreover, due to the baroclinic-like nature of this mode, it has weaker covariance in the upper atmospheric levels than SNAO mode and hence it becomes the 2nd mode of co-variance. Another interesting feature of the NEW mode is the downstream high-pressure anomaly which is enhanced considerably in magnitude in the mid atmospheric levels and it is surrounded by the two low pressure anomalies. The composite with respect to C-E European SAT Index resembles the same vertical structure (not shown). This vertical structure is indicating a blocking like condition related to the NEW mode. We further discuss about this blocking like feature while finding the impact of the NEW mode on European climate.

The previous studies suggest that in presence of a strong non-linear transient eddy forcing the direct linear response to surface heating can change largely from a baroclinic low pressure anomaly downstream to an equivalent barotropic high through a secondary circulation (Kushnir et al., 2002). The transient eddy forcing to the mean flow explains why the atmospheric response in winter is mainly barotropic (Czaja and Frankignoul, 2002). However, the forcing also depends on the climatological mean flow of the season (Peng and Whitaker, 1999). Hence, to confirm that the NEW mode is in accordance to the linear QG theory, we should get a negligible influence from the transient eddies in summer compared to winter.

The transient eddies affect the mean flow through eddy-heat flux and eddy-momentum flux. The eddy-heat flux is denoted by $v'T'$ where v' and T' are the 2-6 day band pass filtered component of the meridional wind and temperature field. The lower tropospheric eddy heat flux combined with the Coriolis force creates a secondary circulation which accelerates the surface westerly flow where the $v'T'$ is maximum. Fig 3.7a shows the composite of the eddy-heat flux at 850 hPa with respect to the time series of the leading EOF of multidecadal SLP variations in winter, the North Atlantic Ocsillation (NAO). The climatological mean eddy-heat flux (in black contours) shows its strong presence in the mid-latitude and hence it strongly affects the mean westerly flow and the Euro-Atlantic climate in winter. The composite shows that the positive phase of the NAO is related to the enhancement of the eddy-heat flux and it mainly drives the westerly flow more northward which supports the results by Woollings et al. (2014b). In summer, however, the climatology of the transient eddy-heat flux is much weaker than winter (black contours in Fig 3.7b). Moreover, the composite with respect to the NEW mode only shows eddy-heat flux with modest amplitude over the NAE region and it further weakens the climatology over the north-western Atlantic Ocean. Some negative values are seen north of the climatological mean. Over Europe, the magnitude is small and as we show in the next section, they are of an order smaller than the horizontal advection of heat. The same feature is seen in the composite with respect to C-E European SAT index (not shown).

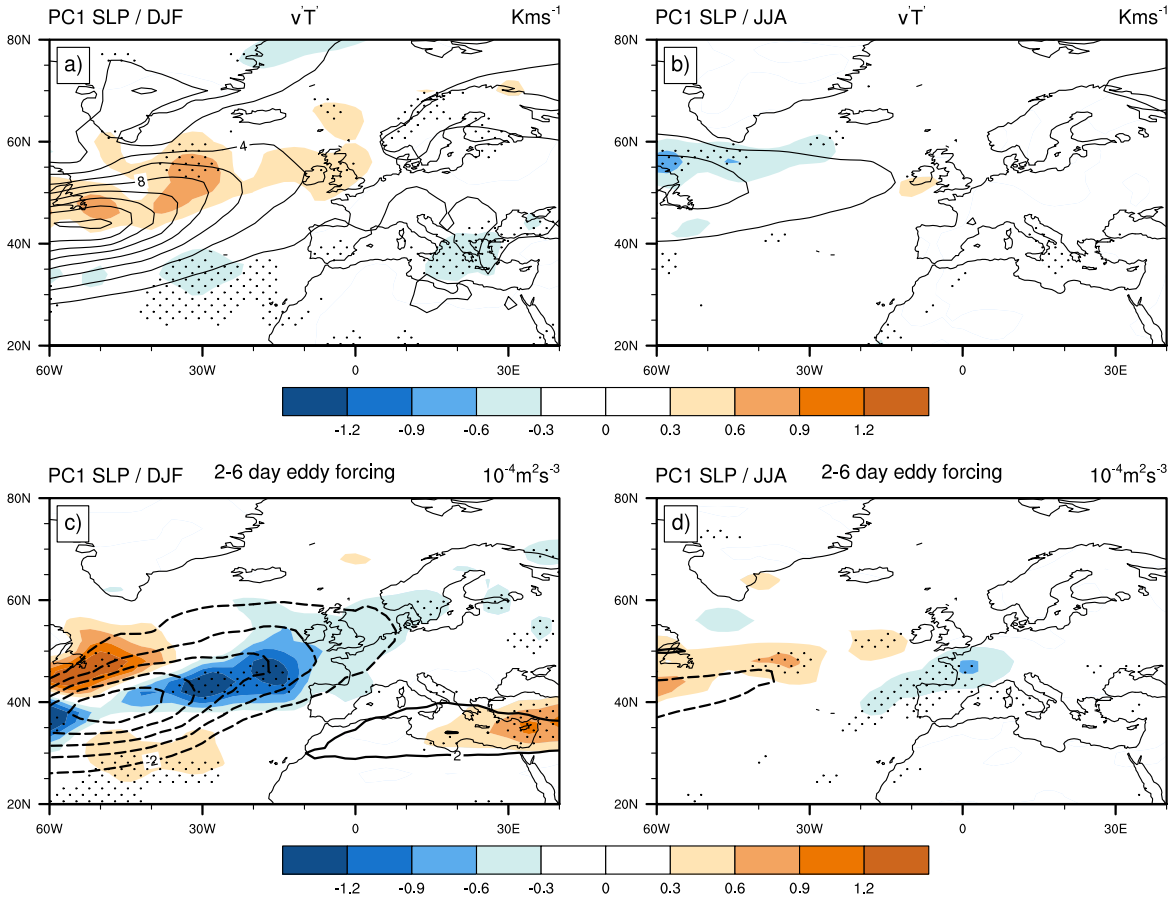

Fig. 2.9 a) The composite of 2-6 day 850 hPa $v'T'$ with respect to the PC1 of SLP EOF in winter (DJF, 11 year running mean). The EOF is constructed over the region 90°W to 30°E and 30°N to 90°N based on the study by Woollings et al. (2014a,b). The climatology is contoured from 4 to 10 with a spacing of 2 Kms^{-1}. b) Same as a) but the composites are with respect to the PC1 of SLP in summer from figure 7. c) Same as a) but the composite of 2-6 day eddy-momentum forcing at 250 hPa (**E**.**D**) in winter. Climatology is contoured from -10 to 10 with a spacing of 2 m^2s^{-3} and negatives contours are dashed. d) Same as b but for the composite of 2-6 day eddy-momentum forcing at 250 hPa (**E**.**D**) in summer. The dotted regions denote areas with significance at 95% level based on block-bootstrap test.

We further investigated the role of eddy-momentum flux by calculating **E**.**D** from the study of Raible et al. (2010). **E** is the E-vector from Hoskins et al. (1983) with the vector components $(v'^2 - u'^2)/2$ and $-u'v'$ where u' and v' are the 2-6 day band pass filtered wind components. **D** is the deformation vector of the time mean flow with the components $(U_x - V_y)$ and $(V_x + U_y)$ where U and V are the seasonal mean wind components. The scalar product of the **E** and **D** vector describes the exchange of the kinetic energy between the eddy and the mean flow (Mak and Cai, 1989). Negative values of **E**.**D** denote that eddy is transferring kinetic energy to the mean flow and positive values denote the opposite. The climatology of **E**.**D** at 250 hpa in winter shows that over the North Atlantic, eddy prominently provides energy to the background mean flow (Fig 3.7c). The composite of **E**.**D** in winter shows

that at the positive phase of NAO, there is a strengthening of the eddy-momentum forcing east and west to the climatology and weakening in the north-south direction. However, in summer the strength of the climatological eddy-momentum forcing itself is much weaker than in winter. The composite with respect to the NEW mode shows further weakening of the climatology in summer through positive anomalies of **E**.**D** which indicates baroclinic production (Fig 3.7d). However, over the western Europe, the composite shows rather weak but significant strengthening of eddy-momentum forcing. It could be a forcing from the baroclinic eddies associated with the downstream linear baroclinic response from the diabatic heating. Nevertheless, in absence of a strong climatological eddy forcing over this region, this localized eddy-momentum flux could not lead to resultant barotropic response. Presumably the same composite with respect to C-E European SAT index shows same feature (not shown).

In summary, these results suggest that at multidecadal time scales the east-west wave like SLP response, which is related to the multidecadal variations of C-E European summer temperature, has a linear baroclinic signature, which is in turn distinctively different from the SNAO and the winter NAO.

2.5 Impact of the NEW mode on European SAT

Having identified the NEW mode as the atmospheric pathway from AMV to the multidecadal variations of European summer temperatures, we proceed to analyze how the NEW mode influences the variations of European summer climate. As shown by the composites and principal components, a positive heat flux is associated with a negative SLP anomaly, which includes temperature advection at its eastern part. To examine the horizontal temperature advection related to the multidecadal variations of the C-E European SAT, we consider the linearized quasigeostrophic thermal energy equation in steady state (e.g. Bader et al., 2013; Hoskins and Karoly, 1981):

$$\bar{u}\frac{\partial \theta'}{\partial x} + v'\frac{\partial \bar{\theta}}{\partial y} + \omega'\frac{\partial \bar{\theta}}{\partial p} = \frac{Q}{C_p}\frac{\theta}{T} \tag{2.1}$$

where Q is the amount of heating, C_p is the heat capacity in constant pressure, θ and T are respectively the potential temperature and temperature at the surface of heating. $\bar{u}$, $\bar{\theta}$ represent the zonal mean of the zonal wind and potential temperature. The pressure is denoted by p. θ', v' and ω' are respectively the deviations of the potential temperature, meridional wind and vertical wind velocity from their zonal means. $\bar{u}\frac{\partial \theta'}{\partial x}$ and $v'\frac{\partial \bar{\theta}}{\partial y}$ are the zonal and meridional temperature advection terms. In this equation, we have assumed the transient eddy term to be small compared to the advective terms. Indeed a quantitative analysis for the preferred regions indicates that eddy heat flux is small compared to the major advection terms (Table 2.1). Further, $\omega'\frac{\partial \bar{\theta}}{\partial p}$ is the vertical temperature advection which could also be negligible since its magnitude is much smaller than the horizontal temperature advcetion

over the diabatic heating region (Table 2.1). $\frac{Q}{C_p}\frac{\theta}{T}$ is the diabatic heating term, where in the northern hemisphere, the $\frac{\partial\bar{\theta}}{\partial y}$ is negative as the meridional temperature gradient is negative, and v' should be negative to balance the diabatic heating $\frac{Q}{C_p}\frac{\theta}{T}$. Therefore, the subpolar colder wind should be driven towards the heating region. The way to advect this subpolar colder wind is through the formation of a low east of the heating. This low will drive the subpolar air towards the heating region (west of the center of the low pressure) due to formation of the low pressure.

Table 2.1 The magnitude of the composite of zonal ($\bar{u}\frac{\partial\theta'}{\partial x}$), meridional ($v'\frac{\partial\bar{\theta}}{\partial y}$), vertical ($\omega'\frac{\partial\bar{\theta}}{\partial p}$) temperature advection terms from Eq. 1 and the advection of eddy heat flux ($\frac{\partial(v'T')}{\partial y}$) with respect to C-E European SAT index, averaged over the North-Western Atlantic diabatic heating region a) 45°N - 55°N, 40°W - 50°W and over the BE region b) 50°N - 60°N, 0°E - 15°E with units K/day for summer. All terms are calculated at the level 850 hPa.

Region	$\bar{u}\frac{\partial\theta'}{\partial x}$	$v'\frac{\partial\bar{\theta}}{\partial y}$	$\omega'\frac{\partial\bar{\theta}}{\partial p}$	$\frac{\partial(v'T')}{\partial y}$
a)	0.02	0.13	0.005	0.02
b)	0.06	0.22	0.19	0.001

2.5.1 Temperature Advection

The composite of the 850 hPa meridional temperature advection ($v'\frac{\partial\bar{\theta}}{\partial y}$ of Eq. 1) with respect to the C-E European SAT index is shown in figure 2.10a. Positive values denote northward advection. Keeping in mind that $\frac{\partial\bar{\theta}}{\partial y}$ is negative in the Northern Hemisphere, the diabatic heating term ($\frac{Q}{C_p}\frac{\theta}{T}$) in equation 1 can be balanced only if v' is negative. Therefore the wind direction is from the pole towards the mid-latitudinal heating area resulting in a cold air advection. Over the north-western Atlantic region, indeed a south-ward temperature advection is identified. The area of this cold air advection coincides with the region of positive heat flux from the ocean. The meridional temperature advection over this region is of magnitude $\sim 0.1 - 0.2$ K/day which is comparable to the diabatic heating rate over this region. Additionally, table 2.1 shows the averaged magnitudes for composites of the advection terms from equation 1 and advection from transient eddy heat flux ($\frac{\partial(v'T')}{\partial y}$) over the diabatic heating region (45°N - 55°N, 40°W - 50°W). The meridional temperature advection is clearly the dominant term compared to all the other advection terms. Hence, we can say that the cold air advection mainly provides the atmospheric counterpart to balance the diabatic heating; in accordance with the linearized quasigeostrophic thermal energy equation (Eq.1).

We further identify a north-ward temperature advection centered over the British Isles and the North Sea, bringing moist air through advection of the subtropical warmer air. The north-ward temperature advection is mainly causing the warming of the north-western European region through advection of the subtropical warmer air.

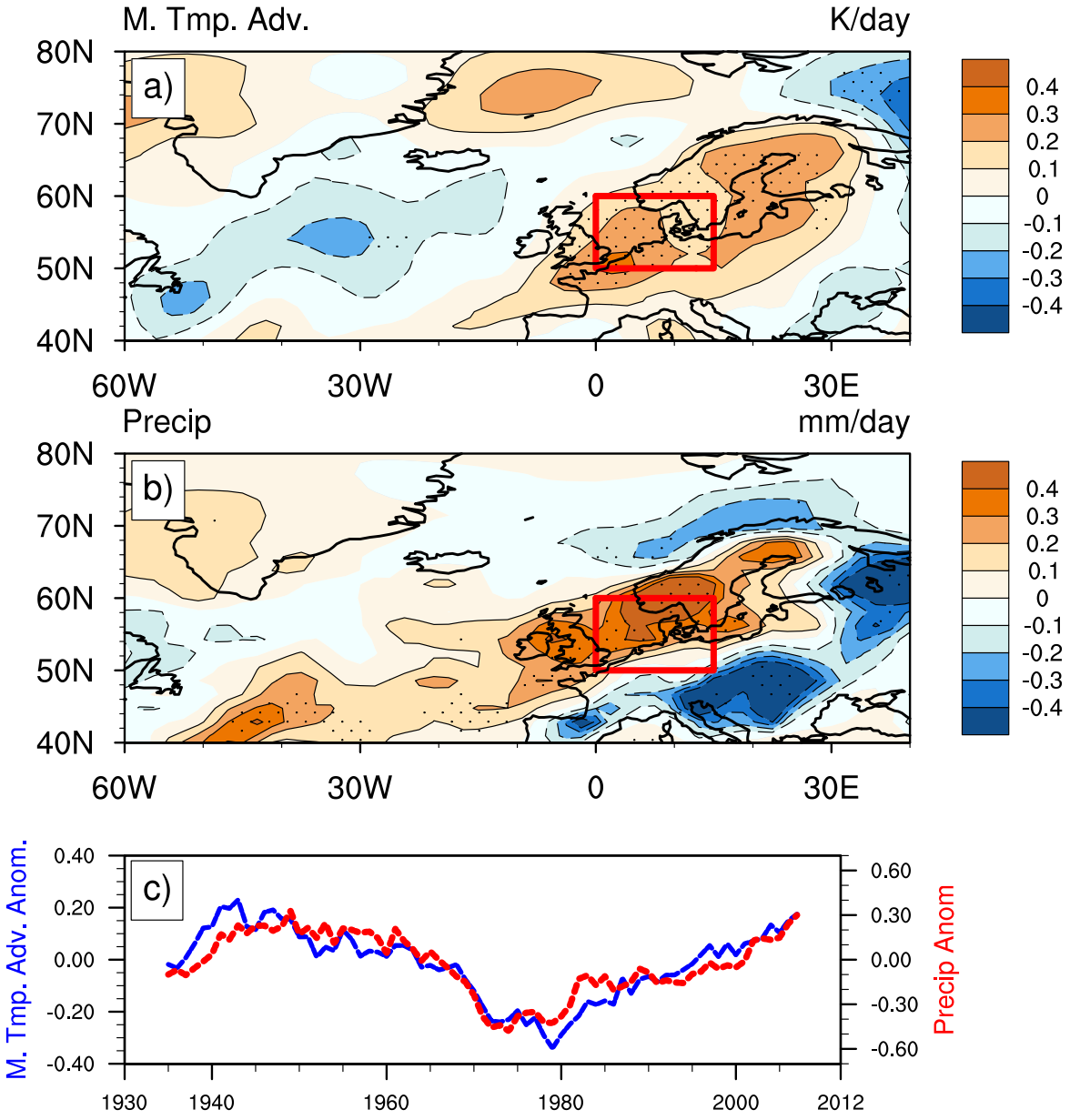

Fig. 2.10 Same as figure 6, but for a) meridional temperature advection $v' \frac{\partial \bar{\theta}}{\partial y}$ at 850 hPa, after Hoskins and Karoly (1981), where v' is the deviation of the meridional velocity from zonal mean and $\bar{\theta}$ is the zonal mean potential temperature and b) the total precipitation. Units for the temperature advection is [K/day] and for precipitation is [mm/day]. The dotted regions denote areas with significance at 95% level based on block-bootstrap test. c) The time series of the precipitation anomaly (red) and the meridional temperature advection anomaly (blue) averaged over the region shown by a red box in figure 7a) and b).

The composites of precipitation are associated with temperature advection and show increasing values over the BE region, in phase with the negative surface pressure anomalies and the respective advection, and vice versa (Fig 2.10b). The time series of the averaged precipitation and the meridional temperature advection over the BE region, show similar variations at multidecadal time scales (Fig 2.10c), and are significantly correlated (r= 0.9). Dong et al. (2013) suggested a relation of multidecadal variations of storm tracks with the precipitation over the same region. Our results suggest that these variations of storm tracks are basically the manifestation of the NEW response which change the pressure response over this region at multidecadal time scales.

The composite of the meridional temperature advection displays major warm air advection over north-western Europe rather C-E Europe, where we identify strong multidecadal variations of temperature. Hence the temperature advection is not directly explaining the temperature variations over C-E Europe.

2.5.2 Atmospheric Blocking

The composite of the outgoing long-wave radiation shows an intensive outward flux of long-wave radiation over the C-E European region (Fig 4.4a). This outward flux indicates a strong localized radiative heating of the C-E European region which also shows significant reduction in precipitation (Fig 2.10b). Moreover, the composite of 500 hPa geopotential height further shows a strong high pressure anomaly over the same region which altogether indicates a blocking high characteristic.

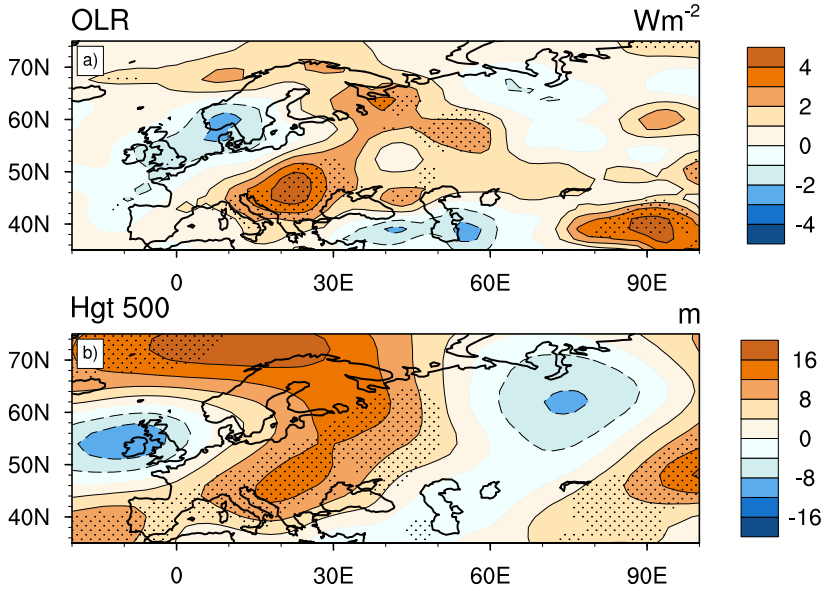

Fig. 2.11 Same as figure 6, but for a) upward long wave radiation (OLR) at the top of atmosphere and b) 500 hPa geopotential height. Units are [Wm^{-2}] for OLR and [m] for 500hPa height. The dotted regions denote areas with significance at 95% level based on block-bootstrap test.

The high pressure anomaly falls under the climatological location of the European blocking region (Masato et al., 2013). A blocking high leads to warmer and drier conditions for an extended period of time. This high pressure anomaly is surrounded by low pressure systems (Fig 4.4b), which is in line with the vertical structure of the NEW mode as shown in Fig 2.8e. This creates a southerly flow downstream of the high pressure which blocks the westerly winds and hence favoring a European blocking-like situation over NAE region with a high just above C-E Europe. Altogether, these findings suggest that the linear baroclinic response to diabatic heating which has wave like pattern downstream, eventually favoring omega blocking like situation over the NAE region with the high pressure anomaly situated above the C-E European region during the positive phase of AMV.

To further confirm the association of blocking over C-E Europe with the NEW mode, a SVD analysis of blocking frequency is performed with respect to SLP (Fig 2.12). The first mode of SVD shows the NEW mode which explains 55% covariance (Fig 2.12a). The second mode shows the negative phase of SNAO, explaining 25% covariance (Fig 2.12d). The blocking frequency with respect to the NEW mode shows enhanced blocking over the C-E European region (Fig 2.12b). Additionally, it shows reduction of blocking over the north-western Europe where we have seen strong temperature advection leading to variation of precipitation on multidecadal time scale. The variations in blocking frequency with respect to SNAO (SVD2) is much lesser than the SVD1 of blocking frequency (Fig 2.12e). It mainly shows the impact of SNAO over the southern Europe. Moreover, the time series of the PCs of the two SVDs are similar to the time series of the EOFs of SLP (Fig 2.12c,f). Therefore, these results confirm that the increase in blocking events over the C-E European region is indeed related to the NEW mode and is in turn leading to the positive temperature anomalies on multidecadal time scale.

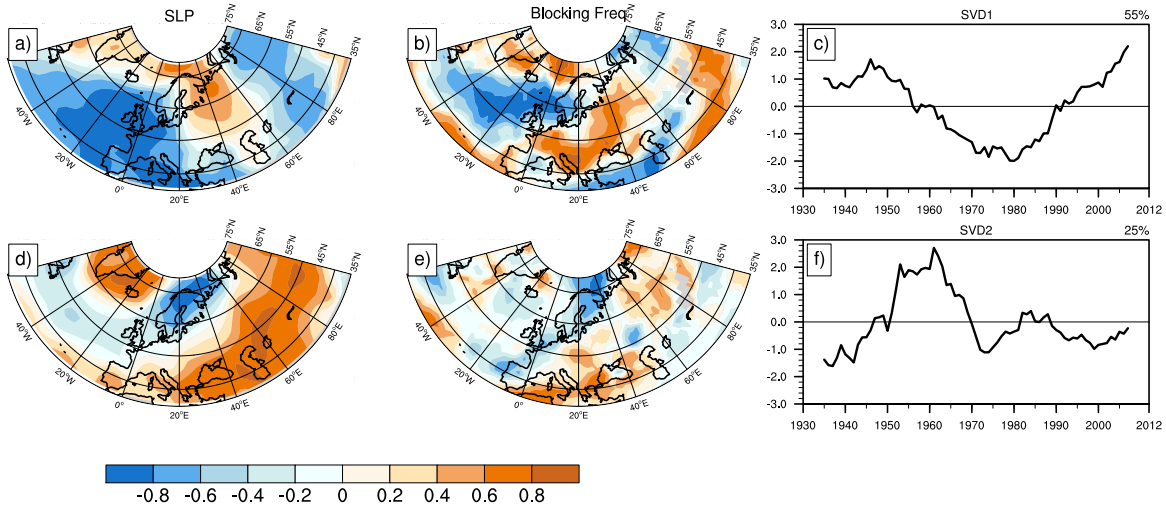

Fig. 2.12 SVD1 of a) SLP with b) blocking frequency (11 year running mean) and SVD2 of d) SLP with e) blocking frequency (11 year running mean) over the respective regions. SVD1 and SVD2 explain 55% and 25% of the total variance respectively and the spatial patterns represent the correlation maps. c) and f) are the corresponding PC1 and PC2 of the SVDs representing the time series of the normalized expansion coefficients.

2.6 Discussion

Here, we have presented an atmospheric pathway bridging the North Atlantic AMV-like SST with the European summer climate. The pathway emerges as a direct linear response to a diabatic heating in the extra-tropical North Atlantic and appears with an East-West-like structure further downstream. This is called the North-Atlantic-European East West (NEW) mode which is affecting precipitation over the BE region and alter the frequency of blocking-like situations over C-E Europe. The pathway is suggested to be a response to mid-latitude forcing and thus is complementary to the recent view of a tropical forcing of the multidecadal climate over the NAE region (Davini et al., 2015; Gastineau and Frankignoul, 2015; Hodson et al., 2010; Terray and Cassou, 2002).

Using 20CRv2, Gastineau and Frankignoul (2015) presented an influence from the tropics to the NAE climate in summer, similar to the processes describing the wintertime atmospheric response to AMV (Davini et al., 2015; Terray and Cassou, 2002). With a lead of 3 months (March-April-May, MAM) in SST, they performed maximum covariance analysis (MCA) with the 500hPa geopotential pattern in summer. Using the time series of the first mode and a regression analysis on the 200hPa velocity potential they showed a decrease in velocity potential over the tropics associated with large scale ascending motion over the tropical Atlantic positive SST anomalies. The extra-tropical climate is thus affected by the Rossby wave propagation. However, their analysis is based on seasonal means, which could have a different characteristic than our study on decadal means. Therefore, to be conclusive with our results, we repeat the cross covariance analysis based on seasonal as well as decadal means. On seasonal means, the regression analysis of velocity potential with the first mode of SVD is similar to findings of (Gastineau and Frankignoul, 2015) (Fig 13a). For the multidecadal time scale, the first mode of SVD MAM SST shows an expected AMV like SST pattern (not shown) and the time series of the first mode has a correlation of 0.9 with the C-E European SAT index. However, the regression of the time series of this first mode on velocity potential shows a much lesser amplitude of negative velocity potential compared to the analysis based on seasonal means (Fig 13b). Moreover, it is confined to the eastern tropical Atlantic ocean which is not in accordance to the previous findings regarding the tropical Atlantic influence over extra-tropics on multidecadal time scales (Davini et al., 2015; Hodson et al., 2010; Sutton and Hodson, 2007). These figures suggest that the influence from the tropics acting on the European summer climate is rather weak on multidecadal time scale in 20CRv2. This is also in line with the analysis of the transient eddy feedback on the mean flow, which is small during summertime (Fig 3.7b,d).

It should be noted that a previous study suggested a similar east-west wave like pattern in the upper tropospheric levels (200hPa), but on the seasonal time scale (Saeed et al., 2014). They also point out the differences in the impact of the east-west wave like pattern from SNAO on European summer precipitation. Given the great similarity of the upper tropospheric east-west wave like pattern with the NEW mode, it would be worth studying if there is any relation between these two features.

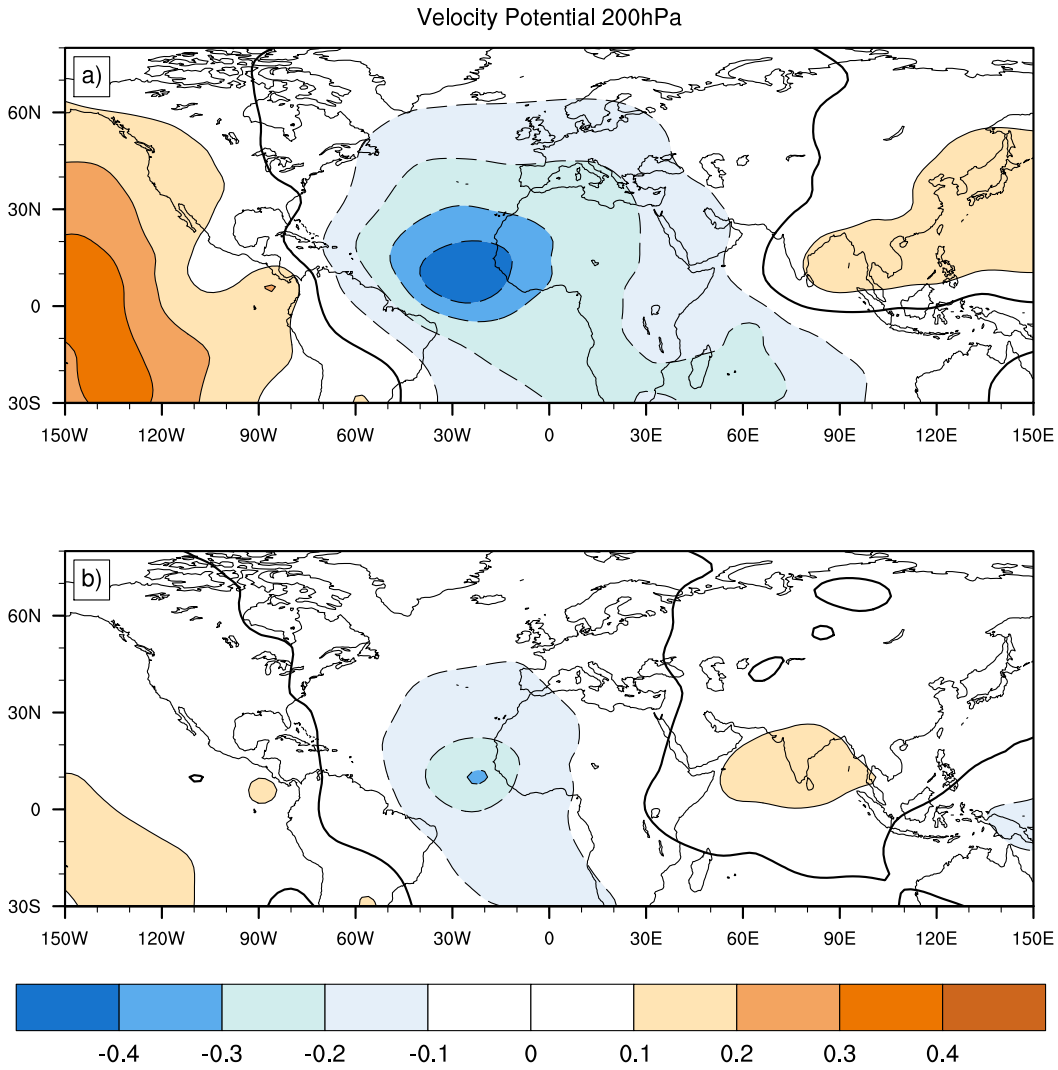

Fig. 2.13 a) Velocity potential at 200 hPa ($10^5 m^2 s^{-1}$) regressed onto the PC1 of SVD of interannual SST (MAM) and 500 hPa geopotential (JJA). b) Velocity potential at 200 hPa regressed onto the PC1 of SVD of multidecadal SST (MAM) and 500 hPa geopotential (JJA).

The analysis in this study is based on 20CRv2, for which there is large uncertainty in the quality of the data before 1930s (Fig 3b). This uncertainty limits our investigation to the last 83 years of data, which consists of only one full cycle of AMV. To understand the robustness and persistence of the atmospheric response from AMV, we must look into the General Circulation Models (GCM) to see whether we can reproduce the NEW response. However, previous studies show less promising results regarding the simulation of the observed AMV impact over the European region. Hodson et al. (2010) conducted a multi-model comparison experiment to investigate the effect of the multidecadal change of SST over the Atlantic Ocean on the regional climate. They investigated in 5 different atmospheric GCMs the changes in climate due to the changes in the North Atlantic SST between the warm phase from 1951-1960 to the cold phase from 1961-1990. In this analysis, Hodson et al. (2010)

found a good agreement among the models regarding the changes of temperature over North America. However, for temperature over Europe, they could not find a consistent change among the atmospheric models. This can be due to the atmospheric model misrepresentation of the teleconnection pathways. On the other hand, coupled GCMs show a substantial bias in the North Atlantic (Jungclaus et al., 2013). The too strong zonal structure of the North Atlantic current and associated distribution of water masses results in displacement of the diabatic heating and associated heat fluxes. As such, further investigation is required into the capability of the atmospheric stand alone models and also the coupled GCMs to verify the proposed hypothesis of the observed atmospheric pathway from North Atlantic SSTs to European summer climate by the NEW pattern.

The relevance of the North Atlantic multidecadal variations for the European summer climate further bears prospects for decadal climate predictions. The North Atlantic has been shown to be a key region for the prediction of climate on decadal time scales. Robust prediction skill has been established for various parameters, such as temperature and heat content (Doblas-Reyes et al., 2013; Kröger et al., 2012; Pohlmann et al., 2009). Prediction skill is further assessed for climate impacts, such as for the multidecadal variability of Atlantic tropical cyclones, which have been considered to origin from the sub-polar gyre region (Dunstone et al., 2011; Smith et al., 2010), or the European summer climate (Hermanson et al., 2014; Müller et al., 2012; Sienz et al., 2016). For the predictability of the European summer climate, however, the underlying processes are not yet understood. There has been some indication that the connections presented here could be relevant also for the assessment of prediction skill for European summers (Müller et al., 2012). In their prediction system prepared for CMIP5, only oceanic temperature and salinity fields are assimilated in the coupled model, with no atmospheric quantities used. Nevertheless, the correlation between the SLP and North Atlantic SST maintained an East-West-like structure similar to the NEW pattern proposed in this study. This signal, however, could not be maintained during the predictions, which may be due to the unresolved processed in the atmospheric component in their model and/or the strong bias in the North Atlantic.

And finally, during the recent positive phase of the multidecadal cycle of C-E European SAT, different parts of C-E Europe have encountered some of the warmest summers on record (Barriopedro et al., 2011; Founda and Giannakopoulos, 2009; Luterbacher et al., 2004; Schär et al., 2004). Increasing greenhouse gas concentrations and anthropogenic aerosols have been suggested to be the major drivers for this increase in the frequency of summer extreme events over the European region (Dong et al., 2016; Schär et al., 2004). However, we also find a considerable role of the multidecadal variations behind these extreme summers. To determine the frequency or return period of such extreme events, both multidecadal variations and the effect of green house gases need to be considered.

2.7 Conclusions

From our analysis of the 20CRv2 data on the mechanism behind the multidecadal variations of the C-E European summer SAT, we conclude:

- The SAT over the central to eastern (C-E) European region and the precipitation over the British Isles and north-western European (BE) region show similar multidecadal variations related to the Atlantic Multidecadal Variability (AMV) and associated surface heat fluxes over the north-western Atlantic.
- The surface heat flux provides the source of a shallow diabatic heating which in turn generates a linear baroclinic-like atmospheric response with a surface pressure low east of the centre of the heating. This low-pressure anomaly is indicative of a quasi-geostrophic response to the extra-tropical diabatic heating, in accordance with the linear quasigeostrophic theory.
- Further downstream, the SLP anomaly has an east-west wave-like structure over the European continent. A principal component analysis of the SLP (applying a 11 year running mean) confirms the east-west wave like NEW response pattern as the principal mode of the multidecadal variations. The NEW response is not related to the SNAO, which is the second mode of SLP variability over this region.
- The NEW response can cause strong multidecadal variations in the meridional temperature advection. The meridional temperature advection brings warm moist air from the subtropics to the extra-tropics and influences the precipitation over the BE region on multidecadal time scales.
- The east-west wave like response in SLP can further cause a high pressure anomaly over the European region. This high pressure response is enhanced at higher altitude (500 hPa) indicating a blocking-like situation. The analysis of the composites and the SVD analysis of the blocking frequencies confirm that the blocking over C-E Europe have a high chance of occurrence during a positive phase of the SAT index and is related to the NEW mode. Therefore, apart from the meridional temperature advection, the NEW response mainly affects the C-E European temperature on multidecadal time scales by creating an atmospheric blocking-like situation.

Chapter 3

Linking AMV and summer European climate in a coupled climate model

Abstract: The Atlantic Multidecadal Variability (AMV) is shown to affect the European summer climate through an associated atmospheric baroclinic response called North-Atlantic-European East West (NEW) mode as demonstrated in the 20th Century reanalysis (Ghosh et al., 2016). In addition, it is hypothesized that European summers are modulated by the barotropic response to the tropical Atlantic forcing (Gastineau and Frankignoul, 2015). Here, by using coupled climate simulations, we investigate the model response to AMV type of SST and its similarities and differences from the response in the reanalysis. In the control simulations, both low resolution (LR) and high (HR) resolution versions of MPI-ESM can simulate a similar AMV type of SST pattern like in 20th century reanalysis. The AMV of the HR configuration differs from LR such that higher anomalies are found in the extra-tropical branch of the AMV. LR is found to be more sensitive to the tropical branch of the SST and thus the North-Atlantic-European (NAE) climate is mainly influenced by the stationary Rossby wave response from the tropics. In HR, the impact of the tropical SST variations on the extra-tropics is weaker due to lesser eddy-mean flow interactions. However the NEW mode is not found in any of these control simulations.

3.1 Introduction

In chapter 2 we identified the observed atmospheric pathway between AMV and C-E European summer climate by an east-west wave like SLP pattern, named NEW mode (Ghosh et al., 2016). We showed that this observed mode is the result of a linear baroclinic response to diabatic heating in the north-western Atlantic Ocean. In this chapter, we investigate the atmospheric pathway between AMV and European summer climate in a coupled climate model and we try to find out how far the model response to AMV can replicate the characteristics of the observed NEW mode.

The atmospheric response from the AMV in the model over the surrounding regions in summer is exclusively investigated through idealized experiments where an AMV SST anomaly pattern is added to the climatological global SST, which is then used as a forcing of the atmospheric model (Sutton and Hodson, 2007, 2005). These experiments showed a robust linear response from the tropical branch of the AMV SST anomaly. The response was attributed to a combination of the off-equatorial Gill response to diabatic heating over the western tropical Atlantic due to increased precipitation and the northward shift of the Inter-tropical Convergence Zone (ITCZ) due to anomalous cross-equatorial SST gradient. The off-equatorial Gill response to diabatic heating generates stationary Rossby waves from the tropics which then propagate to the extra-tropics and influence the mid-latitude climate. However, this study did not show any relation of the AMV to NAE climate and specifically European summer climate where we have seen a prominent response in the reanalysis. This could be due to the non-linear characteristics of the extra-tropical climate, which kept the AMV impact on the European climate in summer unclear.

The summer atmospheric response to AMV is found to be similar to the winter response (Davini et al., 2015; Terray and Cassou, 2002). The response is related to the stationary Rossby wave generation from the diabatic heating in the western tropical Atlantic which increases the transient eddy feedback to the mean flow and shifts the mean position of the mid-latitude storm track equator-ward. The alteration of the mean storm track position influences the climate over the NAE region. However, our studies from reanalysis in summer showed that the eddy activity is much weaker in summer than in winter. Therefore, the summer response over the NAE region to tropical AMV SST anomalies could be different in summer than in winter. Moreover, we must also investigate if the model is able to capture the observed weakening of the transient eddy feedback in summer. Failing to capture the weakening can lead to stronger tropical influence in the model. Altogether, these results indicate that the summer mid-latitude response to AMV SST in the model is still unresolved. Clearer understanding of the model dynamics over this region is highly required.

Regarding the response from the multi-decadal variations of SST over the extra-tropical Atlantic Ocean, there are studies which indeed found a linear baroclinic response from the diabatic heating of the ocean as we have seen in the reanalysis (Kushnir, 1994; Kushnir and Held, 1996). However, their response was much weaker than observed. Further, it was stated that in winter the baroclinic nature of the response can turn into equivalent barotropic due to strong eddy-mean flow interaction (Kushnir et al., 2002). Even though the nature of the summer response under weaker eddy-mean flow interaction is still to be explored. Moreover, these studies did not account for the tropical branch of the SST anomalies, which might be more influential in determining the overall response of the AMV SST on NAE climate in the model. These evidences motivate us to further investigate the model response from the summer AMV SST and its link to European climate.

All the model experiments discussed above are based on prescribed AMV type SST in an AMIP type of setup. In the coupled model setup, only one study addresses the influence of the Atlantic Meridional Overturning Circulation (AMOC) on the summer NAE climate where AMOC induced SST pattern is shown to have resemblance with the AMV structure of

the coupled model (Msadek and Frankignoul, 2009). However, no study directly addressed the summer AMV response to the atmosphere in a coupled model setup, which could be mainly due to a large SST bias over the North Atlantic in the coupled model (Jungclaus et al., 2013). The climatological SST over the north western Atlantic in the Max Planck Institute Earth System Model (MPI-ESM) for both of its low resolution (LR) and high resolution (HR) versions shows a negative bias of magnitude greater than 4K compared to the observations (Fig 3.1). The negative bias is largest over the east of Newfoundland which is the main region for generating extra-tropical diabatic heating. The magnitude of the bias over that region could be large enough to suppress the extra-tropical response from the model AMV. However, there is no clear picture of how the spatial structure of the model AMV could be under this climatological SST bias. Moreover, a basic understanding of the impact of coupled model simulated summer AMV on the surrounding atmosphere would be an added knowledge in assessing the model characteristics which can additionally help improving the decadal prediction skill in the model. Therefore, we start our investigation of the summer AMV response with the coupled model MPI-ESM in this chapter and in the next chapter proceed towards the prescribed AMV SST type experiments.

3.2 Model, Experiments and Data

For the coupled model analysis, we use the MPI-ESM1.2 in low resolution (LR) and high resolution (HR) which consists of the atmospheric model ECHAM version 6.3 coupled with the oceanic model MPIOM version 1.6.2. The ECHAM 6.3 in spectral resolution of T63 (92x196) with 47 vertical levels and in spectral resolution of T127 (192x384) with 95 vertical levels are used for the LR and HR versions of the MPI-ESM, respectively. The improvements in the model physics in ECHAM6 from its previous version, ECHAM5, could be found in Stevens et al. (2013). The main changes are regarding shortwave radiative transfer with a revised surface albedo scheme, the land surface representation with interactive vegetation and the inclusion of the middle atmosphere in the default configuration. The updated version ECHAM6.3 is built upon the version ECHAM6.1 and the detailed description of the changes made can be found in Roeckner et.al. 2016 (in preparation). For the ocean model MPIOM, GR1.5 grid is used for the LR version which has two poles, one over southern Greenland and the other over Antarctica with a nominal resolution of 1.5 degrees implying a grid spacing of 15 km around Greenland to a grid spacing of 185 km around tropical Pacific. The HR version uses a tripolar quasi-isotropic grid at nominal 0.4° resolution for the ocean model which has been constructed following Murray, 1996. Both versions of the ocean model have 40 unevenly spaced vertical layers, ranging from 12 meters near the surface to several hundred meters in the deep ocean. The MPIOM model physics remained almost unchanged from its previous version and the details of the references regarding the ocean model physics and parameterizations can be found in Jungclaus et al. (2013). Ocean and atmosphere are coupled daily in LR and hourly in HR using Ocean Atmosphere Sea Ice Soil (OASIS3) coupler (Valcke et al., 2003).

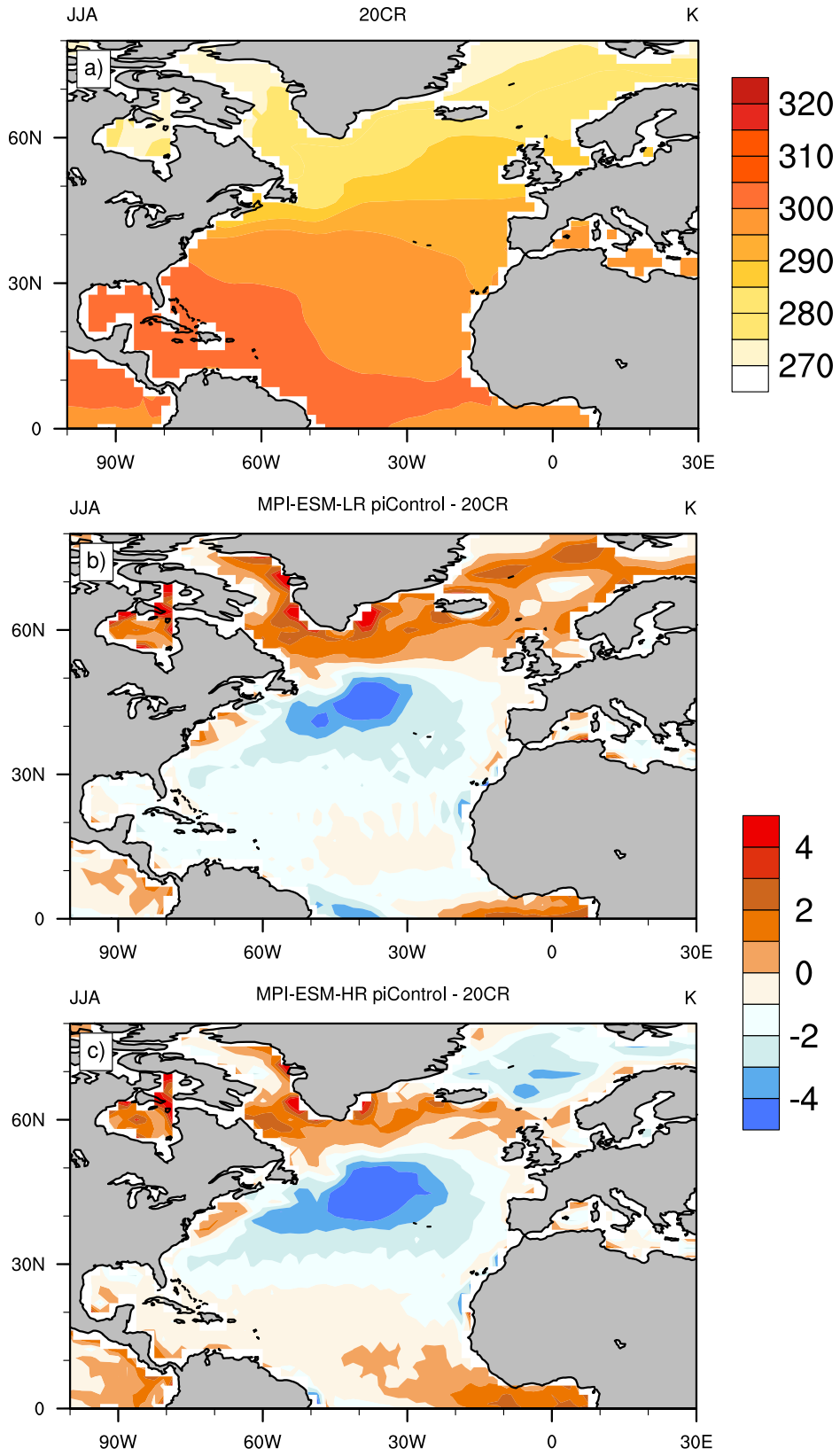

Fig. 3.1 a) Climatology of summer (JJA) sea surface temperature (SST) over the North Atlantic Ocean in the 20th century reanalysis v2 for the period 1871-2012. b) Climatological SST difference in summer of the coupled model MPI-ESM in low resolution (LR, T63) pre-industrial control simulation from 20 CRv2. c) Same as b) but for the MPI-ESM in high resolution (HR, T127). Units are in Kelvin [K]

The pre-industrial control (piCTRL) simulations of LR and HR are used for our coupled model study. The model setup and the forcing are similar to that described in Georgetta, et al., 2013. A total of 500 years is simulated for both the model resolutions. The forcings are set constant with the average of the 1944 to 1956 spectral solar irradiance and with the orbital parameters set to the year 1850 values. The greenhouse gas forcing is fixed to its 1850 values during the entire simulation and the monthly ozone concentration corresponds to the average of the year 1850 to 1860. The aerosol forcing accounts for only the tropospheric natural aerosols. There is no volcanic aerosol forcing.

From the 500 years of simulations, a time slice of 250 years is considered from both the LR and HR piCTRL simulations. We use daily outputs to analyse the transient eddy activity in the model. Therefore, in the case of LR, the last 250 years (3100-3349) of simulations, which consists the daily output data, is considered for our analysis. For the simulation with HR, the entire period consists of daily output data. However, while studying the AMV characteristic for the entire period, we see that as the time progresses there is strong non-stationarity in the model generated internal variability. This implies that the model produces prominent multi-decadal oscillations in the North Atlantic SST for the first half of the simulations and at the later half of the simulation the model generated North Atlantic SST variations is lesser in amplitudes with noisy oscillations. Therefore the first half (1850-2100) of the HR piCTRL simulation is considered for our analysis. 20CRv2 data is used as a proxy for observations to compare the model results (Compo et al., 2011).

3.3 The summer AMV in the coupled model

The summer AMV in the reanalysis shows a distinct horse-shoe like pattern in the SST anomalies over the North Atlantic (Fig 3.2a). There is a region of large SST anomalies over the north western Atlantic, east of the Newfoundland which is the region of the strong diabatic heating for the generation of the proposed baroclinic response as shown in the observations.

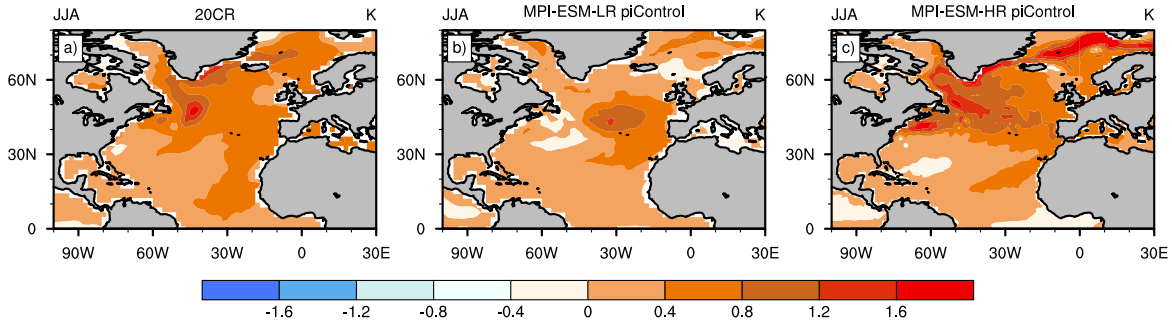

Fig. 3.2 The composite of the SST (11 years running mean) with respect to the time series of averaged 11 years running mean SST from 0°- 60°N and 90°W - 0°E for a) 20CRv2 b) LR piCTRL and c) HR piCTRL. Composites are based on the years above and below ± 1 standard deviation of the reference time series. Units are in kelvin [K].

In the piCTRL simulation of the LR, there is a similar SST anomaly but located over the central North Atlantic Ocean (Fig 3.2b). The piCTRL simulation of the HR shows more similarities in the spatial structure of the AMV with the reanalysis than the LR version (Fig 3.2c). It can simulate the intense SST anomaly over the north western Atlantic and the tropical section of the AMV. In spite of the cold SST bias in the model, this implies that the increase in resolution can help getting closer to the observed spatial structure and the variations of the AMV. However, we must keep in mind the effect of the cold SST bias which, in spite of the AMV SST variations, might lead to an overall colder mean state of the ocean SST over the extra-tropical region than observed and the effect of the extra-tropical SST variations might get suppressed in the coupled model. Therefore, we further proceed to investigate the atmospheric response related to the model simulated AMV in both LR and HR.

3.3.1 AMV related variations of European summer SAT and associated atmospheric pathways

In the piCTRL simulation of the LR version, negative surface temperature anomalies are located over the C-E Europe with respect to the positive AMV SST anomalies (Fig 4.2a). This SAT anomaly is entirely opposite from the observed anomalies in decadal mean SATs as in Ghosh et al. (2016) (Fig. 2.2a). Therefore LR piCTRL simulation could not represent the observed link between AMV and Europe in summer. The piCTRL simulation of the HR also shows negative SAT anomalies over the C-E-Europe with respect to the AMV. However, the negative SAT anomalies are much less pronounced than in LR (Fig 4.2b).

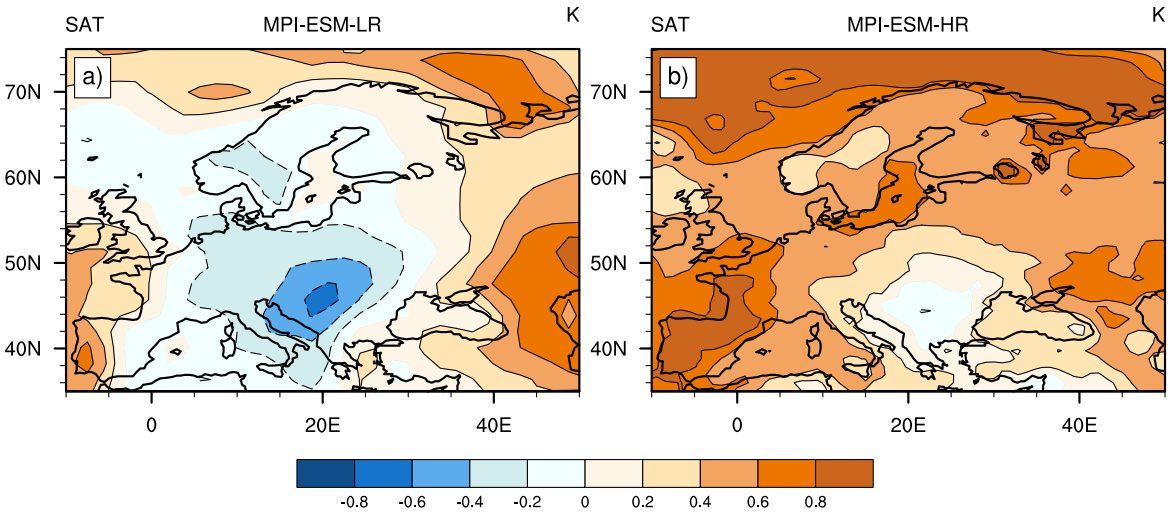

Fig. 3.3 The composite of the SAT (11 years running mean) with respect to the time series of averaged 11 years running mean SST from 0°- 60°N and 90°W - 0°E for a) LR piCTRL and b) HR piCTRL. Composites are based on the years above and below ± 1 standard deviation of the reference time series. The unit are in Kelvin [K].

The HR response in SAT seems to indicate a different characteristic of the AMV impact than LR. However, the SAT response still does not replicate the observed SAT response to AMV over C-E Europe. This implies that a different mechanism in the first place is present in the model and which is more prominent than in observations. In case of LR, the mechanism could be related to the tropics as described by Hodson et al. (2010). To further understand this mechanism, we analyze the sea level pressure (SLP) to understand the atmospheric responses related to the AMV in the model.

The composite of the SLP in LR shows a wave like response starting from the subtropics around 30°N with a surface low, and a subsequent high pressure north-east and then downstream alternating low and high pressure anomalies (Fig 4.3a). This wave like characteristic indicates a stationary Rossby wave like response from the tropics similar to those described by Terray and Cassou (2002). This response brings in a surface low over the C-E Europe and high pressure anomaly in its west which can drive the colder winds from the polar Greenland-Iceland regions towards the C-E European region and, hence, lead to colder temperatures (Fig 4.3a). However, in the case of HR, the SLP response shows a surface low located over the eastern extra-tropical Atlantic just east of the intense SST anomalies (Fig 4.3b). This surface low advects warmer air over the Western Europe and causes warming (figure 4.2b). Although, the magnitude of the surface low is much weaker than the observed north-east Atlantic surface low as in Ghosh et al. (2016) and it could not lead to the observed SAT response over the C-E European region. However, the response is clearly different from LR and it does not show a strong influence from the tropics. To fully understand these differences we examine the upper level (500hPa) geopotential height field together with SLP. This gives an indication of the vertical structure of the responses.

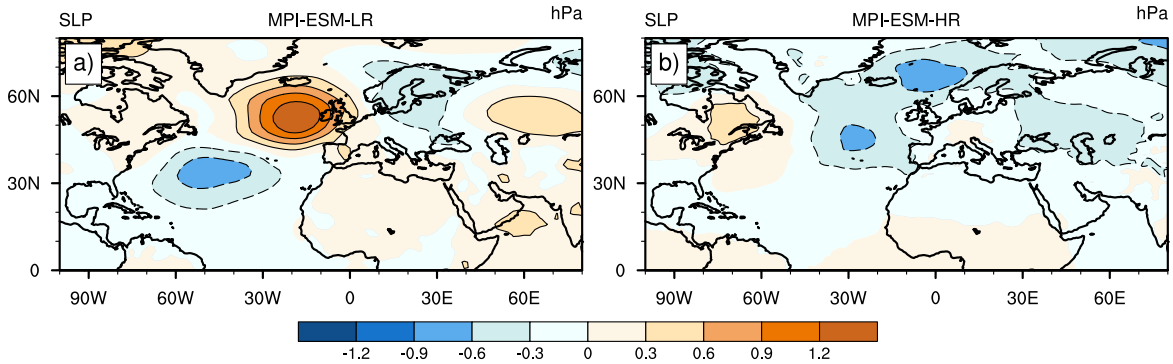

Fig. 3.4 Same as Fig 4.2 a) and b) but for sea level pressure (SLP). The units are in hPa.

The 500 hPa geopotential field shows a prominent wave like characteristic in the LR (Fig 4.4a) associated with AMV. This wave like response resembles the SLP response in figure 4.3a but with more enhanced magnitude which indicates a barotropic nature of the response, and thus supports our assertion about the nature of the response from the tropics as a stationary Rossby wave (similar to those shown by Terray and Cassou (2002)). In case of HR, the response is different from the LR with center of high pressure anomalies over the north-western Europe and over the Eastern North America (Fig 4.4b). The high over

the eastern North America seems to have barotropic nature as it shows an enhancement of the mild surface high over that region (Fig 4.3b). On the contrary, the geopotential height response over the Western Europe has more of a baroclinic characteristic due to the reversal of the anomalies from a surface low to upper level high. This suggests that the response from the tropical branch of the AMV SST has much weaker role on the NAE climate in HR than in LR. To clearly identify the generation of the tropical response in the models, we have a closer look into the upper level divergence field over the tropics which is indicative to the Gill type of response over the tropics (Gill, 1980).

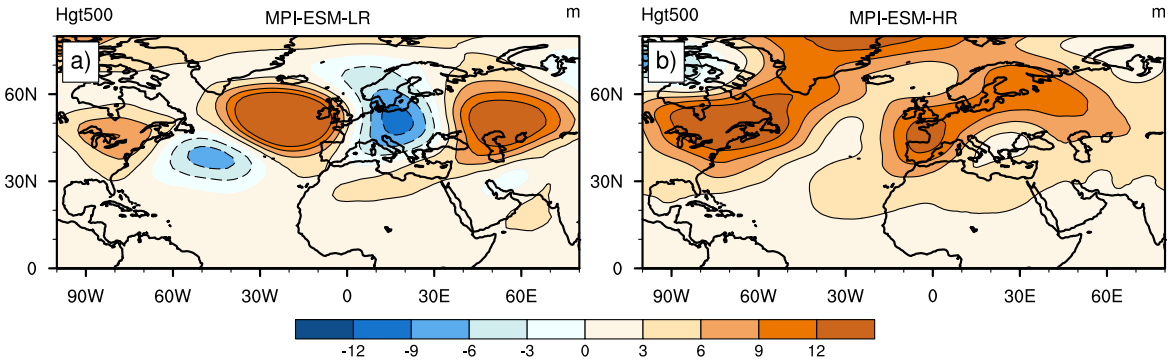

Fig. 3.5 Same as Fig 4.2 a) and b) but for 500 hPa geopotential height. The units are in meter [m].

The 200 hPa velocity potential is used to examine the upper level divergence as a response to the tropical convection. The velocity potential field shows a strong upper level divergence over the tropical Atlantic in case of LR (Fig 4.6a). This upper level divergence is expected in case of Gill type response to off-equatorial heating in the tropics which in turn leads to the stationary Rossby waves propagating to the extra-tropics. This supports our hypothesis about the wave like response emanating from the tropics which is seen in figure 4.4a.

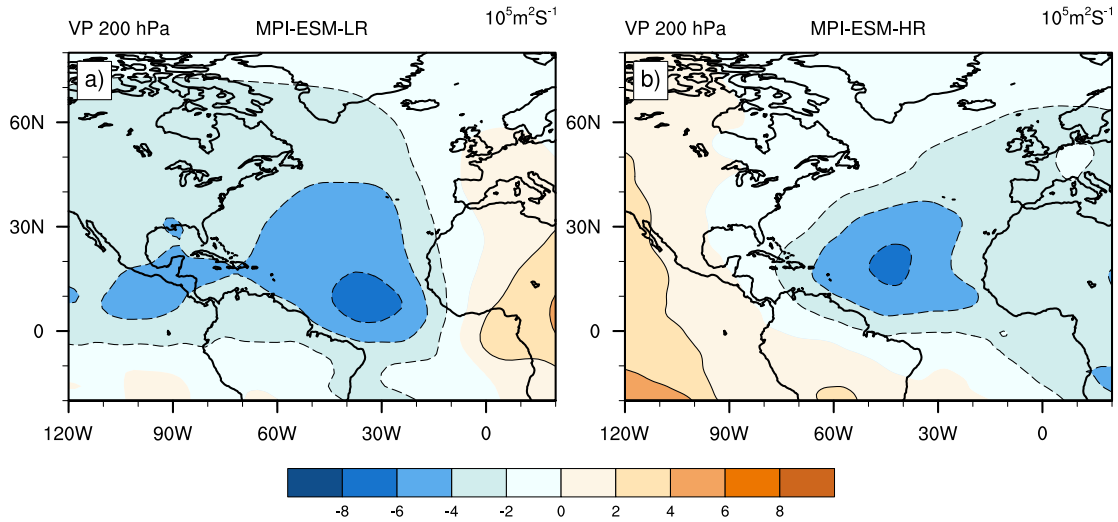

Fig. 3.6 Same as Fig 3.3 a) and b) but for 200 hPa velocity potential. The unit are in $10^5 m^2 s^{-1}$.

Similar to LR, the HR also shows an upper level divergence in the velocity potential field over the tropical region (Fig 4.6b). The center of the divergence is slightly north-westward than LR. Nevertheless, we did not see a wave like response from the tropics in the HR version (Fig 4.4b). This implies that, in spite of the off-equatorial heating in the tropics, the HR version is not able to generate the stationary Rossby wave response. According to Terray and Cassou (2002), a mandatory ingredient for the stationary wave propagation from the tropics is the transient eddy-mean flow interaction, which helps to sustain such response over the higher latitudes and gives the barotropic structure. Hence, an investigation on the eddy feedback strength in both versions of the model gives further insight regarding the different appearance of stationary Rossby waves in HR and LR.

3.3.2 Transient Eddy-Mean Flow Interaction

For understanding the eddy feedback with the mean flow in the coupled models we use the **E**.**D** as described in the section 2.4 of chapter 2. **E** is the E-vector from Hoskins et al. (1983) with the vector components $(v'^2 - u'^2)/2$ and $-u'v'$ where u' and v' are the 2-6 day band pass filtered wind components. **D** is the deformation vector of the time mean flow with the components $(U_x - V_y)$ and $(V_x + U_y)$ where U and V are the seasonal mean wind components. The scalar product of the **E** and **D** vector describes the exchange of the kinetic energy between the eddy and the mean flow (Mak and Cai, 1989). Negative values of **E**.**D** denote that eddy is transferring kinetic energy to the mean flow and positive values denote the opposite. Here, the magnitude of the **E**.**D** is 0.1 times of the magnitude shown in the figure 2.9d due to the lesser amplitude of the summer transient eddy feedback than in winter.

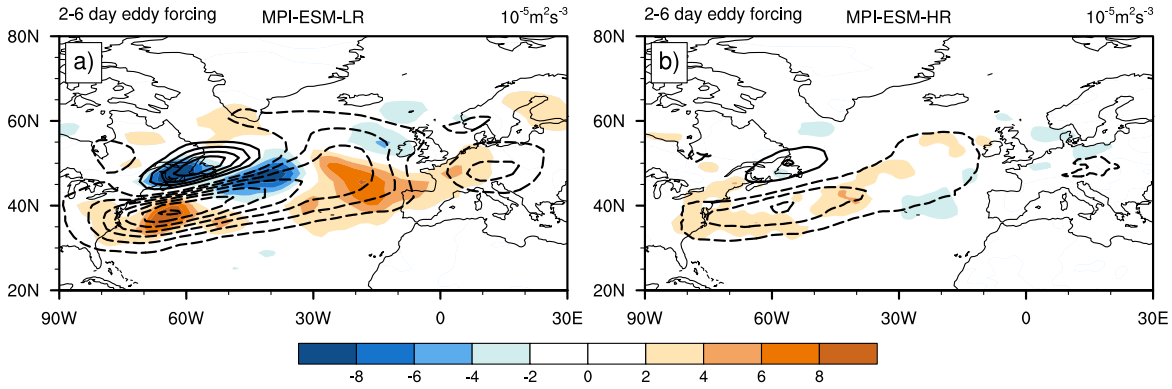

Fig. 3.7 Same as Fig 3.3 a) and b) but for the composite of 2-6 day eddy momentum forcing at 250 hPa (**E**.**D**) in summer. Climatology is contoured from -50 to 50 with a spacing of $5m^2s^{-3}$ and negative contours are dashed. Units are in $10^{-5}m^2s^{-3}$.

In the climatological mean, the LR shows a prominent transient eddy forcing to the mean flow over the North Atlantic region and over the central European region (Fig 3.7a). The composite with respect to the AMV shows a reduction of the transient eddy forcing over the eastern and western North Atlantic Ocean. There is an enhancement of the transient eddy

forcing in the central North Atlantic. Compared to the LR, the intensity of the climatological eddy forcing is less intense in the HR (Fig 3.7b). This result is in accordance to our previous findings in SLP and geopotential height fields which indicated a stronger eddy forcing on to the mean flow in the LR than HR. The stronger eddy forcing corresponds to a prominent stationary Rossby wave response from the tropics in LR which is not seen in HR.

3.4 Summary of the coupled model analysis

The coupled model analysis of the preindustrial control simulations reveal that in spite of a prominent North Atlantic SST bias of magnitude more than 4 K, both the LR and the HR versions of the MPI-ESM can simulate an AMV type SST pattern on multi-decadal time scales. Moreover, the AMV SST pattern in HR has a stronger extra-tropical branch of AMV SST than LR. For European SAT, however, none of the simulated patterns resembles those found in the 20CRv2. The LR shows a large negative SAT anomalies over the C-E Europe in accordance to positive phases to the AMV, which is opposite to what is observed. In case of the HR version, there still are negative anomalies over central Europe, but less pronounced than in the LR configuration.

Further analysis of the SLP, geopotential height at 500 hPa, and 200 hPa velocity potential field reveal that the negative SAT response over the C-E Europe in the LR configuration is due to a prominent stationary Rossby wave response which emerges from the tropics and which favors the polar wind advection that enters into C-E Europe. The stationary Rossby wave response from the tropics is much more reduced in the HR configuration, where the transient eddy-mean flow feedback is much weaker compared to the LR configuration. Such transient eddy feedback is shown to be crucial for sustaining and propagating tropical response to extra-tropics (Terray and Cassou, 2002).

From our coupled model analysis, one outstanding fact is that both versions of the coupled model could not show a linear baroclinic like response from AMV SST, as seen in 20th Century reanalysis. In case of LR, this is due to the prominent transient eddy feedback which retains the stationary Rossby wave response from the tropics over the extra-tropics. Additionally, for both HR and LR versions, the large climatological SST bias in the coupled model over the extra-tropical North Atlantic Ocean could restrict the extra-tropical branch of the AMV SST to produce effective diabatic heating. Therefore, to overcome this effect, we proceed to perform a set of AMIP type experiments using the LR version of the model, in which the observed AMV type SST pattern is added to the observed climatological SST and then used as a boundary condition.

Chapter 4

Atmospheric pathway between AMV and European summer climate in sensitivity experiments

Abstract: The coupled models have a strong SST bias in the North Atlantic which may restrict the model and associated heat fluxes to produce the observed NEW mode. Therefore we conducted AMIP-like sensitivity experiments with prescribed observed AMV type SST pattern, using the atmospheric component of the MPI-ESM-LR, ECHAM version 6.3. The results from the experiments reveal that in the positive phase of the AMV, the North-Atlantic-European (NAE) climate is mainly influenced by the tropical branch of the AMV. Here a stationary Rossby wave response from the tropics is associated with negative surface air temperature (SAT) anomalies over the C-E Europe, which is opposite to what is found in the case of decadal means in the re-analysis. However, in the case of the negative phase of AMV, the NAE climate is mainly governed by the extra-tropical branch of SST through a baroclinic-like response and negative SAT anomalies over C-E Europe. This is similar to what is found in Ghosh et al. (2016). Hence, the model with the AMV type of SST forcing can simulate the observed baroclinic response, but only in the negative phase of the AMV. For the positive phase, in agreement with the previous findings, the model is very sensitive to the tropical branch of the AMV SST.

4.1 Introduction

The nature of the AMV and its impact on the European summer climate in a coupled model is discussed in the chapter 3 and we could not see the replication of the observed link between AMV and European summer climate. However, we have seen that the coupled models have a strong climatological SST bias over the extra-tropical Atlantic Ocean which might restrict the models to reproduce the AMV associated heat fluxes in the North Atlantic and subsequent atmospheric pathway. To overcome the climatological SST bias, we proceed towards Atmospheric Model Inter-comparison Project (AMIP) type of experiments, where the atmospheric component of the coupled model is forced with prescribed observed AMV-type

SST pattern and then investigate the ability of the model to simulate the observed response from AMV to European summer climate.

Nevertheless, as mentioned in the previous chapter, the AMIP-type experiments with AMV SST forcing are already used to study the atmospheric response during summer (Sutton and Hodson, 2007, 2005). Those experiments are conducted with the AMV SST forcing separately applied on the tropical (10°S-30°N), extra-tropical (30°N - 70°N) and combining the tropical and extra-tropical parts (10°S-70°N), for both the positive and the negative AMV phases. Over the midlatitude region, the results from those experiments have shown an equivalent barotropic vertical structure of the geopotential height in the positive AMV phase and a baroclinic structure in the negative AMV phase. This indicates an overall nonlinear response to AMV SST. The positive phase response is indicated to be linked with the stationary Rossby wave emanating from the tropical part of the AMV SST. However, the negative phase response was not attributed to any mechanism, which we hypothesize as the observed baroclinic response from mid-latitude AMV SST (the NEW mode as shown in Ghosh et al. (2016)). This would imply that the model is able to simulate the observed NEW response only in the negative phase of AMV. For the positive phase of AMV, a strong response from the tropical branch of the AMV SST could prevail in the model which we do not find in the reanalysis. However, a rigorous analysis is still lacking to plausibly confirm our hypothesis about the impact of the tropical AMV SST in the positive phase and the role of extra-tropical AMV SST in the negative phase over the NAE region.

Many studies focused mainly on the impact of the tropical branch of the AMV SST on the surrounding continents (e.g. Hodson et. al. 2010). As an example Hodson et al. (2010) used 5 atmospheric GCMs and performed idealized simulations with the forcing of averaged positive AMV SST from 1951 to 1960 and averaged negative AMV SST from 1961 to 1990. The simulations are different from the previous idealized simulations in using seasonally varying AMV SST anomalies such as Rodwell et al. (1999). Hodson et al. (2010) revealed a consistent impact from the tropical branch of the AMV SST to the northern part of South America and over the United States. The response was attributed to a combination of the off-equatorial Gill response to diabatic heating over the western tropical Atlantic due to increased precipitation and the northward shift of the Inter-tropical Convergence Zone (ITCZ) due to anomalous cross-equatorial SST gradient. The off-equatorial Gill response to diabatic heating is the reason of the stationary Rossby wave generation from the tropics which then propagates to the extra-tropics and influences the mid-latitude climate. However, Hodson et al. (2010) did not show any linear robust relation of the AMV to NAE climate and specifically European summer climate, where we have found a prominent response in the reanalysis. Hence, a thorough analysis of the non-linear characteristics of the mid-latitude response to AMV is undertaken which can provide us with more insight about to which extent the model can reproduce the observed pathways.

4.2 Experimental setup

The atmospheric component of the MPI-ESM, ECHAM6.3 is used for the sensitivity experiments. We use the LR version of the model with spectral resolution of T63 (92x196) and with 47 vertical levels. For having the base climate state, we run a control simulation with the monthly global climatological SST forcing. The monthly climatological SST conditions are derived by using Hadley center SST data for the period 1870 to 2014 (Rayner et al., 2003). This simulation is performed for 50 model years where the monthly varying observed climatological SST forcing has been repeated every year. Hence the 50 years of simulations can be considered as 50 sample members.

Next, a set of experiments were performed, where the monthly AMV-like SST anomaly pattern is added on top of the climatological SST. The monthly AMV-like SST anomaly pattern is prepared using the same Hadley center SST data, spanning from 1870 to 2014 (Rayner et al., 2003). For this, we first constructed the AMV index for each month. The monthly AMV index is then defined as the 11 year running mean time series of the averaged detrended North Atlantic SST anomalies over the region 35°N - 50°N. This region is selected as a representative of the AMV index by following the study of Gulev et al. (2013). Further, the AMV SST anomaly patterns are constructed by making positive and negative composites over the North Atlantic Ocean based on the AMV index. The positive and negative composites are the averaged detrended SST anomaly states of all those years when the AMV SST index was above and below + 1 and - 1 standard deviation, respectively. The positive and negative composites are referred to as the AMV SST positive and negative phases in the experiments.

For the AMV sensitivity experiments we choose several regions. The AMV SST anomaly pattern has first been applied from 0°latitude to 60°N, which is referred as "ENTIRE" hereafter. Due to the presence and variations of the seas-ice, we mask out the regions further than 60°N by applying zero weighting. The AMV SST anomaly pattern is further multiplied by a factor of 2 to increase the signal to noise. However, outcomes of the simulations are scaled by a factor of 1/2 for comparing with the observations. This procedure is in line with the previous studies, where the anomaly patterns are inflated even 4 times from their observed values (Sutton and Hodson, 2007, 2005). The averaged summer (JJA) AMV SST anomaly pattern for the positive and negative phases are shown in figure 4.1a,d.

To understand which part of the AMV SST has a greater impact over the NAE climate, further experiments are conducted by adding the AMV SST pattern for only over the extra-tropical North Atlantic (30°N-60°N, "EXTRA-TROP") and the tropical North Atlantic (0°-30°N, "TROP") respectively. A cosine squared smoothing is applied for continuity in the SST gradient at the edges of the added AMV SST pattern. The respective AMV SST anomaly patterns used for the summer months over the EXTRA-TROP and TROP case for both positive and negative phases are shown in figure 4.1b,c,e and f. Each of these experiments is conducted for 50 model years where for each year, the same seasonally varying AMV SST anomaly imposed global climatological SST pattern is repeated.

The atmospheric response to a certain AMV SST anomaly forcing is defined as the difference of the 50 year averaged response of the field in AMV SST forced experiments from the 50 year averaged response of the field in control experiment. Further, we perform a student t-test at each grid point to understand if the atmospheric response in AMV forced experiment is significantly different from the response in the control experiment at the 95% level.

For being consistent with the observational study in chapter 2, the 20th century reanalysis has been used to evaluate the simulated atmospheric responses from the positive and negative AMV forced experiments. The positive and negative phase composites have been constructed using the C-E European SAT index as defined in chapter 2 (black line, Fig 2.2b) and these composites are defined as the average anomalous response of those years when the C-E European SAT index are above and below the zero line, respectively. Due to the close association of the C-E European SAT index with the AMV index for summer in the 20CRv2, the composites would also represent positive and negative phase atmospheric responses with respect to AMV index.

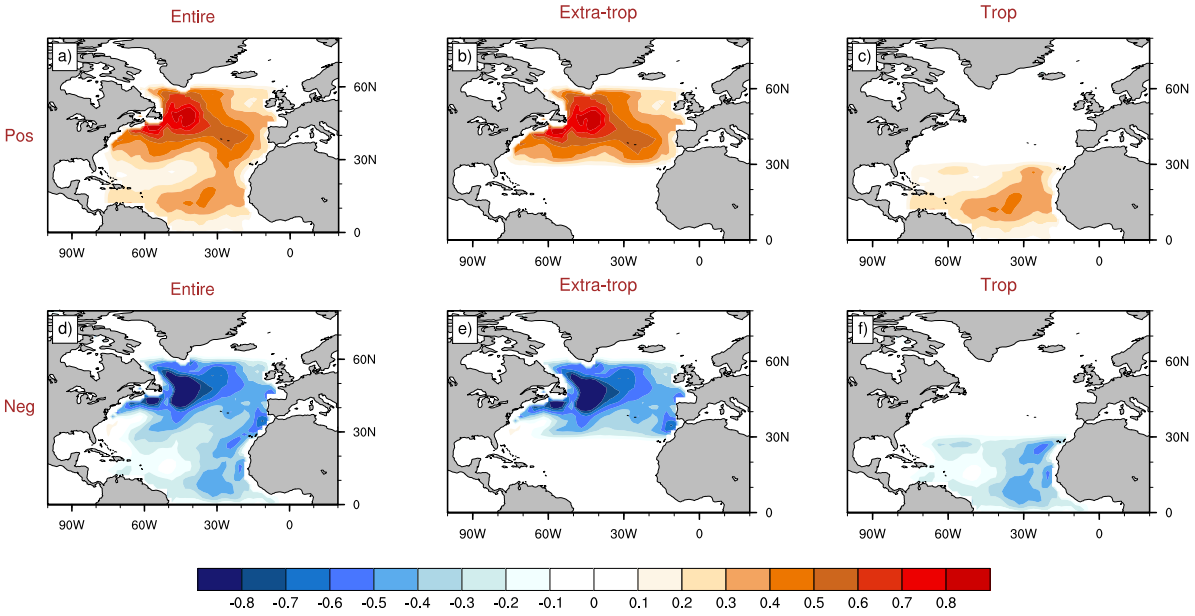

Fig. 4.1 AMV SST anomaly pattern averaged for the summer months (JJA) in positive phase for a) Entire North Atlantic, b) Extra-tropical North Atlantic c) Tropical North Atlantic Ocean and d), e) and f) are the same for the negative phase. See section 4.2 for explanation of the procedure to create the patterns. The units are in Kelvin [K].

4.3 Surface Air Temperature

The SAT response to the ENTIRE, EXTRA-TROP and TROP experiments for both positive and negative phases are shown in figure 4.2a-f. For the positive AMV phase of the ENTIRE

experiment, the C-E European region shows negative SAT anomalies (Fig 4.2a). This response is completely opposite to what we have expected from the observational study in Ghosh et al. (2016) (Fig. 2.2a). In TROP experiment, we find a similar strong negative SAT anomaly over the C-E European region with respect to the positive AMV phase (Fig 4.2c). The EXTRA-TROP experiment also shows negative SAT anomaly response over the C-E Europe (Fig 4.2b). However, it is much lesser in amplitude than the response from the TROP experiment. These results imply that for the positive AMV phase, the response in the model over the C-E Europe is opposite than what is observed and the main contributor is the tropical branch of the AMV SST. This could be due to the inability of the model to simulate the observed NEW response to the positive extra-tropical AMV SST anomalies. Further details regarding these inferences are shown in the following sections.

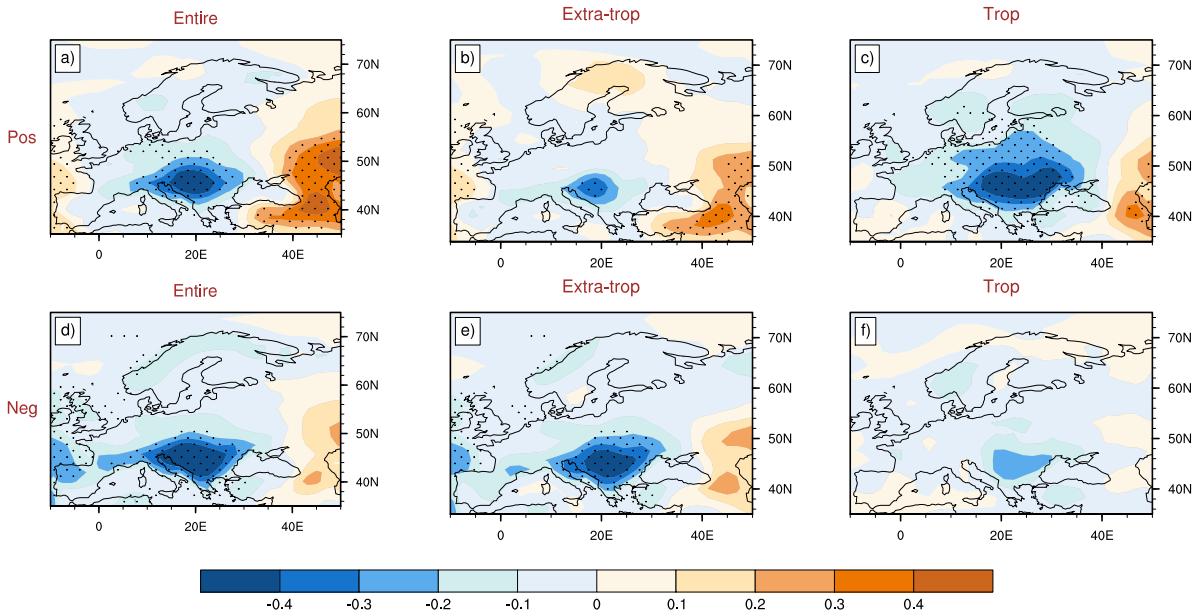

Fig. 4.2 The SAT response from the AMV SST anomaly patterns shown in figure 4.1 averaged for the summer months (JJA) in positive phase for a) Entire North Atlantic, b) Extra-tropical North Atlantic c) Tropical North Atlantic Ocean and d), e) and f) are the same for the negative phase. See section 4.2 for explanation of the procedure to create the patterns. The dotted regions denote areas with significance at the 95% level. The units are in Kelvin [K].

For the negative AMV phase, the ENTIRE experiment also shows negative SAT anomalies over the C-E European region (Fig 4.2d). During this phase, this response however is similar to what we expect from the observations (Ghosh et al., 2016). The EXTRA-TROP experiment also shows similar negative SAT anomaly response over the C-E Europe with the same amplitude as in the ENTIRE experiment (Fig 4.2e). The TROP experiment also shows negative SAT anomaly response, which is however not significant (Fig 4.2f). Therefore, in the negative AMV phase, the response over the C-E Europe in the model resembles the observed response emerging from the extra-tropical branch of the AMV SST anomaly. These results

indicate that the model could be able to generate the NEW response to the extra-tropical AMV SST anomalies at least in the negative phase.

We now further investigate the atmospheric pathways for the positive and then the negative phase for all the experiments, to identify the responses and hence understand the characteristics of the processes related to the response.

4.4 Atmospheric pathways during the positive AMV phase

4.4.1 Sea levels pressure and vertical structure

The SLP response in the TROP, EXTRA-TROP and ENTIRE experiments for the positive AMV phase is shown in figure 4.3a-c. For comparison, the positive phase composite response with respect to C-E European SAT index from the 20CRv2 is shown in figure 4.3d.

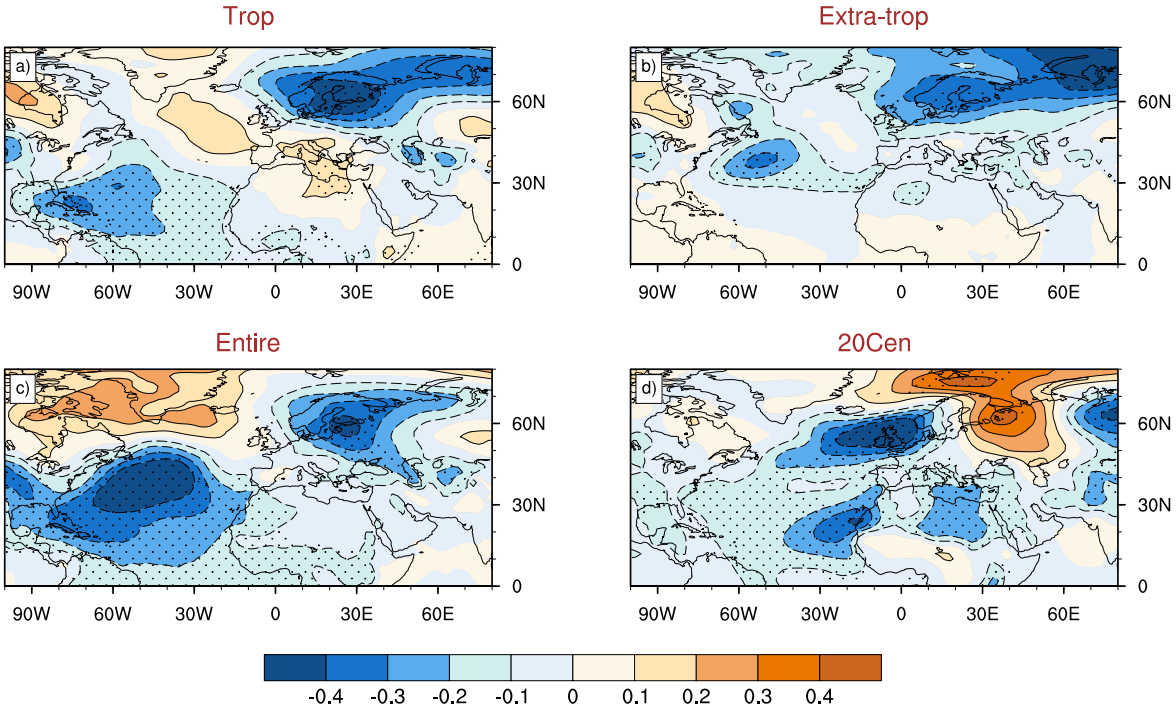

Fig. 4.3 The SLP response from the positive AMV SST anomaly patterns as shown in Fig 4.1a-c averaged for the summer months (JJA) for the a) TROP, b) EXTRA-TROP and c) ENTIRE experiments. d) The positive phase composite with respect to the C-E European SAT index (black line, fig 2.2b) from the 20th century reanalysis. The dotted regions denote areas with significance at the 95% level. The units are in hPa.

It is apparent that for all of the model experiments, the SLP response to positive AMV SST anomalies has no resemblance to the SLP response in the 20CRv2 over the NAE region. The clear presence of the east-west wave like SLP response, with a surface low pressure

anomaly over the west coast of the European continent, is entirely missing in the experiments. This supports our hypothesis that the model experiments in the positive phase are unable to simulate the observed NEW response and hence the observed SAT response over the C-E Europe. Moreover, over the tropical part, the response in the TROP and ENTIRE experiments shows a surface low over the western tropical Atlantic Ocean. However, in the 20th century analysis, the response to the tropical branch of the AMV SST is over the eastern tropical Atlantic Ocean. This suggests a strong tropical forcing in the sensitivity experiments during the positive AMV phase in the model.

The SLP response to the tropical branch of AMV SST shows a negative SLP anomaly pattern emanating from the Caribbean region, as shown in the TROP experiment (Fig 4.3a). Further, the SLP response consists of surface high pressure north-east of the low and the surface high is followed by a surface low pressure anomaly downstream. The pattern resembles the SLP signature of a stationary Rossby wave emanating from the tropics due to positive tropical SST anomalies (Terray and Cassou, 2002). In case of the extra-tropical AMV SST, there is a negative SLP anomaly pattern situated over the east of the North American continent (Fig 4.3b). The figure 4.1b shows strong positive SST anomalies just below this negative SLP anomalies, hence indicating convection from localized heating over this region. For the ENTIRE experiment, the SLP response shows a stronger negative SLP anomaly over the same western to central North Atlantic similar to the TROP experiment (Fig 4.3c). The SLP pattern over the NAE region however has similarities with both tropical and extra-tropical AMV SST forced experiments. This indicates that both the tropical and extra-tropical branches of AMV SST play their role to determine the overall atmospheric response over the NAE region in the positive AMV phase of the model. However, we have seen that the role over C-E region seems to be mainly controlled by the tropical branch of AMV SST (Fig 4.2c).

We investigate the 500 hPa geopotential height fields to understand the vertical structure of the SLP responses, and to further confirm the dominant role of the tropical forcing in the positive AMV SST phase. The geopotential height response to the tropical, extra-tropical and entire North Atlantic positive AMV SST anomalies are shown in figure 4.4a-c. In case of the tropical AMV SST anomalies, the surface low over the Caribbean region is diminished in magnitude at the upper levels (Fig 4.4a). However, the following north-eastward high pressure anomaly and low pressure anomaly further downstream seem to get strengthened in the higher altitudes. This indicates a barotropic nature of the response over the extra-tropics, which starts with a baroclinic nature over the lower latitudes. This again refers to the characteristics of the stationary Rossby wave response from the tropics (Terray and Cassou, 2002). Apparently, this wave response creates a favorable situation to advect the colder winds from the higher latitudes over the European region. The response in height fields at 500 hPa for the ENTIRE experiment also shows a quite similar atmospheric pattern over the NAE region, indicating a dominant contribution from the tropical branch of AMV SST through stationary Rossby wave generation (Fig 4.4c). However, the extra-tropical AMV SST response also shows similar atmospheric pattern over the NAE region, where the surface low is diminished in the upper levels and the downstream high pressure is strengthened

(Fig 4.4b). Nevertheless, the low pressure response over the European region which plays a crucial role to bring colder winds to C-E Europe is much stronger and significant in the TROP experiment compared to the EXTRA-TROP experiment. These results confirm that the response over the C-E Europe during the positive phase in the model is due to the tropical branch of AMV SST through stationary Rossby waves.

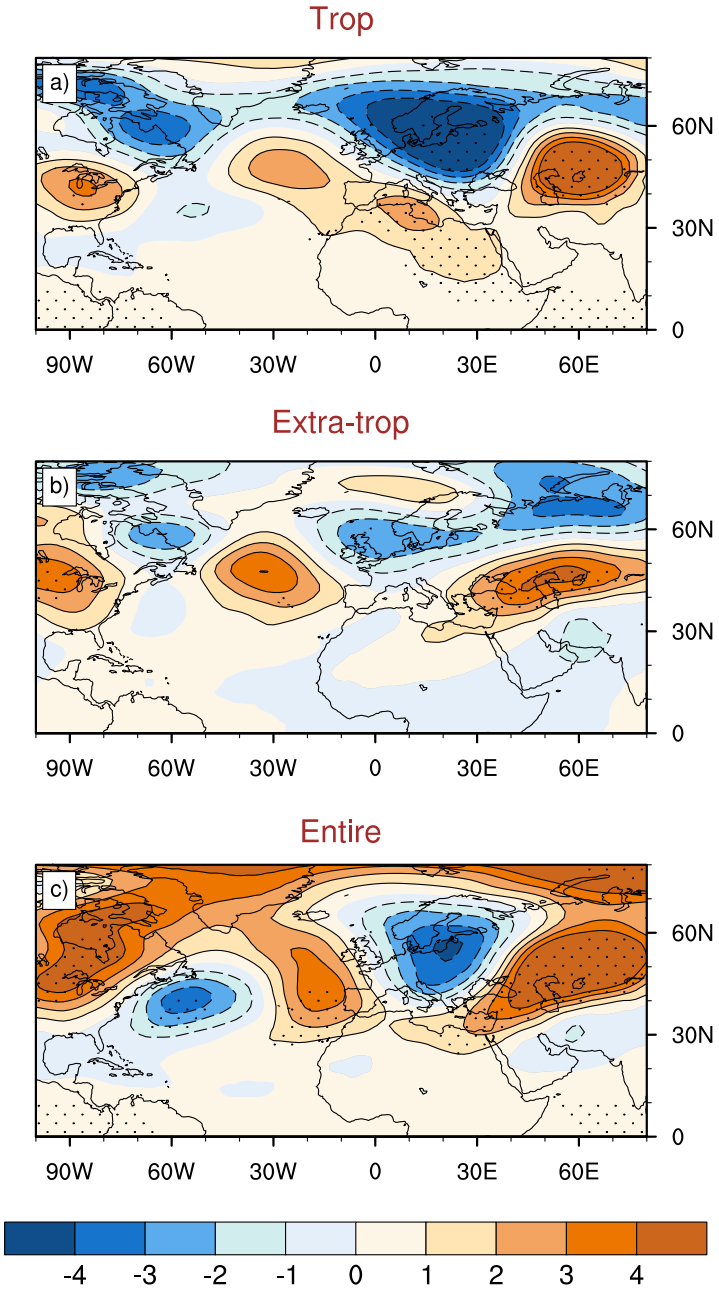

Fig. 4.4 The geopotential height at 500 hPa response from the positive AMV SST anomaly patterns as shown in Fig 4.1a-c, averaged for the summer months (JJA) for the a) TROP, b) EXTRA-TROP and c) ENTIRE experiments. The dotted regions denote areas with significance at 95% level. The units are in meters [m].

To further confirm the barotropic and baroclinic natures of the responses over the mid-latitudes in the positive AMV phase experiments, we show the vertical structure of the geopotential height fields averaged over the latitude 30°N to 60°N (Fig 4.5). Over the North Atlantic Ocean (80°W-0°W/E), the response from the TROP and EXTRA-TROP experiments looks quite similar with a baroclinic low (45°W and westward) and an equivalent barotropic high east of the low (Fig 4.5a,b). However, the high seems stronger and significant at the upper levels in case of the extra-tropical AMV SST forcing. Proceeding towards the east, the response over the European region (0°E-60°E) shows a low pressure anomaly with barotropic structure regarding the TROP experiment and baroclinic structure with respect to the EXTRA-TROP experiment. Moreover, the response in the ENTIRE experiment resembles more the TROP experiment, with a barotropic structure of the low pressure anomaly (Fig 4.5c). This again indicates that the European region is mainly influenced by the tropical AMV SST in the model during the positive phase.

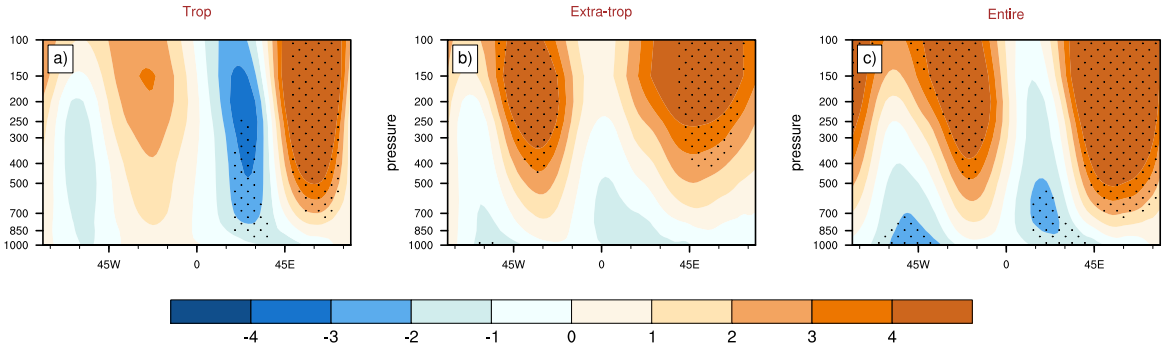

Fig. 4.5 The zonal vertical structure of the geopotential height response averaged over the latitude 30°to 60°N from the positive AMV SST anomaly patterns, as shown in Fig 4.1a-c in the summer period (JJA) for the a) TROP b) EXTRA-TROP c) ENTIRE experiments. The dotted regions denote areas with significance at the 95% level. The units are in meters [m].

4.4.2 Tropical AMV SST influence

To further confirm the dominant role of the tropical branch of the AMV SST in the positive phase, we briefly show the precipitation and 200 hPa velocity potential responses for the ENTIRE, TROP and EXTRA-TROP experiments in figure 4.6. Typically, the tropical off equatorial heating produces a Gill type response, which can be detected through high positive precipitation anomalies and strong upper level divergence of the wind (Hodson et al., 2010). This Gill type of response over the tropical region is a source for the stationary Rossby wave generation which then propagates poleward and east ward from the tropics (Hoskins and Karoly, 1981). In both the ENTIRE and TROP experiments, there are intense positive precipitation anomalies over the tropical Atlantic region (Fig 4.6a,b). Further, the 200 hPa velocity potential field shows intense negative anomalies, indicating strong divergence of the wind at the upper levels over the anomalous precipitation region in the tropics (Fig 4.6d,e). This confirms the prominent presence of the Gill type of response from the tropics in the

TROP, as well as ENTIRE experiment. Presumably, there is no sign of such response in the EXTRA-TROP experiment (Fig 4.6c,f). However, in case of the precipitation anomalies for the EXTRA-TROP experiment (Fig 4.6c), there is significant positive precipitation anomaly associated with the surface low over the North Atlantic (Fig 4.3b). This supports the hypothesis of a convective response from localized heating regarding the response from the extra-tropical AMV SST anomalies.

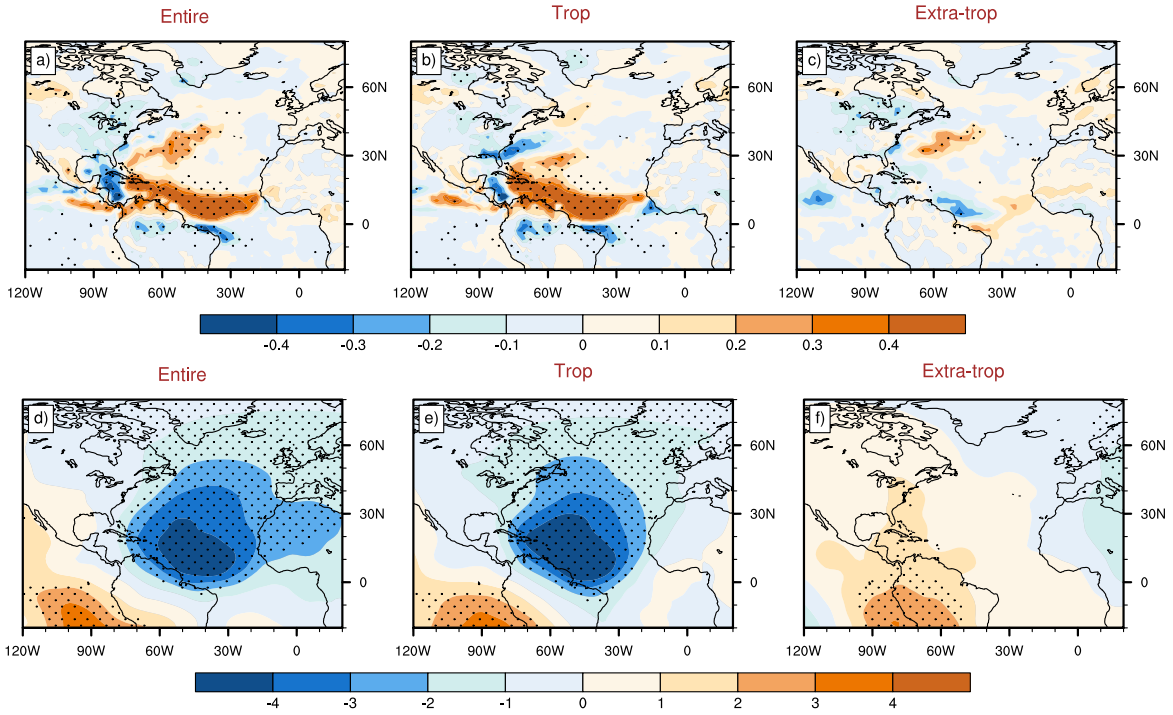

Fig. 4.6 The precipitation response from the positive AMV SST anomaly patterns as shown in Fig 4.1a-c averaged for the summer months (JJA) for the a) ENTIRE, b) TROP and c) EXTRA-TROP experiments. The units are in mm/day. d), e),f) are same as a),b),c) but for 200 hPa velocity potential. Units are in $10^5 m^2 s^{-1}$. The dotted regions denote areas with significance at the 95% level.

4.5 Atmospheric pathway during the negative AMV phase

4.5.1 Sea level pressure

The SLP responses in the TROP, EXTRA-TROP and ENTIRE experiments for the negative AMV phase are shown in figure 4.7a-c. Further the negative phase composite response with respect to C-E European SAT index from the 20th century reanalysis is shown in figure 4.7d. In the TROP experiment there is a weak high pressure anomaly over the tropical region which is expectedly opposite to the response in the positive AMV forcing and hence confirming the linear nature of the tropical response (Fig 4.7a). However, we do not see any significant SLP anomalies over the extra-tropical Atlantic, as well as European region with respect

to tropical negative AMV SST anomaly. On the contrary, in case of the EXTRA-TROP experiment, there is a significant and intense surface high pressure anomaly centered over the north-eastern Atlantic Ocean, which encompasses its influence over the NAE region (Fig 4.7b). Moreover, the position and structure of this high is very similar to the high pressure anomaly in 20th century reanalysis negative phase response (Fig 4.7d). In reanalysis, this high pressure anomaly is related to the negative phase response from the extra-tropical AMV SST, which means the NEW mode in its negative phase. Hence the close resemblance of the high SLP anomaly in the EXTRA-TROP experiment with the negative AMV phase 20th century reanalysis SLP response suggests that the model is able to simulate the NEW response from the negative phase AMV SST anomalies. For the ENTIRE experiment, though slightly reduced in magnitude, we can still find the significant presence of the surface high over the north-eastern Atlantic Ocean (Fig 4.7c). This indicates that irrespective of tropical Atlantic AMV SST anomalies, the response from the extra-tropical AMV SST (Fig 4.7b), which resemble with the observed NEW response, can retain its characteristics and influence over the NAE region in the negative AMV SST phase of the model.

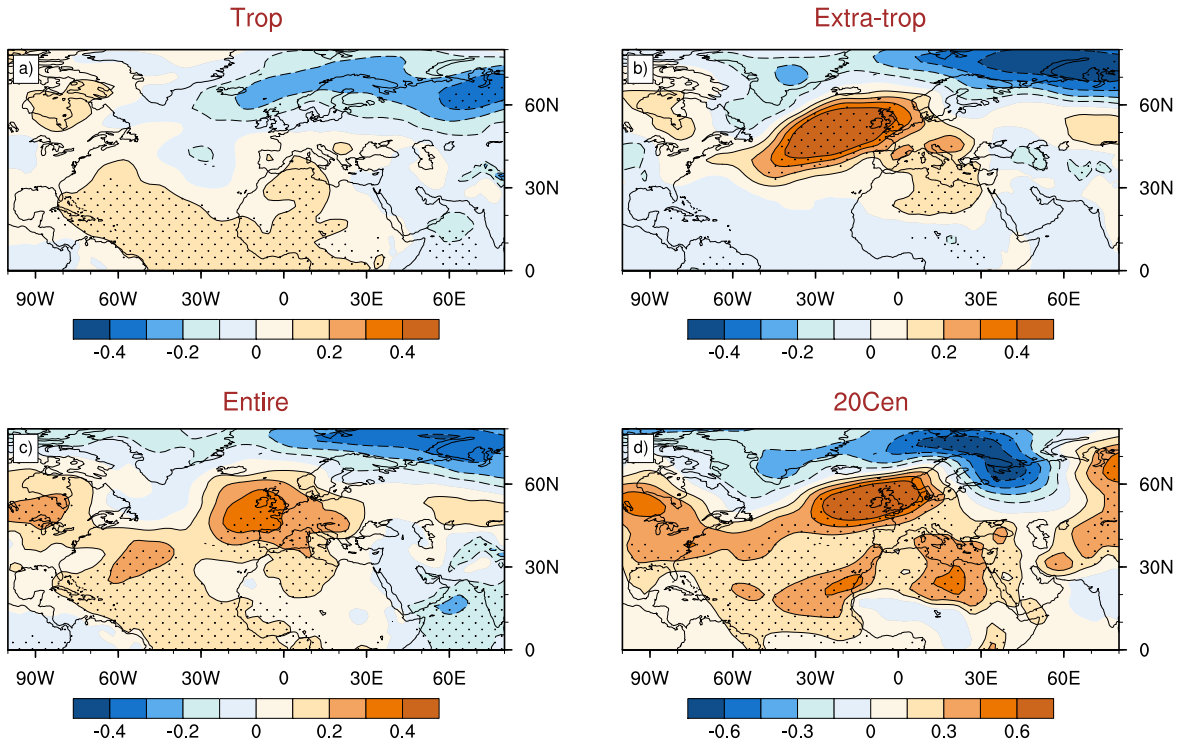

Fig. 4.7 The SLP response from the negative AMV SST anomaly patterns as shown in Fig 4.1d-f averaged for the summer months (JJA) for the a) TROP, b) EXTRA-TROP and c) ENTIRE experiments. d) The negative phase composite of SLP with respect to the C-E European SAT index (black line, fig 2.2b) from the 20th century reanalysis. The dotted regions denote areas with significance at the 95% level. The units are in hPa.

4.5.2 Vertical structure and temperature advection

For being confirmed that the surface high in the negative AMV SST phase EXTA-TROP experiment is indeed the NEW mode, we must ensure that the vertical structure of the high pressure anomaly has a baroclinic-like nature. Therefore, we proceed to look into the vertical structure of the responses in the experiments with the response in 20CRv2. The zonal vertical structure of the geopotential height field averaged over the latitude 30°N-60°N for the negative AMV SST forced TROP, EXTRA-TROP and ENTIRE experiments are shown in figure 4.8a-c. Additionally, the same geopotential height field for the negative phase composite with respect to the C-E European SAT index from 20CRv2 is shown in figure 4.8d.

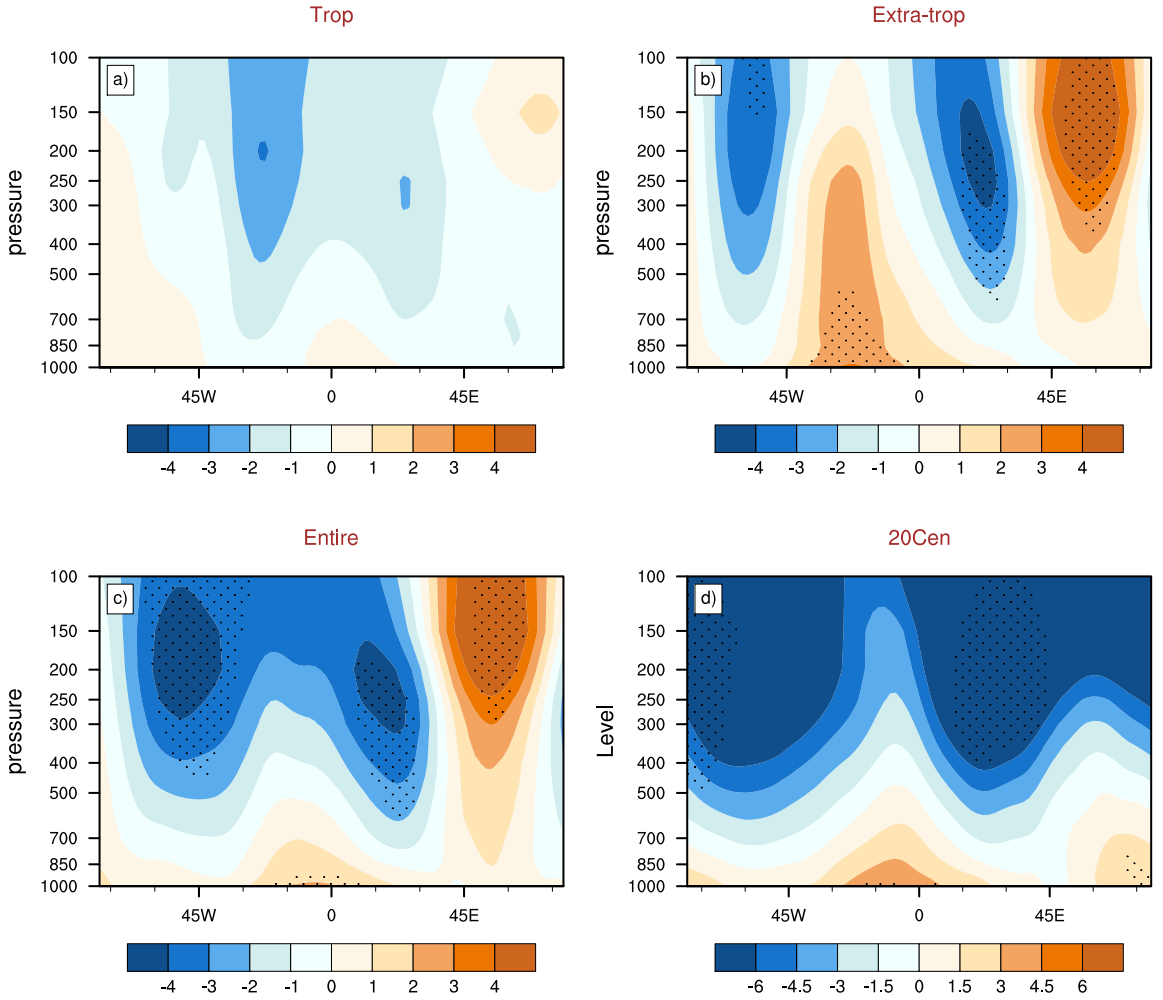

Fig. 4.8 The zonal vertical structure of the geopotential height response averaged over the latitude 30°to 60°N from the negative AMV SST anomaly patterns as shown in Fig 4.1d-f in the summer period (JJA) for the a) TROP b) EXTRA-TROP c) ENTIRE experiments and d) for the negative phase composite with respect to the C-E European SAT index (black line, fig 2.2b) from the 20th century reanalysis. The dotted regions denote areas with significance at the 95% level. Units are in meter [m].

From the TROP experiment, it is evident that the tropical negative AMV SST anomaly forcing has no significant impact over the extra-tropical region in the negative AMV phase (Fig 4.8a). However, the EXTRA-TROP experiment shows a baroclinic-like vertical structure of the surface high seen in figure 4.7b (Fig 4.8b). The response from the ENTIRE experiment also shows the baroclinic nature of the surface high over the NAE region (Fig 4.8c). Moreover, the vertical geopotential height structure of the ENTIRE experiment closely resemble the structure of the EXTRA-TROP experiment with two barotropic lows surrounding the surface baroclinic high and further eastward a barotropic high. Therefore, it is apparent that in negative AMV SST forcing condition the model atmospheric response over the NAE region is mainly contributed by the extra-tropical branch of the AMV SST. Further, the negative phase composite from the 20CRv2 shows a vertical structure quite similar to the structure in the ENTIRE as well as EXTRA-TROP experiments with the same baroclinic surface high surrounded by two barotropic low over the NAE region (Fig 4.8d). Hence, it implies that the model response to the extra-tropical negative AMV SST forcing can very closely replicate the observed response in the negative AMV phase, which is the part of the NEW mode in the negative phase.

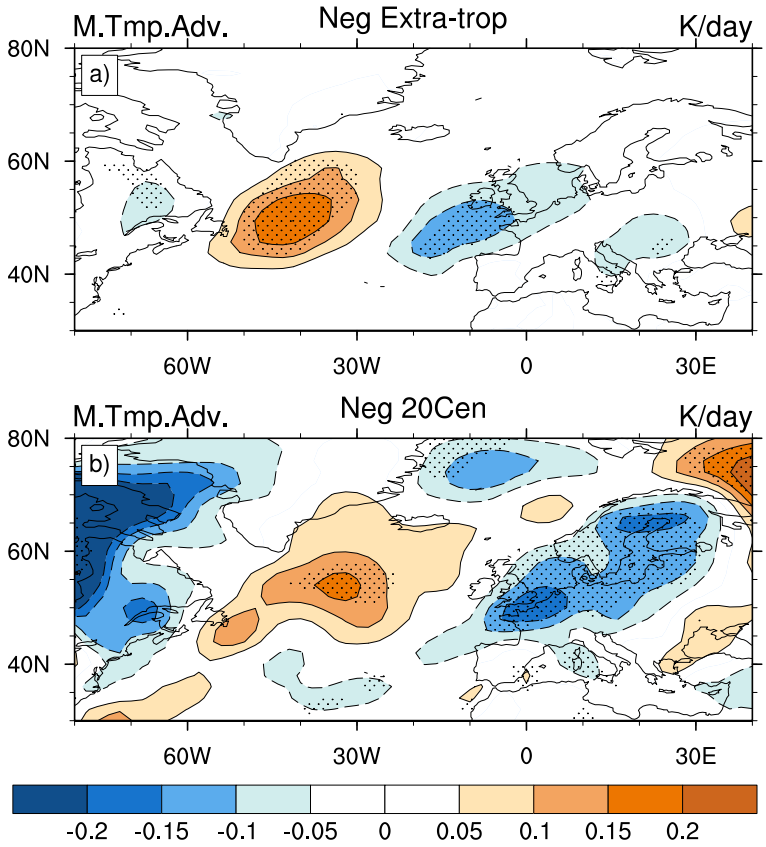

Fig. 4.9 The response of the meridional temperature advection $v' \frac{\partial \bar{\theta}}{\partial y}$ at 850 hPa, after Hoskins and Karoly (1981), where v' is the deviation of the meridional velocity from zonal mean and $\bar{\theta}$ is the zonal mean potential temperature a) in the EXTRA-TROP experiment with the negative AMV SST and b) in the negative phase composite with respect to the C-E European SAT index (black line, fig 2.2b) from the 20th century reanalysis. The dotted regions denote areas with significance at the 95% level. Units are in Kevin per day [K/day].

To further confirm the similarities in the response from the negative AMV phase in the EXTRA-TROP experiment and the negative phase composite response in the 20CRv2, figure 4.9 shows the meridional temperature advection $v' \frac{\partial \bar{\theta}}{\partial y}$ response as derived from Hoskins and Karoly (1981), following the thermodynamic energy equation with the quasi-geostrophic approximation. The positive values denote the advection is north-ward and the negative values denote that the advection is south-ward. The response in the EXTRA-TROP experiment shows cold air advection over the European region and north wards warm air advection over the negative SST anomalies over the north-western Atlantic Ocean (Fig 4.9a). This temperature advection pattern follows the surface high that we see in the SLP response over the NAE region (Fig 4.7b). The temperature advection response over the NAE region in the 20CRv2 for the negative phase composite is very similar to the response seen in the experiment, with the same cold air advection over the Europe and warmer air advection over the north-west Atlantic Ocean (Fig 4.9b). This close resemblance strongly suggest that the model generated response in the negative AMV phase EXTRA-TROP experiment is following a linear quasi-geostrophic response to the midlatitude cooling as elaborated in chapter 2.

4.6 Discussions

The results from the sensitivity experiments show that in the positive phase, the response from the extra-tropical AMV SST anomalies does not resemble the linear baroclinic response from midlatitude heating as found in the 20CRv2. Hence, we do not find the observed SAT response from positive AMV SST anomalies in the sensitivity experiments. One of the reasons for this could be the differences in the turbulent heat flux response from the SST anomalies between the model and the reanalysis. The turbulent (sensible + latent) heat flux response over the midlatitudes is shown for the positive AMV phase ENTIRE, EXTRA-TROP experiments and for the positive phase composite with respect to the C-E European SAT index from 20CRv2 in figure 4.10.

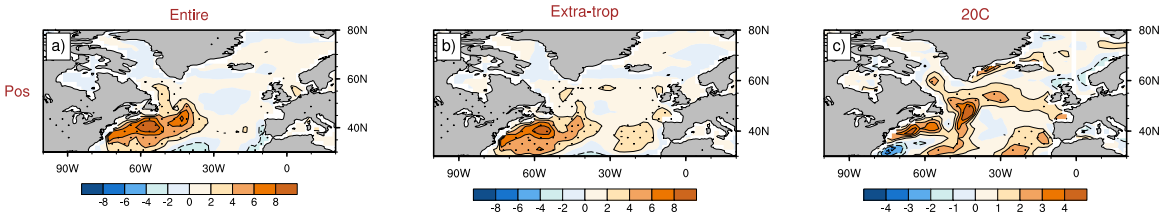

Fig. 4.10 The sensible + latent heat flux response from the positive AMV SST anomaly patterns as shown in Fig 4.1a-c, averaged for the summer months (JJA) for the a) ENTIRE, b) EXTRA-TROP experiments and c) for the positive phase composite with respect to the C-E European SAT index (black line, fig 2.2b) from the 20th century reanalysis. Positive values denote that the flux is from the ocean to the atmosphere. The dotted regions denote areas with significance at the 95% level. Units are in Wm^{-2}.

There is a distinct difference in the heat flux response over the north-western Atlantic Ocean in the experiments (Fig 4.10a,b) in comparison to the reanalysis (Fig 4.10c). In both the EXTRA-TROP and ENTIRE experiments, the most intense heat flux anomalies are over the east coast of the North-American continent around 40°N. Moreover, the low pressure anomaly response and the positive precipitation anomaly response coincide with the region of the intense heat flux anomalies in the experiments. However, in the 20CRv2 the most intense heat flux anomalies are further north-east ward, just east of the Newfoundland, around 50°N. It could be possible that due to the model deficiency to simulate the observed diabatic heating region, the model is not able to simulate the observed SLP response from the heat flux anomalies. Instead, the model tends to create a convective response from the localized heating over the lower latitudes.

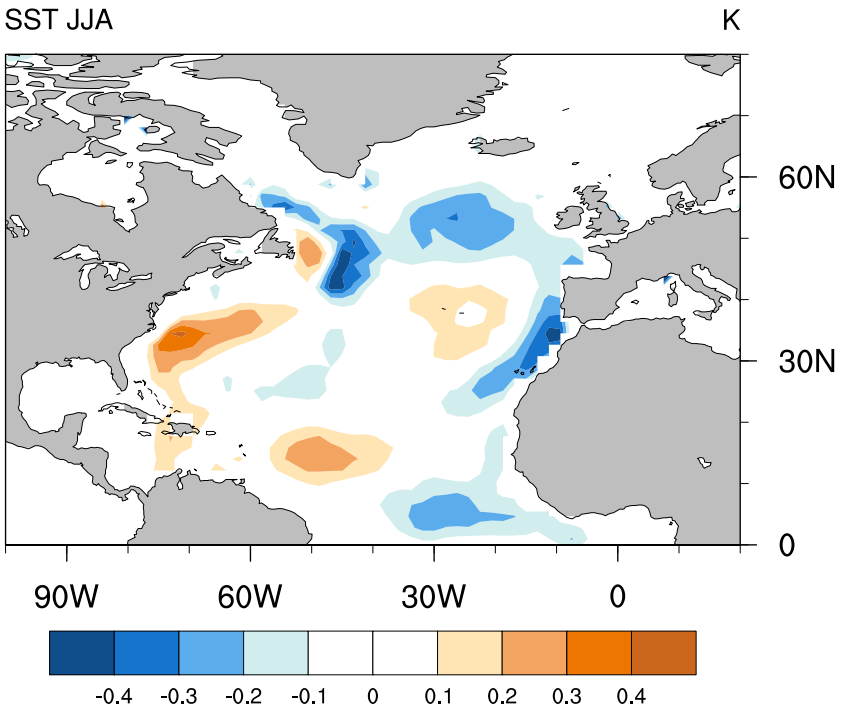

Fig. 4.11 The difference of the SST pattern over the Atlantic Ocean in summer (JJA) between the positive AMV SST ENTIRE experiment and the negative AMV SST ENTIRE experiment. Units are in Kelvin [K].

The non-linearity in the atmospheric response over the extra-tropical region between the positive and negative AMV SST phase experiments could be due to the non-linearity in the AMV SST forcing itself. The difference in the SST conditions between the positive AMV SST forcing and the negative AMV SST forcing is shown in figure 4.11. It clearly shows that the positive and negative AMV SST forcing is not entirely linear. The positive values denote the regions where the positive AMV SST forcing is stronger and the negative values denote the opposite. The positive AMV SST forcing is stronger over the western tropical Atlantic Ocean and the east coast of North America. The western North Atlantic starting from the tropics to the subtropical region is more sensitive to generate the stationary Rossby

wave response (Terray and Cassou, 2002) which we indeed find in the positive AMV SST experiments. Whereas the negative AMV SST forcing is stronger over the north-western, eastern Atlantic Ocean and over the eastern tropical Atlantic Ocean. The strength of SST anomalies over the north-western Atlantic Ocean, east of Newfoundland, is the main region for generating linear baroclinic response from midlatitude heating. Therefore, this indicates that the magnitude of SST anomalies over the north-western Atlantic Ocean is stronger in the negative AMV SST phase than in the positive AMV SST phase and, hence, we have been able to see the observed NEW response in negative AMV SST phase of the model. It would be interesting to see if the model is able to simulate the observed NEW response in the positive phase, if the negative AMV SST forcing is applied after changing its phase by multiplying with -1. This will make the forcing stronger over the desired location and also will enable us to understand the response with the linear forcing. However, the experimental condition used for the present study is more realistic and the desired atmospheric response for the positive AMV SST phase is ultimately expected to be simulated with the present SST forcing.

4.7 Conclusions

The results from the AMIP type sensitivity experiments with the positive and negative AMV SST forcing can be summarized as follows:

- The SAT response from the positive AMV SST forced experiments shows negative anomalies over the C-E European region, which is opposite from the observed anomalies in decadal mean SATs as in Ghosh et al. (2016) in the positive AMV SST phase.
- The SAT response over the C-E European region is mainly generated by the tropical branch of the AMV SST in the positive phase.
- The results for SLP, 500 hPa geopotential height field, precipitation, and 200 hPa velocity potential field strongly suggest that the tropical positive SST anomalies tend to emanate a stationary Rossby wave response, which then propagates towards the extra-tropics. This creates an atmospheric condition, which advects colder polar winds towards C-E Europe and brings the negative SAT anomalies.
- There is no evidence of the extra-tropical forcing over the C-E Europe in the positive phase experiment.
- In the negative AMV SST forced experiment, the SAT response over the C-E Europe shows negative anomalies, similar to the observed anomalies for decadal mean SATs in the negative AMV SST phase, as found in Ghosh et al. (2016).
- The SAT response over C-E Europe in the negative phase is due to the extra-tropical branch of the AMV SST, in association with a baroclinic response from the extra-tropical SST anomalies.

- The SLP response in the extra-tropical AMV SST forced experiment shows very high resemblance with 20th century reanalysis.
- The analysis of the meridional temperature advection and the vertical structure of the geopotential height field reveal that the response from the negative extra-tropical AMV SST experiment shows similar characteristics of the observed NEW mode.

Altogether, we can conclude that the model SAT response over C-E Europe with the positive AMV SST forcing is opposite to what we have found in reanalysis Ghosh et al. (2016). However, in case of the negative AMV SST forcing, the model is indeed able to simulate the observed SAT response over the C-E Europe and the related dynamical mechanism shows the characteristics of the observed linear baroclinic response to diabatic heating.

Chapter 5

Conclusions and Thesis outlook

The thesis investigated the atmospheric pathway between AMV and European summer climate in the observations, coupled models and in the idealized AMIP type sensitivity experiments. This investigation, as mentioned in the introduction, is split into three chapters each addressing a specific aspect. At the end of the thesis, these aspects and the respective findings related to that are addressed chapter wise as following:

Chapter 2: What is the observed atmospheric pathway between AMV and European summer climate? What is a plausible dynamical mechanism which can lead to the observed atmospheric pathway?

Using 20th century reanalysis as a proxy of observations, we find an east-west wave like pattern in sea level pressure (SLP) as an observed atmospheric pathway between AMV and Central to Eastern (C-E) European summer surface air temperature (SAT). Associated with its spatial pattern, this response is named as North-Atlantic-European East West (NEW) response (Ghosh et al., 2016). The principle component analysis of the decadal mean SLP (11 year running mean) shows that this NEW response is the principle mode of multidecadal variations in summer over the NAE region and it is not related to summer North Atlantic Oscillation, which is the second mode of variability over this region.

We find that the NEW response is baroclinic in nature and agrees well with the characteristics of the linear baroclinic response from the diabatic heating of the midlatitiude ocean. According to the linear quasigeostrophic theory, in the extra-tropical ocean, a shallow diabatic heating induces a surface low east of the center of heating. The surface low deviates the colder polar wind towards the heating region and drives sub-tropical warmer air to the east of the centre of the low pressure (Hoskins and Karoly, 1981). In 20CRv2, the surface heat flux over the north-west Atlantic Ocean indeed provides the source of a shallow diabatic heating by generating a linear baroclinic-like atmospheric response with a surface pressure low east of the centre of the heating. By analyzing the linearized quasigeostrophic thermal energy equation in steady state, we find that the induced surface low advects warmer subtropical air over the north-western European region.

The AMV related warming over the C-E Europe, however, mainly happens due to the increase in the atmospheric blocking situation. The east-west wave like NEW response favours the European blocking condition, which increases the blocking frequency over the C-E European region. Therefore, apart from the warm air advection, we suggest that the NEW response mainly affects the C-E European temperature on multidecadal time scales by increasing the liklihood of atmospheric blocking-like situations over this region.

Chapter 3: What is the relation of the AMV and European summer climate in a coupled climate model? Can it represent the observed link and the atmospheric pathway?

Using the coupled model MPI-ESM in its low (LR) and high (HR) resolutions we investigate the atmospheric pathway between AMV and C-E Europe in summer. Both LR and HR are unable to capture the observed response in SAT over C-E Europe from AMV.

Instead, the LR shows a prominent response from the tropical branch of AMV SST through stationary Rossby waves emanating and propagating towards the NAE regions and bringing negative SAT anomalies over C-E Europe, which is opposite to what is in the observations. In HR, however, such overestimation of the tropical response is reduced. This difference is found to be related to different transient eddy-mean flow interactions. The transient eddy feedback to the mean flow, which is crucial to sustain and propagate the tropical response to the extra-tropics, is much stronger in LR than HR.

Chapter 4: What is the relation of the AMV and European summer climate in idealized sensitivity experiments with observed AMV like SST pattern? Can we find the observed response over Europe and associated atmospheric pathway?

The inability of the coupled models to simulate the desired response is inferred to be link with a large cold climatological SST bias ($\sim 4^{\circ}$C) over the extra-tropical North Atlantic Ocean, which is shown to be the key region for generating the observed heat fluxes and the linear baroclinic response from diabatic heating. Therefore, to overcome this shortcoming in the coupled model, we performed a set of AMIP type sensitivity experiments with the observed AMV type SST pattern.

The AMIP type sensitivity experiments with the positive and negative AMV SST forcing are conducted using the LR version of the atmospheric component of MPI-ESM, ECHAM6.3. Having been known that the LR version has a strong forcing from the tropical SST anomalies, these experiments enabled us to clearly understand the role and influence of strong tropical forcing over C-E Europe.

The SAT response from the positive AMV SST forced experiments shows negative anomalies over the C-E European region which are opposite from the observed anomalies in decadal mean SATs as in Ghosh et al. (2016). This opposite response is mainly contributed by the tropical branch of the AMV SST. The results from the SLP, 500 hPa geopotential height field, precipitation and 200 hPa velocity potential field strongly suggest that the tropical positive SST anomalies tend to emanate stationary Rossby wave response. This response then propagates towards extra-tropics and creates an atmospheric condition which advect colder

polar winds towards C-E Europe to bring negative SAT anomalies. There is no evidence of the extra-tropical forcing over the C-E Europe in the positive AMV phase experiments.

In the negative AMV SST forced experiment, the SAT response over the C-E Europe shows negative anomalies similar to the observed anomalies for decadal mean SATs in the negative AMV SST phase as found in Ghosh et al. (2016). This is due to the extra-tropical branch of the AMV SST, in association with a baroclinic response from the extra-tropical SST anomalies. The analysis of the SLP, meridional temperature advection and the vertical structure of the geopotential height field reveal that the response from the negative extra-tropical AMV SST experiment shows similar characteristics of the observed NEW mode.

Hence, it can be concluded from that the model SAT response over the C-E Europe with the positive AMV SST forcing has appeared opposite to what we have found in observations (Ghosh et al., 2016). However, in case of the negative AMV SST forcing, the model is indeed able to simulate the observed SAT response over the C-E Europe and the related dynamical mechanism shows the characteristics of the observed linear baroclinic response to diabatic heating.

In summary, the thesis is able to find the observed atmospheric pathway between AMV and European summer climate and it successfully establishes a dynamical mechanism related to extra-tropical AMV SST anomalies which can bring such atmospheric pathway (Ghosh et al., 2016). Moreover, the analysis of the link between AMV and European summer climate in the model reveals the strong sensitivity of the LR to the tropical positive AMV SST anomalies and the corresponding inability to bring the observed response over C-E Europe from AMV. However, in the negative AMV SST phase, the model shows promising results by replicating the observed response as found in Ghosh et al. (2016).

The thesis further opens directions for new studies. For example, the AMV sensitivity experiments are done with the LR version of the model which helped us understand the role of strong tropical forcing on the NAE climate in summer. However, from our coupled model study, we know that the HR version has much lesser influence of the tropical SST anomalies over Extra-tropics. Hence, it would be interesting to conduct a similar set of sensitivity experiments with observed AMV SST forcing using the HR to investigate whether the model is able to better simulate the response from AMV SST as in Ghosh et al. (2016).

Another direction could be to investigate the atmospheric pathway between AMV and North American climate during summer in observations using 20th century reanalysis. Using general circulation models, previous studies suggested that the tropical branch of the AMV SST plays a main role for the link between AMV and North American climate by emanating Gill-type of response (Hodson et al., 2010; Sutton and Hodson, 2007). However, our study with the 20th century reanalysis shows different characteristics regarding the position and the strength of the response from the tropical branch of the AMV SST. Moreover, we also found that the climate model is more sensitive to the tropical branch of the AMV SST. Therefore, it would be worth investigating the dynamical reason behind the link between AMV and North American summer climate in the 20th century reanalysis, which seemed to be different from the proposed Gill type of response from the tropics.

List of figures

List of tables

References

Bader, J., Flügge, M., Kvamsto, N. G., Mesquita, M. D. S., and Voigt, A. (2013). Atmospheric winter response to a projected future Antarctic sea-ice reduction: a dynamical analysis. *Climate Dyn.*, 40:2707–2718.

Barriopedro, D., Fischer, E. M., Luterbacher, J., Trigo, R. M., and García-Herrera, R. (2011). The hot summer of 2010: Redrawing the temperature record map of Europe. *Science*, 332(6026):220–224.

Bengtsson, L., Semenov, V. A., and Johannessen, O. M. (2004). The Early Twentieth-Century Warming in the Arctic—A Possible Mechanism. *J. Climate*, 17:4045–4057.

Bjerknes, J. (1964). *Atlantic Air-Sea Interaction*. Academic Press.

Bladé, I., Liebmann, B., Fortun, D., and van Oldenborgh, G. J. (2012). Observed and simulated impacts of the summer NAO in Europe: implications for projected drying in the mediterranean region. *Climate Dyn.*, 39:709–727.

Bretherton, C. S., Smith, C., and Wallace, J. M. (1992). An Intercomparison of Methods for Finding Coupled Patterns in Climate Data. *J. Climate*, 5:541–560.

Compo, G. P., Whitaker, J. S., and Sardeshmukh, P. D. (2006). Feasability of a 100-year reanalysis using only surface pressure data. *Bull. Amer. Meteor. Soc.*, 87:175–190.

Compo, G. P., Whitaker, J. S., Sardeshmukh, P. D., Matsui, N., Allan, R. J., Yin, X., B. E. Gleason, J., Vose, R. S., Rutledge, G., Bessemoulin, P., Bronnimann, S., Brunet, M., Crouthamel, R. I., Grant, A. N., Groisman, P. Y., Jones, P. D., Kruk, M. C., Kruger, A. C., Marshall, G. J., Maugeri, M., Mok, H. Y., Nordli, O., Ross, T. F., Trigo, R. M., Wang, X. L., Woodruff, S. D., and Worley, S. J. (2011). The Twentieth Century Reanalysis Project. *Quart. J. Roy. Meteor. Soc.*, 137:1–28.

Czaja, A. and Frankignoul, C. (2002). Observed Impact of Atlantic SST Anomalies on the North Atlantic Oscillation. *J. Climate*, 15(6):606–623.

Davini, P., von. Hardenberg, J., and Corti, S. (2015). Tropical origin for the impacts of the Atlantic Multidecadal variability on the Euro-Atlantic climate. *Environ. Res. Lett.*, 10(9):094010.

Delworth, T. L. and Mann, M. E. (2000). Observed and simulated multidecadal variability in the northern hemisphere. *Climate Dyn.*, 16(9):661–676.

Doblas-Reyes, F., Andreu-Burillo, I., Chikamoto, Y., Garcıa-Serrano, J., Guemas, V., Kimoto, M., Mochizuki, T., Rodrigues, L., and van Oldenborgh, G. (2013). Initialized near-term regional climate change prediction. *Nat. Commun.*, 4(1715).

Dong, B., Sutton, R. T., and Shaffrey, L. (2016). Understanding the rapid summer warming and changes in temperature extremes since the mid-1990s over Western Europe. *Climate Dyn.*, pages 1–18.

Dong, B., Sutton, R. T., Woollings, T., and Hodges, K. (2013). Variability of the North Atlantic summer storm track: meachanisms and impacts on the European climate. *Environ. Res. Lett.*, 8:034037.

Dong, B. W., Sutton, R. T., and Woollings, T. (2012). The extreme European summer 2012. *Bulletin of American Meteorological Society*, 94(9):S28–32.

Duchon, C. E. (1979). Lanczos Filtering in One and Two Dimensions. *J. Appl. Meteor.*, 18:1016–1022.

Dunstone, N. J., Smith, D. M., and Eade, R. (2011). Multi-year predictability of the tropical Atlantic atmosphere driven by the high latitude North Atlantic Ocean. *Geophys. Res. Lett.*, 38(14).

Enfield, D. B., Mestas-Nunez, A. M., and trimble, P. J. (2001). The atlantic multidecadal oscillation and its relation to rainfall and river flows in the continental u.s. *Geophys. Res. Lett.*, 28:2077–2080.

Folland, C. K., Knight, J., Linderholm, H. W., Fereday, D., Ineson, S., and Hurrell, J. W. (2009). The Summer North Atlantic Oscillation: Past, Present, and Future. *J. Climate*, 22:1082–1103.

Founda, D. and Giannakopoulos, C. (2009). The exceptionally hot summer of 2007 in Athens, Greece - A typical summer in the future climate. *Global Planet. Change*, 67:227–236.

Gastineau, G. and Frankignoul, C. (2015). Influence of the North Atlantic SST Variability on the Atmospheric Circulation during the Twentieth Century. *J. Climate*, 28:1396–1416.

Ghosh, R., Müller, W. A., Baehr, J., and Bader, J. (2016). Impact of observed North Atlantic multidecadal variations to European summer climate: a linear baroclinic response to surface heating. *Climate Dyn.*, pages 1–17.

Gill, A. E. (1980). Some simple solutions for heat-induced tropical circulation. *Quart. J. Roy. Meteor. Soc.*, 106:464–467.

Gulev, S. K., Latif, M., Keenlyside, N., Park, W., and Koltermann, K. P. (2013). North Atlantic Ocean control on surface heat flux on multidecadal timescales. *Nature*, 499:464–467.

Harris, I., Jones, P. D., Osborn, T. J., and Lister, D. H. (2014). Updated high-resolution grids of monthly climatic observations—The CRU TS 3.1 dataset. *Int J Climatol*.

Hermanson, L., Eade, R., Robinson, N. H., Dunstone, N. J., Andrews, M. B., Knight, J. R., Scaife, A. A., and Smith, D. M. (2014). Forecast cooling of the Atlantic subpolar gyre and associated impacts. *Geophys. Res. Lett.*, 41:5167–5174.

Hodson, D. L. R., Sutton, R. T., Cassou, C., Keenlyside, N., Okumura, Y., and Zhou, T. (2010). Climate impacts of recent multidecadal changes in Atlantic Ocean Sea Surface Temperature: a multimodel comparison. *Climate Dyn.*, 34(7-8):1041–1058.

Hoskins, B. J., James, I. N., and White, G. H. (1983). The shape, propagation and mean-flow interaction of large scale weather systems. *Journal of Atmospheric Science*, 40:1595–1612.

Hoskins, B. J. and Karoly, D. J. (1981). The Steady Linear Response of a Spherical Atmosphere to Thermal and Orographic Forcing. *J. Atmos. Sci.*, 38:1179–1196.

Jungclaus, J., Fischer, N., Haak, H., Lohmann, K., Marotzke, J., Matei, D., Mikolajewicz, U., Notz, D., and Storch, J. (2013). Characteristics of the ocean simulations in the Max Planck Institute Ocean Model (MPIOM) the ocean component of the MPI-Earth system model. *J. Adv. Model. Earth Syst.*, 5(2):422–446.

Knight, J. R., Folland, C. K., and Scaife, A. A. (2006). Climate impacts of the Atlantic Multidecadal Oscillation. *Geophys. Res. Lett.*, 33:L17706.

Kröger, J., Müller, W. A., and von Storch, J.-S. (2012). Impact of different ocean reanalyses on decadal climate prediction. *Climate Dyn.*, 39(3-4):795–810.

Krueger, O., Schenk, F., Feser, F., and Weisse, R. (2013). Inconsistencies between Long-Term Trends in Storminess Derived from the 20CR Reanalysis and Observations. *J. Climate*, 26:868–874.

Kushnir, Y. (1994). Interdecadal variations in North Atlantic sea surface temperature and associated atmospheric conditions. *J. Climate*, 7:141–157.

Kushnir, Y. and Held, I. M. (1996). Equilibrium Atmospheric Response to North Atlantic SST Anomalies. *J. Climate*, 9(6):1208–1220.

Kushnir, Y., Robinson, W. A., Blade, I., Hall, N. M. J., Peng, S., and Sutton, R. (2002). Atmospheric GCM Response to Extratropical SST Anomalies: Synthesis and Evaluation. *J. Climate*, 15:2233–2256.

Luterbacher, J., Dietrich, D., Xoplaki, E., Grosjean, M., and Wanner, H. (2004). European seasonal and annual temepearture variability trends and extremes since 1500. *Science*, 303(5663):1499–1503.

Mak, M. and Cai, M. (1989). Local barotropic instability. *J. Atmos. Sci.*, 46(21):3289–3311.

Masato, G., Hoskins, B. J., and Woollings, T. (2013). Winter and Summer Northern Hemisphere Blocking in CMIP5 Models. *J. Climate*, 26(18):7044–7059.

Matthews, A. J. and Kiladis, G. N. (1999). Interaction between ENSO, transient circulation and tropical convection over the Pacific. *J. Climate*, 12:3062–3086.

McCabe, G. J., Palecki, M. A., and Betancourt, J. L. (2004). Pacific and atlantic ocean influences on multidecadal drought frequency in the united states. *Proc. Natl. Acad. Sci. U. S. A.*, 101:4136–4141.

Mestas-Nunez, A. M. (2000). Orthogonality properties of rotated empirical modes. *Int J Climatol*, 20:1509–1516.

Msadek, R. and Frankignoul, C. (2009). Atlantic multidecadal oceanic variability and its influence on the atmosphere in a climate model. *Climate Dyn.*, 33(1):45–62.

Müller, W. A., Baehr, J., Haak, H., Jungclaus, J. H., Kröger, J., Matei, D., and Notz, D. (2012). Forecast skill of multi-year seasonal means in the decadal prediction system of the Max Planck Institute for Meteorology. *Geophys. Res. Lett.*, 39:L22707.

Müller, W. A., Pohlmann, H., Sienz, F., and Smith, D. (2014). Decadal climate predictions for the period 1901-2010 with a coupled climate model. *Geophys. Res. Lett.*, 41:2100–2107.

North, G. . R., Bell, T. L., Cahalan, R. F., and Moeng, F. J. (1982). Sampling errors in the estimation of empirical orthogonal functions. *Mon. Wea. Rev.*, 110.

Peng, S. and Whitaker, J. S. (1999). Mechanisms Determining the Atmospheric Response to Midlatitude SST Anomalies. *J Climate*, 12:1393–1408.

Pohlmann, H., Jungclaus, J. H., Köhl, A., Stammer, D., and Marotzke, J. (2009). Initializing Decadal Climate Predictions with the GECCO Oceanic Synthesis: Effects on the North Atlantic. *J. Climate*, 22:3926–3938.

Polyakov, I. V., Bhatt, U. S., Simmons, H. L., Walsh, D., Walsh, J. E., and Zhang, X. (2005). Multidecadal Variability of North Atlantic Temperature and Salinity during the Twentieth Century. *Journal of Climate*, 18:4562–4581.

Raible, C. C., Ziv, B., Saaroni, H., and Wild, M. (2010). Winter synoptic-scale variability over the Mediterranean Basin under future climate coconditions simulated by the ECHAM5. *Climate Dyn.*, 35:473–488.

Rayner, N. A., Parker, D. E., Horton, E. B., Folland, C. K., Alexander, L. V., Rowell, D. P., Kent, E. C., and Kaplan, A. (2003). Global analysis of sea surface temperature, sea ice, and night marine air temperature since the late nineteenth century. *J. Geophys. Res.*, 108:D14:4407.

Robson, J., Sutton, R., Lohmann, K., Smith, D., and Palmer, M. D. (2012). Causes of the Rapid Warming of the North Atlantic Ocean in the Mid-1990s. *J. Climate*, 25:4116–4134.

Rodwell, M. J., Rowell, D. P., and Folland, C. K. (1999). Oceanic forcing of the wintertime North Atlantic Oscillation and European climate. *Nature*, 398:320–323.

Saeed, S., Lipzig, N. V., Müller, W. A., Saeed, F., and Zanchettin, D. (2014). Influence of the circumglobal wave-train on European summer precipitation. *Climate Dyn.*, 43:503–515.

Schär, C., Vidale, P. L., Luethi, D., Frei, C., Haeberli, C., Liniger, M. A., and Appenzeller, C. (2004). The role of increasing temperature variability in European Summer heatwaves. *Nature*, 427:332–336.

Scherrer, S. C., Croci-Maspoli, M., Schwierz, C., and Appenzeller, C. (2006). Two-Dimensional Indices of Atmospheric Blocking and their Statistical Relationship with Winter Climate Patterns in the Euro-Atlantic region. *Int J Climatol*, 26:233–249.

Schlesinger, M. E. and Ramankutty, N. (1994). An oscillation in the global climate system of period 65–70 years. *Nature*, 367:723–726.

Schreck, C. J., Shi, L., Kossin, J. P., and Bates, J. J. (2013). Identifying the MJO, Equatorial Waves, and Their Impacts Using 32 Years of HIRS Upper-Tropospheric Water Vapor. *J. Climate*, 26:1418–1431.

Sienz, F. H., Müller, W. A., and Pohlmann, H. (2016). Ensemble size impact on the decadal predictive skill assessment. *Meteorol. Z.*

Smagorinsky, J. (1953). The dynamical influence of large-scale heat sources and sinks on the quasi-stationary mean motions of the atmosphere. *Quart. J. Roy. Meteor. Soc.*, 79:342–366.

Smith, D. M., Eade, R., Dunstone, N. J., Fereday, D., Murphy, J. M., Pohlmann, H., and Scaife, A. A. (2010). Skilful multi-year predictions of Atlantic hurricane frequency. *Nat Geosci*, 3:846–849.

Stevens, B., Giorgetta, M., Esch, M., Mauritsen, T., Crueger, T., Rast, S., Salzmann, M., Schmidt, H., Bader, J., Block, K., Brokopf, R., Fast, I., Kinne, S., Kornblueh, L., Lohmann, U., Pincus, R., Reichler, T., and Roeckner, E. (2013). Atmospheric component of the mpi-m earth system model: Echam6. *JAMES*, 5:146–172.

Sutton, R. T. and Dong, B. (2012). Atlantic Ocean influence on a shift in European climate in 1990s. *Nat Geosci*, 5:788–792.

Sutton, R. T. and Hodson, D. L. (2007). Climate response to basin-scale warming and cooling of the North Atlantic Ocean. *J. Climate*, 20(5):891–907.

Sutton, R. T. and Hodson, D. L. R. (2005). Atlantic Ocean Forcing of North American and European Summer Climate. *Science*, 309(5731):115–118.

Terray, L. and Cassou, C. (2002). Tropical Atlantic Sea Surface Temperature Forcing of Quasi-Decadal Climate Variability over the North Atlantic-European Region. *J. Climate*, 15:3170–3187.

Valcke, S., Calubel, D., and Terray, L. (2003). OASIS ocean atmosphere sea ice soil user's guide. techreport TR/CMGC/03/69, CERFACS, Toulouse, France.

Whitaker, J. S., Compo, G. P., Wei, X., and Hamill, T. M. (2004). Reanalysis without radiosondes using ensemble data assimilation. *Mon. Weather Review*, 132:1190–1200.

Woollings, T., Czuchnicki, C., and Franke, C. (2014a). Twentieth century North Atlantic jet variability. *Quart. J. Roy. Meteor. Soc.*, 140:783–791.

Woollings, T., Franzke, C., Hodson, D. L. R., Dong, B., Barnes, E. A., Raible, C. C., and Pinto, J. G. (2014b). Contrasting interannual and multidecadal NAO variability. *Climate Dyn.*, pages 1–18.

Acknowledgements

This PhD journey holds some of the most memorable years in my life, which grew me not only scientifically as a researcher but also philosophically and spiritually as a human being. There are many who played very important roles during this journey. First of all, I would like to thank Wolfgang, one of the coolest supervisors one can have during this crucial journey. During these years, he not only guided me in my research but also supported me as a true friend. He has given me all the freedom and showed complete trust on my potential, which allowed me to fully flourish and grow in my own way. I am really grateful to him on that regard.

Next, my gratitude goes to Johanna, who was always there with her help and support whenever I needed. There are times when her kind and inspiring words helped me to keep my strength and confidence. I would like to thank Jochem and Hartmut for keeping my PhD voyage on track and very smooth through their knowledge and vast experience in the field of climate science. Their valuable comments and inputs during the panel meetings allowed me to keep a high quality in my work. Moreover, Jochem accompanied by Dallas improved my writing skills which erased a long-lived fear of writing within me.

I would like to thank Jürgen for all his guidance that he provided regarding the dynamical understanding of my results. I am thankful to Frank for helping me conduct some statistical analysis correctly. I also thank Johan for his valuable comments on my first work, which helped me improve certain aspects of the study.

I would also like to thank Google whose support is undeniable and one of the most significant during my research. From knowing all other relevant researches to dealing with technical issues, Google was the place, which helped me almost each and every day. It is like the experience and help of the entire humanity is on your door step, without which this PhD journey could have been longer.

I like to thank Max Planck Society for creating and supporting the international PhD school, which allowed us to be a part of this novel institute and to develop world class research skills. I want to thank the European project, SPECS, which funded my PhD. Moreover, I also want to thank my masters supervisors, Arindam and Ravi sir, for their encouragement and support which paved my path to this PhD school.

As an International student, coming from India and settling in a new culture were a bit challenging in the beginning. I am grateful to Antje for all the guidance, help and support during these years which made this transition and adaptation really smooth. Additionally, the

help from Wiebke at the beginning and afterwards from Connie made the official aspects of the PhD very much hassle free. Thank you so much for that. I would like to thank Christina for introducing me to all the concerned people around at the beginning and for always helping me regarding translations of the official documents. I am thankful to Kornelia for always helping me regarding smoothly fixing panel meetings and especially for helping me move in a brighter office room.

Being away from my home, the people who made me feel home in Hamburg are my friends. I am thankful to them for making these years so lively and full of nice memories. Thanks Suvi, for the awesome time we had which made our friendship epic and forever. Thanks Roger and Vika for being one of my closest buddies in Hamburg and for all your encouragements. Thanks Jörg for the cool friendship and for all the delicious lunch sessions together which helped me keep the flavours in my work. Thanks a lot Edu, for all our lunch breaks, cool discussions and for being so inspiring in your work. Thanks Laura for your suggestions on the thesis. Thanks Dirk, Manita, Katharina, Max, Jan, Felix, Matthias, Ritthik, Pierre, Kamesh, Anurag, Ashu, Pavan, Hanna and Ketan for all your friendship and for making these PhD years special in my life.

The way to my PhD and its accomplishment would be impossible without the support of my parents. They always supported me with what I wanted to do in my life. It is their unconditional love, trust and blessings, which brought me here and will continue to guide me in the days ahead. I am grateful to my big brother, Bhaia, for being such a great support as a friend, philosopher and guide in my life. Thanks a lot Bhaia. At the end, I want to thank my love, Armelle, for being my companion and giving me all the strength on this journey. This journey became so lovely and full of joy and happiness with you. Its a blessing to have you in my life.